

Analysis and Modeling of Vehicular Movement in no-lane-disciplined Heterogeneous Traffic Stream

*A thesis submitted in partial fulfilment of the requirements
for the degree of*

Doctor of Philosophy

In

Civil Engineering

By

Dibyendu Pal

Under the Supervision of

Dr. C. Mallikarjuna



**DEPARTMENT OF CIVIL ENGINEERING
INDIAN INSTITUTE OF TECHNOLOGY GUWAHATI
GUWAHATI-781039, ASSAM, INDIA
October 2015**

Analysis and Modeling of Vehicular Movement in no-lane-disciplined Heterogeneous Traffic Stream

*A thesis submitted in partial fulfilment of the requirements
for the degree of*

Doctor of Philosophy

In

Civil Engineering

By

Dibyendu Pal

(09610413)

Under the Supervision of

Dr. C. Mallikarjuna



**DEPARTMENT OF CIVIL ENGINEERING
INDIAN INSTITUTE OF TECHNOLOGY GUWAHATI
GUWAHATI-781039, ASSAM, INDIA**



Department of Civil Engineering
Indian Institute of Technology Guwahati
Guwahati-781039
Assam, India

CERTIFICATE

This is to certify that the work contained in this thesis entitled “Analysis and Modeling of Vehicular Movement in no-lane-disciplined Heterogeneous Traffic Stream” submitted by Mr. Dibyendu Pal (09610413) to the Indian Institute of Technology, Guwahati, India, for the award of the degree of Doctor of Philosophy, in Civil Engineering, has been carried out under my supervision. This work has not been submitted elsewhere for the award of any other degree or diploma.

Dr. C. Mallikarjuna
Associate Professor
Department of Civil Engineering
Indian Institute of Technology Guwahati
Guwahati-781039, Assam, India

Acknowledgements

I would like to express my deep gratitude and heartfelt thanks to my supervisor Dr. C. Mallikarjuna, Associate Professor, Department of Civil Engineering, Indian Institute of Technology Guwahati, Assam, India, for his consistent supervision, guidance, encouragement and gracious support throughout my research work. His valuable suggestions, effusive co-operation and encouraging interactions were great driving force for me to carry out this research work. Conducting the research and writing this dissertation would not have been possible without his patience, guidance and tireless devotion to this work.

I deeply express my sincere thanks to the chairman of doctoral committee Prof. Subashisa Dutta and the committee members Prof. S. V. Rao and Dr. Akhilesh Kumar Maurya for their sincere advice and suggestions to improve the quality of work. I would also like to extend my sincere gratitude to the Head, Department of Civil Engineering, IIT Guwahati, for all the support and encouragement extended to me directly or indirectly to carry out my research. I am also thankful to Prof. Anjan Dutta, Prof. S. K. Deb, Dr. T. L. Ryntathiang and the other faculty members for their support and encouragement extended to me at various stages of work. I also express my sincere thanks to all the staff for their help and support in various aspects.

I would like to convey my thanks to all the post graduate students who have extended their support in traffic data extraction and collection from various cities of India. I am also grateful to my fellow research scholars Dr. Partha Partim Sarkar, S. Omar, Tanmoy, Polash, Geetimukta, Madhulisha, Thainswemong and others for their inspiration, interesting discussions, and encouragement.

I would also like to take this opportunity to thanks the Director, NERIST, Head, Department of Civil Engineering, NERIST, and all the other faculty members, staff and students of NERIST, Nirjuli, who has supported and encouraged me directly or indirectly in various aspects.

I express my great gratitude to my parents, siblings, in-laws and all other family members for their constant support and encouragement. Last but not the least; I would like to appreciate my better half and my son, for their support and sacrifice, without which I would not have reached to the status which I have achieved now.

Dibyendu Pal

Abstract

Increasing number of personal vehicles in cities of developing countries has resulted in a significant growth of urban traffic. Prevalent traffic jams observed in Indian cities can be partly attributed to this vehicular growth. Solutions to such problems can be either in terms of efficient traffic management and operational strategies or by expanding the existing infrastructure according to the emergent requirements. Both strategies cannot be implemented without using suitable traffic flow models. Traffic flow models meant for lane disciplined homogeneous/heterogeneous traffic cannot be directly used for modeling the no-lane-disciplined heterogeneous traffic observed in Indian cities.

Understanding the behavior of vehicles moving in no-lane-disciplined heterogeneous traffic stream is essential in developing the simulation model. To gain the necessary understanding it is required to analyze the vehicular movement at the microscopic level.

Based on the empirical observations it has been found that one of the important characteristics of no-lane-disciplined heterogeneous traffic is the variable lateral gap maintaining behavior of different types of vehicles. In this study the total lateral gap maintaining behavior of vehicles has been analyzed using the trajectory data obtained from the video image processing software, TRAZER. Total minimum lateral gap (gap on both the sides of vehicle) maintained by four types of vehicles, namely, Light motor vehicle (LMV), Motorized two wheeler (MTW), Motorized three wheeler (MThW), and Heavy motor vehicle (HMV) has been modeled in this study. Field observations suggest significant variability in the lateral gaps even when the passing/overtaking vehicle was traveling at more or less constant speed. Logistic regression model has been used to model the total lateral gaps. From the estimated models it has been observed that the speed of the subject vehicle, size and speed of both the adjacent vehicles affect the lateral gaps. The impact of side vehicle has been found to be prominent even at lower speed of the subject vehicle in case of a relatively wide road.

A modified cellular automata (CA) based microscopic traffic simulation model has been developed in this study to analyze the no-lane-disciplined heterogeneous traffic. The variable lateral gap maintaining behavior of vehicles of no-lane-disciplined heterogeneous traffic has been incorporated in the current CA based simulation model. The cell structure of the current CA model is modified to adequately represent the

smaller vehicles and finer variable lateral movements of vehicles. Updating procedures and the corresponding parameters of the current CA model is modified in accordance with the modified cell structure.

In no-lane-disciplined heterogeneous traffic stream, following vehicle encounters multiple leading vehicles. In this study, Front leading vehicle (FLV), left front leading vehicle (LFLV) and right front leading vehicle (RFLV) have been considered as the leading vehicles and the closest among these vehicles is considered as the effective leading vehicle. The movement of the following vehicle is governed by the effective leading vehicle. The impact of the side vehicles has also been considered in indentifying the effective leading vehicle. The movement of vehicles in no-lane-disciplined heterogeneous traffic stream is characterized by the finer lateral movements. To represent this behavior the road section was divided into multiple sub-lanes in terms of finer cells. With the help of finer cell structure, gradual lateral shifting has been introduced in the present model.

Effect of the finer cell structure on the updating procedures and on the corresponding parameters has been thoroughly analyzed. Based on the previous research efforts, field observations, and parametric analysis, some of the parameters have been modified. The impact of variable lateral gap and the interaction headways were found to be prominent on the traffic stream behavior. The developed model has been macroscopically validated using the field observed speed, flow, and occupancy data of two different road sections. Simulated free flow conditions are further validated by comparing the observed and simulated free flow speed distributions. Model's ability to simulate the congested traffic conditions has also been validated by comparing the observed and simulated queue formation and dissipation characteristics. The developed model has been used to analyze the effect of two-lane road width being used in urban regions. It has been observed that slight changes in the road width, between 6.9 to 8.4 m, significantly influence the traffic stream behavior.

Contents

Certificate	ii
Acknowledgements	iii
Abstract	iv
Contents	vi
List of Figures	x
List of Tables	xiii
Abbreviations	xiv
Chapter 1 Introduction	1
1.1 General	1
1.2 Need for the Study	3
1.3 Research Goal and Objectives	4
1.4 Scope of the Present Study	4
1.5 Thesis Outline	4
Chapter 2 Literature Review	7
2.1 Microscopic Modeling	7
2.2 Application of car-following Model for Heterogeneous Traffic	9
2.2.1 Field observations on car-following in heterogeneous traffic	10
2.3 Microscopic Data Collection	11
2.3.1 Trajectory correction	11
2.3.2 Speed estimation from the smoothed trajectory	13
2.3.3 Lateral gap maintaining behavior of vehicles	14
2.4 Cellular Automata Based Traffic Flow Model	16
2.4.1 Homogeneous traffic flow modeling using CA	16
2.4.2 Heterogeneous traffic flow modeling using CA	19
2.4.2.1 Evolution of the updating procedure	20
2.5 Summary of the Literature Review	22

Chapter 3	Data Collection and Analysis	23
3.1	Introduction	23
3.1.1	Site selection	24
3.1.2	Trajectory extraction using TRAZER	24
3.1.3	Details of the traffic data	26
3.1.4	Analysis of the raw trajectory extracted using TRAZER	26
3.2	EMD based Trajectory Smoothing	27
3.2.1	Empirical Mode Decomposition (EMD) and its Noise Assisted Versions	28
3.2.2	The EMD method	29
3.2.3	The ensemble EMD method	30
3.2.4	The CEEMDAN method	31
3.2.5	Trajectory data smoothing using CEEMDAN	33
3.3	Speed Estimation	37
3.3.1	Wavelet Transforms	38
3.3.2	Extraction of speed from the smoothed trajectory	40
3.3.3	Internal consistency	42
3.4	Summary and Conclusions	43
Chapter 4	Modeling of Lateral Gap Maintaining Behavior of Vehicles	45
4.1	Introduction	45
4.2	Data Collection	47
4.2.1	Identification of passing/overtaking vehicles	47
4.2.2	Field observations on total lateral gaps	49
4.3	Analysis of the Variations in the Total Lateral Gap	49
4.3.1	Logistic curve for modeling the total lateral gaps	51
4.3.2	Framework for optimization	51
4.4	Lateral Gap Modeling	52
4.4.1	Effect of the adjacent vehicles' speed	53
4.4.2	Effect of the adjacent vehicles' size	54
4.5	Analyses of the Results	55
4.5.1	Effect of the road width on the total lateral gap	58

4.6 Summary and Conclusions	61
Chapter 5 CA Model Development for no-lane-disciplined Traffic	63
5.1 Vehicular Movement in no-lane-disciplined Heterogeneous Traffic Stream	63
5.2 Cell Structure	65
5.3 Updating rules of the CA Model	66
5.3.1 Assumptions used in the updating procedure	66
5.3.2 Decision to maintain the current lateral position	67
5.3.2.1 Detection of the side influencing vehicle	67
5.3.2.2 Effective leading vehicle detection	67
5.3.3 Decision to change the current lateral position	69
5.3.3.1 Possible lateral positions for the SV	69
5.3.4 Lateral movement rules	70
5.3.4.1 Incentive criteria	70
5.3.4.2 Safety criteria	70
5.3.5 Forward movement rules	70
5.4 Data Collection from the Model	74
5.4.1 Global measurements	74
5.4.2 Local measurements with a detector of finite length	75
5.4.3 Local measurements with a detector of unit length	75
5.5 Parameter Analysis	76
5.5.1 Parameters of forward movement rules	76
5.5.1.1 Interaction headway (h)	76
5.5.1.2 Security distance (SD)	78
5.5.1.3 Slow down probability (p_{dec})	78
5.5.1.4 Slow-to-start probability (P_0)	79
5.5.1.5 Lateral gap	80
5.5.1.6 Acceleration characteristics	82
5.5.2 Parameters of lateral movement rules	83
5.5.2.1 Probability of lateral movement (p)	83
5.5.2.2 Look back distance	84
5.5.3 Effect of traffic composition	85

5.6 Summary and Conclusions	85
Chapter 6 Model Validation and Application	87
6.1 Simulation Model Set-up	87
6.2 Validation of the CA Model	88
6.2.1 Traffic stream moving on 10 m wide road	88
6.2.1.1 Macroscopic validation	90
6.2.1.2 Microscopic validation	92
6.2.2 Traffic stream moving on 8.3 m wide road	93
6.2.2.1 Macroscopic validation	95
6.2.2.2 Microscopic validation	97
6.3 Microscopic Validation of Queue Formation and Dissipation	98
6.4 Analysis of the Global Measurements	99
6.4.1 Global flow-occupancy relation for the 10 m wide road	100
6.4.2 Global flow-occupancy relation for the 8.3 m wide road	101
6.5 Effect of Road Width on Maximum Flow	102
6.6 Summary and Conclusions	104
Chapter 7 Summary and Conclusions	105
7.1 Summary	105
7.2 Conclusions	106
7.2.1 Trajectory correction	106
7.2.2 Lateral gap model	107
7.2.3 Traffic characteristics	108
7.2.4 Simulation model	108
7.2.5 Effect of road width	109
7.3 Contributions	110
7.4 Further Scope	110
REFERENCES	113
Publications	121

List of Figures

Fig. 1.1	Comparison of traffic streams with lane discipline (left photograph); without lane discipline (right photograph)	1
Fig. 2.1	Computation of transverse clearances for overtaking maneuver (Arasan and Koshy 2005)	15
Fig. 3.1	Trajectory data extraction using TRAZER	25
Fig. 3.2	Raw trajectory of Vehicle id_36004 extracted using TRAZER	27
Fig. 3.3	Arbitrary sinusoidal function and IMF extraction process	28
Fig. 3.4	CEEMDAN of longitudinal position (x, t) data of Vehicle id_36004	33
Fig. 3.5	IMF of lateral trajectory data obtained using CEEMDAN	34
Fig. 3.6	Comparison of trajectories estimated using various methods with the observed trajectory	34
Fig. 3.7	Comparison of smoothed trajectories obtained using various methods	35
Fig. 3.8	Statistical measures of trajectory corrections for Vehicle id_36004 (a); and arbitrary trajectory(b) by various methods.	36
Fig. 3.9	Observed and estimated paths of the vehicle corresponding to Fig. 3.2.	36
Fig. 3.10	Average RMSE and MAE of the trajectories	37
Fig. 3.11	Original (a) and smoothed (b) trajectories of vehicles	37
Fig. 3.12	Variation of RMSE with dilation parameter (a), and decomposition level (b)	41
Fig. 3.13	Speed profiles obtained using various techniques	42
Fig. 3.14	Error measures of the consistency of position(a); and speed (b) estimated using various methods	43
Fig. 4.1	Variable lateral gap maintained by MTW at two different scenarios	46
Fig. 4.2	Hypothetical no-lane-disciplined traffic stream with passing/overtaking vehicles and the representation of total lateral gap	48
Fig. 4.3	Speed of the passing/overtaking vehicle versus total lateral gap, in case of LMV (a), MTW (b), MThW (c), and HMV (d)	50
Fig. 4.4	Variation of total lateral gap maintained by the subject vehicle when travel- ling at different speeds: LMV (a); MTW (b); MThW (c); and HMV (d)	56
Fig. 4.5	Variation in the threshold values of the subject vehicles' speeds (a); and adjacent vehicles' speeds (b), while assessing the impact of the adjacent vehicle's speed and size	58

Fig. 4.6	Variation of the threshold total lateral gap with road width	60
Fig. 4.7	Validation of total lateral gap for LMV (a) and MTW (b)	60
Fig. 5.1	Various vehicles affecting the SV's movement in the heterogeneous traffic stream	64
Fig. 5.2	Cell structure of the proposed CA model and the hypothetical representation of vehicles moving in the no-lane-disciplined heterogeneous traffic stream	64
Fig. 5.3	Effective route width available for the SV at various speeds	73
Fig. 5.4	Relationship between global flow and global occupancy for various interaction headways for homogeneous traffic, consisting of only cars (a); and heterogeneous traffic (b)	77
Fig. 5.5	Relationship between global flow and global occupancy for various security distances for homogeneous traffic, consisting of only cars	78
Fig. 5.6	Relationship between global flow and global occupancy for various values taken by p_{dec} , for homogeneous traffic, consists of only cars	79
Fig. 5.7	Relationship between global flow and global occupancy for various slow-to-start parameters for homogeneous traffic consists of only cars; current model (a); results from Mallikarjuna (2007) (b)	80
Fig. 5.8	Relationship between global flow and global occupancy for constant and variable total lateral gap for homogeneous traffic consists of only cars (a); and heterogeneous traffic (b)	81
Fig. 5.9	Relationship between global flow and global occupancy for constant and variable acceleration for homogeneous traffic consists of only cars (a); and heterogeneous traffic (b)	83
Fig. 5.10	Relationship between global flow and global occupancy for different probability of lateral movement (p) for homogeneous traffic consists of only cars	84
Fig. 5.11	Global flow-occupancy relationship of heterogeneous traffic for various beta (β) values	84
Fig. 5.12	Effect of traffic composition on Global flow-density relationships	85
Fig. 6.1	Observed and simulated Flow-Occupancy relationship for Jubilee hills Road	91
Fig. 6.2	Observed and simulated Speed-Flow relationship for Jubilee hills Road	91

Fig. 6.3	Observed and simulated Speed-Occupancy relationship for Jubilee hills Road	92
Fig. 6.4	Comparison of observed and simulated cumulative distributions of FFS for LMV (a); MTW (b); MThW(c); HMTV(d)	93
Fig. 6.5	Observed and simulated Flow-Occupancy relationship for Kodihalli Road	96
Fig. 6.6	Observed and simulated Speed-Flow relationship for Kodihalli Road	96
Fig. 6.7	Observed and simulated Speed-Occupancy relationship for Kodihalli Road	97
Fig. 6.8	Comparison of observed and simulated cumulative distributions of FFS for LMV (a); MTW (b); MThW(c); HMTV(d)	98
Fig. 6.9	Comparison of the simulated (a) and observed (b) queue formation and dissipation	99
Fig. 6.10	Simulated global flow and global occupancy relationship for 10 m wide road	100
Fig. 6.11	Simulated global flow and global occupancy relationship for 8.3 m wide road	101
Fig. 6.12	Variation of Global flow-occupancy relationships for homogeneous traffic (a); and heterogeneous traffic (b), with changing two-lane road width	103
Fig. 6.13	Variation of capacity on slight changes in the width of a two lane road	104

List of Tables

Table 3.1	Road geometry and traffic characteristics observed at data collection sites	26
Table 4.1	Observed total lateral gap data and number of observations considered in modeling	49
Table 4.2	Parameters of the lateral gap models, for Maharani Bagh road	55
Table 4.3	Threshold values corresponding to the speeds of subject and the adjacent vehicles	56
Table 4.4	Parameters of the lateral gap models, for various other roads	57
Table 4.5	Parameters for speed and size effects, for different types of vehicles	59
Table 6.1	Representation of 10 m wide road (Jubilee hills, Hyderabad) and the corresponding vehicles related parameters used in the simulation model	89
Table 6.2	Coefficients and threshold total lateral gap for 10 m wide road	90
Table 6.3	CA model Parameters corresponding to validated model (10 m wide road)	90
Table 6.4	Statistical comparison of observed and simulated free flow speeds of various types of vehicles	93
Table 6.5	Representation of 8.3 m wide road (Kodihalli, Bangalore) and the corresponding vehicles related parameters used in the simulation model	94
Table 6.6	Coefficients and threshold total lateral gap for 8.3 m wide road	95
Table 6.7	CA parameters corresponding to the validated model (8.3 m wide road)	95
Table 6.8	Statistical comparison of observed and simulated free flow speeds of various types of vehicles	98
Table 6.9	Conversion of global flows obtained in cells /sub-lane/sec to vehicles/hr, in case of three lane road	101
Table 6.10	Conversion of global flows obtained in cells /sub-lane/sec to vehicles/hr, in case of two lane road	102

Abbreviations

CA	Cellular Automata
LMV	Light Motor Vehicle
HMV	Heavy Motor Vehicle
MThW	Motorized Three Wheeler
MTW	Motorized Two Wheeler
GPS	Global Positioning System
EMD	Empirical Mode Decomposition
EEMD	Ensemble Empirical Mode Decomposition
CEEMDAN	Complete Ensemble Empirical Mode Decomposition With Adaptive Noise
NADA	Noise Assisted Data Analysis
RMSE	Root Mean Squared Error
MAE	Mean Absolute Error
FFS	Free Flow Speed
2D-KS	Two Dimensional Kolmogorov-Smirnov
SV	Subject Vehicle
LFLV	Left Front Leading Vehicle
RFLV	Right Front Leading Vehicle
LV	Leading Vehicle
LSV	Left Side Vehicle
BV	Back Vehicle
LBV	Left Back Vehicle
RBV	Right Back Vehicle
SD	Security Distance

Introduction

1.1 General

Increasing number of personal vehicles in cities of developing countries has resulted in a significant growth of urban traffic. Prevalent traffic jams observed in Indian cities can be attributed to this traffic growth. This has been recognized as a major problem faced by the city administrations, with significant effect on the economy, air quality, and a cause of discomfort for the millions of commuters. Solutions to such problems can be either in terms of efficient traffic management and operational strategies or by expanding the existing infrastructure according to the emergent requirements. Both strategies cannot be implemented without using suitable traffic flow models. Traffic flow models meant for lane disciplined homogeneous/heterogeneous traffic cannot be directly used for modeling the no-lane-disciplined heterogeneous traffic observed in the Indian cities. Differences in the traffic streams moving on the Indian roads and the lane based traffic streams can be clearly seen in Fig. 1.1.



Fig. 1.1 Comparison of traffic streams with lane discipline (left photograph); without lane discipline (right photograph)

Vehicles moving in homogeneous traffic stream (Fig. 1.1) follow lane discipline. Hence, the movement of following vehicle can be said to be directly influenced by the characteristics of the leading vehicle such as the type of vehicle, the longitudinal gap, and the expected movement of the leading vehicle in the next time step.

Heterogeneous traffic stream consists of motorized vehicles such as Motorized two wheelers (MTW); Light motor vehicles (LMV) such as cars, jeeps, vans; Heavy motor vehicles (HMV) such as buses, trucks; Motorized three wheeler (MThW) such as auto-rickshaws; light commercial vehicles (LCV), and non-motorized vehicles such as bicycles and tricycles. Small sized vehicles (MTW, bicycle) often use gaps between the larger vehicles to weave through the traffic. The no-lane-discipline of vehicles moving in the heterogeneous traffic stream can be attributed to the above two factors. In no-lane-disciplined traffic stream a moving vehicle can laterally be closer to the adjacent standstill vehicle. But, it requires to maintain safe lateral gap if the adjacent vehicle is in motion. That means the impact of neighboring vehicle speed is felt on the movement of any vehicle moving in the no-lane-disciplined traffic stream. Similarly, the type of the adjacent vehicle also influences the movement of a vehicle. Therefore, the lateral gap or the frictional clearance between the vehicles is an important characteristic of heterogeneous traffic. Ideally any microscopic simulation model meant for modeling no-lane-disciplined traffic stream should capture this behavior. Similarly all the other important factors affecting the vehicle movement need to be considered in the model.

Many researchers have worked on modeling the heterogeneous traffic and developed the microscopic simulation models. Most of these efforts were based on limited field observations and in many of these models convenient assumptions were made regarding the vehicular movement. Unlike the lane base traffic, in case of no-lane-disciplined traffic it is difficult to get the field data on vehicular movement such that a clear understanding of the traffic stream behavior can be gained. Trajectory data on all the vehicles need to be collected to understand the vehicular movement. If the trajectory data over a long road stretch are available, it is possible to understand the vehicular movement and the relevant influencing factors. If the trajectory data are available on a short road stretch, some understanding of lateral gap maintaining behavior can be gained.

Traditional microscopic traffic simulation models describe the behavior of individual vehicles at every instant of time and location of the road. Given the complex interaction of vehicles, it is difficult to develop a similar model for no-lane-disciplined heterogeneous traffic stream. Cellular Automata (CA) is widely used in developing the microscopic traffic simulation model and it has been found that this approach is computationally efficient and less time consuming. Numerous models have been

developed using CA concept for lane-based traffic (Nagel and Schreckenberg 1992; Knospe et al. 2000; Maerivoet 2005; Barlovic et al. 1998) and no-lane-disciplined heterogeneous traffic (Lan and Chang 2005; Lan and Hsu 2006; Gundaliya 2005; Mallikarjuna and Rao 2011). With CA it is also possible to model the vehicular movements at closely spaced time and space intervals (Knospe et al. 2000; Mallikarjuna and Rao 2011). This leads to the possibility of modeling finite lateral movements and variable lateral gap maintaining behavior observed in no-lane-disciplined traffic conditions using the CA models. Few researchers have incorporated this concept in CA model, but did not adequately represent the actual behavior. Also, to model the no-lane-disciplined the present concept of lanes may not be useful. The cell width needs to be decided in such a way that the small vehicles such as motorized two wheelers and three wheelers are appropriately represented in the model. To simulate the real world traffic conditions it is also necessary to incorporate the static and dynamic behavior of all the vehicles observed in the no-lane-disciplined heterogeneous traffic stream. Therefore, a systematic study of all the relevant characteristics of traffic, with enough data, is required to comprehend this type of traffic scenario.

1.2 Need for the Study

Microscopic traffic data of all the vehicles are necessary to understand the no-lane-disciplined heterogeneous traffic stream behavior. Also, data needs to be collected on various states of traffic stream. The requisite microscopic data can be extracted from the vehicle trajectories. Manual extraction of the trajectories from traffic video film is a tedious job and random parallax errors may occur. Image processing based methods are useful in collecting huge data covering various scenarios. Serious errors may also occur due to various reasons while extracting the vehicle trajectory using image processing software. A suitable approach for the correction of trajectory data, corresponding to no-lane-disciplined traffic stream, is required. Besides the longitudinal interaction, vehicles moving in no-lane based heterogeneous traffic stream are affected by the lateral interactions. Therefore, a comprehensive study on various factors that affect the lateral interactions (lateral gap maintaining behavior) of vehicles is required.

Most of the existing microscopic traffic simulation models have been developed for lane based traffic streams. Some of the microscopic traffic simulation models, developed for no-lane based traffic streams, have considered the lateral gap maintaining

behavior of vehicle in a rigid manner. Variability in the lateral gap maintaining behavior was not thoroughly analyzed and modeled. Moreover, in case of no-lane based heterogeneous traffic stream, the factors that affect the movement of a follower have not been clearly identified. This lead to the present study with the objectives detailed in the following section.

1.3 Research Goal and Objectives

The goal of this research is to develop a microscopic traffic simulation model for no-lane-disciplined heterogeneous traffic stream. The main objectives of the current research effort to achieve this goal are as follows:

- To analyze the vehicle trajectory data extracted through image processing.
- To analyze the vehicular movement in no-lane-disciplined heterogeneous traffic stream using trajectory data.
- To modify the cell structure and vehicle's updating procedures of CA based model for heterogeneous traffic.
- To study the effect of lane widths, presently being used in India for two lane roads on traffic movement using the proposed simulation model.

1.4 Scope of the Present Study

The scope of the present study is limited to the analysis of traffic stream behavior on divided urban roads with widths varying from 8.3 to 12.5 m. It was also assumed that non-motorized traffic is not present in the traffic stream. Trajectory data collected in the present study would be used only for the modeling of lateral gaps.

1.5 Thesis Outline

This thesis is organized into seven chapters. **Chapter 1** presents general introduction, need for the present study, research objectives, and the scope of the present work. A State-of-the-art literature review has been presented in **Chapter 2**. **Chapter 3** describes the details of the data collected for present study. Methodology to extract trajectory from traffic video film, estimation of corrected position and instantaneous speed from discrete trajectory data are also presented in this chapter. **Chapter 4** provides the details of lateral gap modeling. **Chapter 5** describes the microscopic traffic simulation

modeling framework and parameter analysis of the proposed model. **Chapter 6** deals with the results and analysis of the proposed simulation model. Finally, **Chapter 7** provides the summary and important conclusions of the present work, and future scope of research.





Literature Review

Traffic flow models for lane disciplined traffic have evolved over time and the same is not the case with the models dealing with heterogeneous traffic. Traffic flow models for no-lane-disciplined heterogeneous traffic have taken most of the concepts meant for lane disciplined traffic. With the evolution of data collection techniques researchers have started differentiating the fundamental behavior of these traffic streams. This chapter presents a systematic literature review of the development of models for no-lane-disciplined traffic stream either on the basis of existing lane based models or based on the observed behavior of heterogeneous traffic streams. Image processing techniques are being used for trajectory data collection under heterogeneous traffic conditions and in this chapter a review of trajectory correction methodologies has been presented. A brief history of microscopic traffic flow modeling is described in section 2.1. Car following models adopted for no-lane-disciplined heterogeneous traffic streams are presented in section 2.2. Correction of the trajectory data and the models developed based on the analysis of trajectories are shown in section 2.3. Brief review on CA models is presented in Section 2.4. Summary and important aspects of the literature review are presented in section 2.5.

2.1 Microscopic Modeling

In microscopic modeling dynamics of different types of vehicles and their interactions are modeled using analytical and empirical relations. Microscopic traffic simulation models are based on the individual vehicle entities, and many of these models consider the driver behavior. In microscopic models the interaction between the vehicles is determined by the influence of each vehicle's movement (Chowdhury et al. 2000), driver's behavior, state of surrounding vehicles, etc. In microscopic modeling vehicle's movement can be divided into longitudinal movement and lateral movement. The car-following model is mainly used in modeling the longitudinal movement and lane-changing model is used in modeling the lateral movement of individual vehicle.

Common car-following models are safe distance or behavioral model, stimulus response model, psychological-physical/action point model, artificial intelligence based

model, cellular automaton (CA) model etc. Car-following models consider the time and position of two consecutive vehicles in the same lane and control the motion of the following car (Pipes 1953; Newell 1961; Gazis et al. 1961; Kesting et al. 2007). But, lane changing models consider the spreading of vehicles across lanes (Brackstone et al. 1998; Laval and Leclercq 2008; Treiber et al. 2010). Compared to the car-following models, in lane-changing models interaction between vehicles depends on many factors, and also getting the data is difficult.

The first car-following model includes a car-following rule based on safe following distance. Pipes (1953) has developed the single lane car-following model without overtaking based on the safe following distance from the preceding vehicle. This safe distance is proportional to the speed of the following vehicle. Gipps (1981) refined the safe following distance based on the assumption that the driver sets limits on desired braking and acceleration rates. Most well-known and extensively used car-following model in 1950s was the stimulus response model, originally developed by General Motors (GM), also known as GHR model (Chandler 1958; Gazis 1961), takes a non-linear form of response as a function of sensitivity and stimuli. Michaels (1965) discussed that the driver would only react when approaching another vehicle. This indicates that at large headway driving behavior is not influenced by the other vehicles. However, Wiedemann (1974) has developed a car-following model, known as action point model, considering that a driver behaves differently in free driving, approaching, following, and braking.

Though car-following is the basis of controlling the motion of following vehicles, in real world lane-changing occurs frequently for faster movement (Laval and Daganzo 2006; Jin 2010) or as a mandatory maneuver (Choudhury et al. 2007). However, many more complicated interactions occur while lane-changing (Sun and Elefteriadou 2014). Zheng (2014) has given a state-of-art review on recent developments in lane changing models. He has emphasized the need of modeling lane-changing at macroscopic as well as at microscopic level with reasonable accuracy. He has also stressed on accurate trajectory data collection.

Since the present study is specifically meant for understanding the behavior of each individual entity in no-lane-disciplined heterogeneous traffic stream moving on multilane road, the main emphasis is given on understanding the microscopic traffic

modeling approaches used for heterogeneous traffic modeling. Some of the important models are discussed in the following section.

2.2 Application of car-following Model for Heterogeneous Traffic

Traffic observed on Indian urban roads is heterogeneous in nature, and due to various reasons vehicles do not follow lane markings. Hence, the models built for lane disciplined homogeneous traffic would not be able to replicate this type of traffic behavior. Many attempts were made in 1980's to develop heterogeneous traffic simulation models (Palaniswamy et al. 1985; Ramanayya 1988). Ramanayya (1988) has modeled mixed traffic moving on one lane roads using the car-following concept. In addition to car-following concept, he has added overtaking criteria and lateral clearance adequacy in the developed model. He has observed that on Indian roads, under mixed traffic conditions, single lane road can support two or three rows of small vehicles with appropriate lateral clearances. Palaniswamy et al. (1985) have modified and developed a discrete event-based simulation model, based on Swedish Road Traffic Simulation model (SWERTS). They have incorporated different road conditions, different shoulder conditions, terrain, power-to-mass ratio, over-taking gap acceptance, passing speeds etc. Four types of roads were considered in this study (single lane bidirectional traffic (3.75 m); intermediate lane road (5.50 m); two-lane road (7.5 m) and four-lane road).

Mathew et al. (2013) have proposed a strip-based approach for simulation of mixed traffic conditions using SiMTraM (Simulation of Mixed Traffic Mobility), implemented on a traditional lane based simulator, SUMO. The road is divided into small strips, which allows continuous lateral movement rather than conventional discrete lane changing. For lateral movement they have calculated a factor called 'benefit' as the difference between the safe speeds on the neighboring and on the current strips. It has been computed using the car-following model, and normalized by the maximum velocity. A positive 'benefit' leads to lateral movement and vice-versa. They have also observed that reduction of strip width increases the throughput; indicates better utilization of empty space. But, this model is unable to analyze the erratic behavior of two wheeler (Lan et al. 2010) which is common in no-lane-disciplined heterogeneous traffic.

2.2.1 Field observations on car-following in heterogeneous traffic

Few researchers have observed the no-lane-disciplined heterogeneous traffic stream at microscopic level and had developed some understanding of vehicular interactions in no-lane-disciplined heterogeneous traffic stream. Gunay (2007) has developed a car-following theory with lateral discomfort. He has formulated the movement of following vehicles as a function of the off-centre effects of the leaders. He has pointed out the effect of the route width on the speed of the following vehicle, and the reduced following distance with increased lateral distance between the leader and follower.

Ravishankar and Mathew (2011) have observed that spacing maintained by a following vehicle is dependent on the type of leading and following vehicles, indicating that the car-following behavior is dependent on type of the leader and follower. They have obtained the data for homogeneous traffic from Next Generation Simulation (NGSIM) project (NGSIM 2009) and for heterogeneous traffic, from Eastern Express Highway, Mumbai, India using global positioning system (GPS) instrumented vehicles. They have observed that the mean speed of the follower is quite close to the lead vehicle speed, suggesting the existence of following behavior. They have modified Gipps's model using vehicle pair (follower-leader) specific parameters such as reaction time and deceleration of the following vehicle, assumed deceleration of the lead vehicle, effective size of the lead vehicle, maximum acceleration and desired speed of the following vehicle etc. They have also introduced a sensitivity parameter in the modified model which represents the variability in gap maintained by various vehicle combinations. These vehicle pair specific (follower-leader) parameter values for different combinations of vehicles have been obtained by optimization. This study did not consider the impacts of surrounding vehicles on the behavior of the following vehicle.

Kanagaraj et al. (2015) have analyzed the flow characteristics of mixed traffic based on the data collected from Chennai, India. The traffic data have been collected using videography technique and the trajectories have been extracted using a semi automated image processing software, called Trajectory Extractor (Lee et al. 2008). They have defined the leading vehicle in no-lane-disciplined heterogeneous traffic as the nearest vehicle from subject vehicle which laterally overlap and within 30 m from the follower's position. Depending on leader type subject vehicle maintains the

longitudinal spacing. In case of heavy vehicles and three wheelers this spacing is higher compared to two wheelers and cars. Similar trends also observed depending on subject vehicle type. The lateral movement is highest in case of two wheelers followed by cars, heavy vehicles and three wheelers.

From the above review it can be inferred that understanding and modeling of no-lane-disciplined heterogeneous traffic requires comprehensive studies on vehicular interactions in lateral and longitudinal directions. The following section deals with the trajectory data required for studying vehicular interactions in no-lane-disciplined heterogeneous traffic.

2.3 Microscopic Data Collection

The vehicular interactions can be captured in terms of positions, speeds, accelerations, time and space headways, lateral gaps etc. All these features can be extracted from the trajectories of the vehicles. The major hindrance in studying this behavior is the availability of accurate vehicle trajectory data. Collection of accurate vehicle trajectories under heterogeneous traffic flow is a major problem encountered by the researchers. A brief review on vehicle trajectory extraction and its correction is highlighted in the following sub-section.

2.3.1 Trajectory correction

Various non-intrusive data collection methods (using GPS (Greaves and Figliozzi 2008), radar (Adnan et al. 2013)) have been used by researchers, among them, video based traffic data collection was found to be more appropriate as this method has minimal effect on driver behavior. Several automated and semi-automated tools have been deployed to extract the vehicle trajectory data from traffic video film, such as VEVID (Wei et al. 2005), NGSIM-Video (Kovvali et al. 2007), Trajectory Extractor (Lee et al. 2008), TRAZER (Mallikarjuna et al. 2009), Traffic Data Extractor (Minugety et al. 2014) etc. Among these tools, TRAZER and Traffic Data Extractor have been utilized to extract trajectory in no-lane-disciplined heterogeneous traffic. Extraction of trajectory by Traffic Data Extractor is semi-automated and manual intervention is required to select the vehicle position in each time step. TRAZER is an automated tool and it can extract the trajectory without manual intervention. Manual intervention is also possible and this enhances the utility of TRAZER in case of false

classification and identification. The accuracy of trajectory extraction by TRAZER is about 85-90% (Mallikarjuna et al. 2009). Although videography based technique is an alternative to collect the trajectory data, due to the complex nature of vehicular movement the processed trajectory data contain several errors. When a vehicle is partially occluded the vehicular tracking becomes difficult and leads to errors in the position data. These errors, in a way, hinder the applicability of video image processing methods under heterogeneous traffic conditions. Hence, correction of the raw trajectory is necessary before extracting the traffic data.

Researchers have tried various methods to correct the trajectory and subsequently the speed. Averaging (Ossen and Hoogendoorn 2008), locally weighted regression technique (Toledo et al. 2007), filtering (Punzo et al. 2005; and Montanino and Punzo 2013) or moving average techniques (Thiemann et al. 2008) etc. were the commonly used techniques for correcting the trajectory data. Locally weighted regression techniques depend on the polynomial order. For a given polynomial order, the deviation from the observed position increases with the window size (Toledo et al. 2007; Kanagaraj et al. 2015). Duell et al. (2014) have pointed out that the large window size may not be suitable for widely displaced datasets. Ervin et al. (1991) have used Kalman filtering to smooth the trajectory data. Punzo et al. (2005) have used a similar approach to correct the GPS based trajectory data. They have used Kalman filter to obtain the average speeds from the raw data. Punzo et al. (2011) have analyzed the trajectory and speed data accuracy based on jerk analysis, consistency analysis, and spectral analysis.

Yuan (2009) has applied EMD (empirical mode decomposition) based trajectory smoothing algorithm on both the lateral and longitudinal positions of the vehicle. He has concluded that EMD is a more convenient method to smooth the trajectory compared to the wavelet based techniques. Correction of the end positions is one of the major problems associated to EMD technique. Wu and Huang (2009) have observed that the mode mixing was a major drawback associated with the original EMD approach. To overcome this problem, they have proposed a noise assisted data analysis (NADA) method termed as ensemble empirical mode decomposition (EEMD). It performs the EMD over an ensemble of the signal plus white Gaussian noise. The addition of white Gaussian noise solves the mode mixing problem, but, the reconstructed signal includes residual noise and different realizations of signal plus

noise may produce different number of modes (Torres et al. 2011). To avoid such problems, Torres et al. (2011) have proposed a complete ensemble empirical mode decomposition with adaptive noise (CEEMDAN).

From the review it can be said that the application of locally weighted regression approach for smoothing the trajectories needs inputs on window size and the order of the polynomial. In case of heterogeneous traffic conditions, where the lengths of the extracted trajectories are not uniform, it is necessary to give variable window size as well as the polynomial order. When the traffic volumes are high it is very difficult to provide such variable inputs. Application of EMD approach has also issues related to end point correction. Also, sometimes the position data obtained from TRAZER do not contain any noise and EMD approach cannot handle this kind of data. EEMD approach minimizes such a kind of errors but this method results in more computational time.

2.3.2 Speed estimation from the smoothed trajectory

The instantaneous speed of the vehicle can be estimated by taking the first derivatives of the smoothed trajectory. The simplest method of derivative calculation is numerical differentiation. In case of high frequency data the intensity of noise gets increased in derivative calculation (Haswell 1992). To improve the signal-to-noise ratio (SNR) of higher order derivatives, noise reduction is usually performed between each order of the successive derivatives (Antonov and Stoyanov 1996). Polynomial method of Savitzky–Golay (Savitazky et al. 1964; Gorry 1990; Barak 1995) and Fourier transform (Kauppinen et al. 1981; Cameron and Moffatt 1987) are the commonly used approaches for numerical differentiation. These approaches have limitations when applied to the experimental signal with low SNR (Shao and Ma 2003).

To handle the data with low SNR, methods based on wavelet transform (Mallat 2008 and Messina 2004), including continuous wavelet transforms (CWTs) and discrete wavelet transforms (DWTs), have been used for first derivative calculation.

WT, with commonly used wavelet functions, can be regarded as a smoothing and differentiation process. The order of differentiation was determined by the property of the wavelet function. The calculation of n^{th} order derivative was achieved by only one transform procedure, instead of repeated transforms (Shao et al. 2000). WT has been introduced in various aspects of civil engineering, such as detection of open

cracks in damaged beams (Gentile and Messina 2003; Messina 2004), evaluation of the seismic performance of the structure (Das and Gupta 2008). Application of WT has also been found in traffic and intelligent transportation engineering. WT has been adopted to investigate various traffic related issues, such as automatic detection of freeway incidents (Adeli and Samant 2000; Zheng et al. 2011), traffic features around freeway work zones (Adeli and Ghosh-Dastidar 2004), traffic flow forecasting (Jiang and Adeli 2005), and traffic pattern recognition (Jiang and Adeli 2004).

2.3.3 Lateral gap maintaining behavior of vehicles

Vehicles moving in the heterogeneous traffic stream interacts both in longitudinal and lateral directions and both these interactions are strongly correlated. Analysis and modeling of these correlated interactions is a complex task and some researchers (Chakroborty et al. 2004; Gunay 2007) have attempted to model this behavior. Many researchers have stressed the need to consider the adjacent moving vehicles in modeling the vehicular movement under heterogeneous traffic conditions (Chakroborty et al. 2004; Gunay 2007; Arasan and Koshy 2005; Mallikarjuna 2007; Dey et al. 2008). Though many have emphasized this requirement, very few attempts were made towards understanding this behavior.

Nagaraj et al. (1990) investigated the linear and lateral placement of vehicles in mixed traffic environment to develop the models for mixed traffic flow. They have done extensive data collection studies on gap maintaining behavior of vehicles. Data collection was limited to certain traffic conditions. They had specified the minimum lateral clearances maintained by various types of vehicles at zero speed and at 60 km/hr speed. In between these speeds the gaps were assumed to vary linearly as a function of subject vehicle's speed.

Singh (1999) has proposed relationships between lateral spacing and the subject vehicle speed. The minimum and maximum lateral spacing have been estimated for two lane road, for different combinations of vehicles. He has also estimated the lateral space from physical barriers like Curb and median etc. Arasan and Koshy (2005) have considered transverse clearance for over taking maneuver. They had assumed linear relationship between the speed of overtaking vehicle and lateral gaps. The lateral gap between two adjacent vehicles has been approximated as the sum of the two independent clearances, each contributed by the type and speed of the vehicles

involved. Fig. 2.1 depicts the computation of lateral gap when Vehicle 2 is overtaking Vehicle 1. The minimum left side clearance to be maintained by Vehicle 2 was represented as C_1+C_2 , where C_1 depends on the type and speed of Vehicle 1 and C_2 on that of Vehicle 2. Similarly, the minimum right side clearance required for Vehicle 2 was C_2+C_3 , and C_3 depends on the type and speed of Vehicle 3.

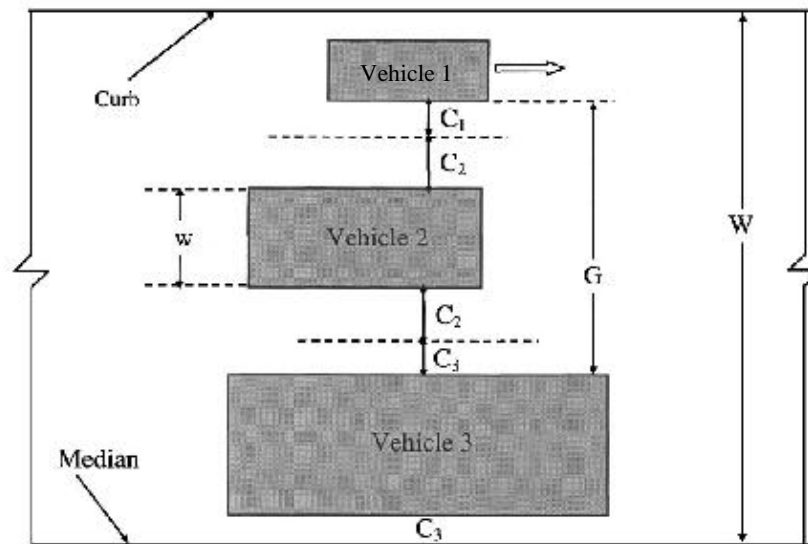


Fig. 2.1 Computation of transverse clearances for overtaking maneuver (Arasan and Koshy 2005)

Gunay (2007) has shown that speeds of the passing vehicles increase with increasing frictional clearance. He has also shown that increasing centre line separation reduces the time headway between the leader and follower. He had assumed that the speed of a vehicle was affected by the effective route width (ERW). In other words it can be said that the vehicle needs certain path width to maintain its speed and if the width is not available it has to slow down. He had also assumed that if frictional clearance (FC) between two vehicles was more than 1.5 m, the effect of the neighboring vehicle was negligible.

Mallikarjuna (2007) have analyzed the variation of average lateral gap with respect to the area occupancy. He has found that the fraction of majority vehicle type present in the traffic stream has significant influence on the gap maintaining behavior of vehicles. Minh et al. (2006) have observed linear relationship between the speed of passing motorcycle and the lateral gap.

Dey et al. (2008) have considered the lateral clearance to be one and half times the width of the passing vehicle. No field data analysis has been provided to

substantiate this assumption. Pal and Mallikarjuna (2010) have analyzed the lateral gap maintaining behavior and its effect on the traffic flows under heterogeneous traffic conditions. From the field gap maintaining behavior they observed that the vehicles were maintaining different gaps when travelling under different traffic conditions and this was also influenced by the lateral position of the subject vehicle. Luo et al. (2013) have observed a linear variation between lateral distance from the surrounding objects and the speed of the passing car. The surrounding objects were shoulder on left side and bicycle on the right side.

From the review it can be said that very few studies have collected the field data to substantiate their findings. Most of the past studies have considered only the speed of the subject vehicle in modeling the lateral gaps.

2.4 Cellular Automata Based Traffic Flow Model

Cellular Automata (CA) concept is used in the development of microscopic traffic flow model. Wolfram (1986) defined CA as the mathematical idealization of physical systems in which space and time are discrete, and physical quantities take on a finite set of discrete values. It expresses the traffic structure as a lattice of cells of equal size. The model contains a set of rules that decide the vehicle movement in the next time step.

CA models have been utilized in representing numerous traffic scenarios starting from rather simple ones such as illustration of highway traffic to more complex ones such as the simulation of lane reduction scenarios (Nassab et al. 2006) and the simulation of mixed traffic (Lan and chang 2003; Lan and Chang 2005; Mallikarjuna 2007). CA rules have also been used to simulate pedestrian (Blue and Adler 2001; Burstedde et al. 2001) and railway traffic (Li et al. 2005). In the following sub-sections a brief description on the evolution of CA model is presented.

2.4.1 Homogeneous traffic flow modeling using CA

Cremer and Ludwig (1986) proposed the first CA model for vehicular traffic. Later, Nagel and Schreckenberg (1992) proposed the CA model which is well known as NaSch model or NS model, to reproduce the basic features of traffic flows, wherein the space, speed, acceleration and time were treated as discrete variables. The state of the road at any time-step was derived from the state in the previous time-step by applying acceleration, braking, randomization and driving rules for all vehicles simultaneously.

The model was defined for a single road lane of L sites and with open or periodic boundary conditions, which may be either empty or occupied by a vehicle with a non-negative integer velocity in between 0 to V_{\max} . The model was developed and validated only for passenger car, and this model has got several computational advantages in modeling the complex systems. Since then number of modified NaSch models have been developed to model the real world traffic conditions. Although CA models are somewhat crude and also different in terms of their rules and dynamics when compared to kinematic wave and car-following models, their output is fairly similar to those models (Nagel 1995; Daganzo 2006).

Though the original NaSch model could able to mimic the real traffic conditions at macroscopic level, it could not reproduce some typical traffic characteristics such as jam propagation and time and space headways. To overcome these problems some modifications have been proposed to the updating procedure (Takayasu and Takayasu 1993; Benjamin et al. 1996; Schadschneider and Schreckenberg 1997; and Barlovic et al. 1998). In order to obtain a correct behavioral picture of stable jam, it is necessary that a vehicle's minimum time headway or reaction time should be smaller than its escape time from a jam, or equivalently, the outflow from a jam (i.e., the queue discharge rate) must be lower than its inflow (Maerivoet 2006). Therefore, a rule to make the vehicles wait a short while longer before accelerating from standstill position, which was known as 'slow-to-start' rule, was introduced. With some probability, the vehicles which were stopped in the prior time remain stationary in the next time step. The probability value was adjusted such that the delay in starting from the stationary position replicated the observed delays. Due to this delay, the out flow from the jam was less than the capacity flow. One of the prominent models that incorporate this feature is Velocity-dependent randomization (VDR) model proposed by Barlovic et al. (1998). This model included stochastic fluctuations as well as slow-to-start rule.

To replicate the synchronized flow (observed by Kerner and Rehborn 1996), Knospe et al. (2000) have proposed the three phase (free-flow, synchronized, and slow to start) traffic flow model (known as BL Model) using brake lights, in which car following behavior was dependent on brake light status (on/off) of the leading and following vehicles. The mathematical model proposed by Knospe et al. (2000) was quite complex compared to standard single-cell CA models. Braking probability, the

interaction time headway and security distance were the important parameters of the BL model.

To reproduce the synchronized flow, Kerner et al. (2002) proposed a parameter called synchronization distance based on which the following vehicle adjusts its speed. The update rules consisted of a deterministic and a stochastic part. In the deterministic part, the velocity value was first chosen between values 0, v_{\max} , v_{safe} , and v_{des} . The term v_{safe} was connected to collision-free driving, and the term v_{des} was the desired speed that was connected to acceleration (for large space headways normal acceleration was used, otherwise the speed of the following vehicle was adjusted to that of the leading vehicle).

Since single lane models do not represent the real traffic scenario, two lane CA models were developed (Rickert et al. 1996; Chowdhury et al. 1997; Wagner et al. 1997; Nagel et al. 1998; Knospe et al. 2000). Nagatani (1993) has first proposed the lane-changing concept in CA model for two-lane road. He has also introduced randomness in lane-changing behavior. Rickert et al. (1996) have developed a CA based traffic simulation model for two-lane road. They had explored the significance of stochastic elements with respect to real traffic. Lane-changing occurs due to several reasons on multilane roads, but the following prerequisites must be fulfilled before the commencement of lane-changing (Rickert et al. 1996; Nagel et al. 1998).

- ✓ there must be incentive for lane change
- ✓ legal constraints must be fulfilled
- ✓ security issues have to be fulfilled

Emmerich and Rank (1997) have tried to improve the CA model by modifying the updating rules including lane-changing. Chowdhury et al. (1997) have introduced asymmetric models with various lane-changing rules for different lanes.

Most of the above referred works were carried out for lane disciplined homogeneous traffic either for single lane road or for multilane road. Therefore, these models cannot be directly implemented for no-lane-disciplined heterogeneous traffic. A systematic vehicle updating procedure is essential in accordance with the dynamics of different types of vehicles plying on the road section, to replicate the no-lane-disciplined heterogeneous traffic.

2.4.2 Heterogeneous traffic flow modeling using CA

Several researchers have modified the original CA model to suit the needs of heterogeneous traffic (Lan and Chang 2005; Lan and Hsu 2006; Gundaliya 2005; Hsu et al. 2007; Mallikarjuna and Rao 2009; Lan et al. 2010; Lin et al. 2013; Luo et al. 2013; Yang et al. 2015). Lan and Chang (2005) have modeled the heterogeneous traffic composed of cars and motorcycles with the help of a refined cell structure. They employed basic CA updating rules to simulate the heterogeneous traffic. Based on the field observations they have reduced the cell size to 1.25 m x 1.25 m. Lan and Hsu (2006) have used a cell of 1.25 m x 1.25 m to explore the traffic stream moving on a two-lane road. Their model could generate free, synchronized, and wide moving jam conditions. Mathew et al. (2006) have used the concept of CA to simulate the heterogeneous traffic. Basic CA structure was modified using a cell of 0.9 m x 1.9 m to suit the heterogeneous traffic. They have also modified the lane changing rules to represent the heterogeneous traffic.

Hsu et al. (2007) have decided the cell size based on the physical dimensions of the vehicle and the required safe gaps. They have used a cell of 1.25 m x 1m and the width of the cell has been arrived at based on motorcycle width and its minimum clearance. Cells used to represent the vehicles include the lateral and longitudinal clearances. Lan et al. (2009) proposed a new revised CA model with piecewise-linear speed variation in place of conventional particle hopping, using the cell sizes proposed by Hsu et al. (2007). This model could overcome the unrealistic deceleration behavior associated to the conventional CA models. Mallikarjuna and Rao (2009) have used the cellular automata model for modeling heterogeneous traffic. Model developed by Kerner et al. (2002) has been modified to incorporate the heterogeneous behavior of traffic. They have considered five types of vehicles in their model. Their model was validated with the field observations at macroscopic level. Lan et al. (2010) have studied the erratic behavior of two wheelers. In addition to the conventional moving forward and lane-change rules, this model has also considered the lateral drift behavior for cars and motorcycles moving in the same lane. Possible motorcycle movements have been categorized into five classes. They have observed and modeled the transverse crossing behavior of motorcycles when stuck in traffic through the gap between two stationary cars on the same lane. Lin et al. (2013) have used CA model for

exploring traffic patterns and phase transitions. They have used the same concept of 'common unit' proposed by Hsu et al. (2007) to represent different vehicle dimensions.

The cell size decided in the above studies is based on the vehicle dimensions, gap requirement and their mechanical characteristics. No specific guideline is given for determining the cell size in most of the cases. If the cell size is taken to be small, the model accuracy for the physical representation is high. Very few studies have changed the updating rules as per the refined cell structure. Some of these studies are reviewed in the following sub-section.

2.4.2.1 Evolution of the updating procedure

Sara et al. (2010) have studied the effect of surrounding traffic characteristics on lane changing behavior. They have analyzed lane changing maneuvers' of 28 heavy vehicles and 28 passenger cars and found the vehicle specific lane changing behavior. The results suggest a substantial difference exists between the traffic characteristics influencing the lane changing behavior of heavy vehicle and passenger car drivers even under lane following heterogeneous traffic conditions. Heavy vehicles speed changes little during a lane changing maneuver. Heavy vehicle drivers mainly move into the slower lanes to prevent obstructing the fast moving vehicles which approach from the rear. However, passenger car drivers increase their speed according to the speeds of the lead and lag vehicles in the target lane. They move into the faster lanes to gain speed advantages. In no-lane-disciplined traffic vehicles are not forced to follow the lane markings hence a wide variety of lateral movements can be observed.

Mallikarjuna (2007) has developed a CA based heterogeneous traffic flow model using the cell size of 1.4 m x .5 m. Reduced cell width was used to capture the finer lateral movements observed in the heterogeneous traffic. According to this cell size, all the updating procedures have been modified. In this model a following vehicle can have more than one leading vehicle and the longitudinally closest vehicle was considered as the effective leading vehicle. He has also considered the effect of other vehicles in the vicinity on the movement of the subject vehicle.

Lan et al. (2010) have elucidated the lateral drift behavior of cars moving in the same lane. They introduced the lateral movement rule of cars in two ways such as lane change and lateral drifts. They have divided a two-lane road of 7.5 m into 6 sub-lanes,

as the cell size for this model was 1.25 m x 1.0 m. In lane change rule, a car may shift from one lane to another lane completely, but, in lateral drift, a car may shift sub-lane within the same lane. They have also assumed that a car would change lane only when it is located along the lane markings. A car located away from lane markings would take longer time to complete the lane change. They have also modeled the lateral drift behavior of motorcycles breaking into two moving cars, and the transverse crossing behavior for motorcycles through the gap between two stationary cars in the same lane. A motorcycle being stuck in traffic jams for a period of 3 sec, would take transverse crossing through the gap between the two queued vehicles.

Luo et al. (2013) have investigated the interaction between car and bicycle using CA concept. They have incorporated the variability of lateral gap maintaining behavior of car in vehicle updating steps. They have shown the impact of variable lateral gap on forward movement of car. Variable lateral gap maintaining behavior may also impact the lateral movement of car. This has not been addressed in their study because of the restriction on lateral movement of car. Therefore, this study need to be further investigated to check the effect of variable lateral gap on lateral movement, as well as on forward movement of different vehicle types. Moreover, interaction between motorized vehicles is needed to be further investigated. Most recently, Yang et al. (2015) have investigated car-truck following combination effect. They have observed that vehicle specific interactions are different. Interactions vary depending on the pair of vehicles in car-following.

Since several types of vehicles are plying on the roads in developing countries, a suitable model is required to understand their behavior in the traffic stream. From the review presented here it is evident that CA model can be a better alternative to model heterogeneous traffic considering its ability to model complex interactions.

From the above review it can be inferred that a comprehensive approach is lacking when modeling the heterogeneous traffic. Complexity in microscopic data collection, specifically when collecting gap related data, has been one of the major problems faced by the researchers working in this area. Hence, development of an appropriate traffic simulation model to replicate the no-lane-disciplined heterogeneous traffic stream, integrating the variable inter vehicular lateral gap maintaining behavior is essential.

2.5 Summary of the Literature Review

Traffic flow modeling requires thorough understanding of the actual traffic stream behavior and this understanding can be gained with the help of field observations. Due to lack of empirical observations such understanding of no-lane-disciplined heterogeneous traffic is almost absent. In this scenario, as shown in the literature review, homogeneous traffic flow models are being adopted for heterogeneous traffic conditions. Some researchers have attempted to incorporate few modifications considering the heterogeneous traffic conditions. Specifically, microscopic models, including car following and CA models have been adopted for modeling the heterogeneous traffic.

Recently, few researchers have made attempts to collect and understand the field data on heterogeneous traffic stream. It was found that field data collection itself is a complicated task and significant efforts are required in collecting and correcting the microscopic data. Image processing techniques were found to be useful in collecting the data but the extracted data were riddled with errors. This aspect needs to be addressed for getting a meaningful insight into the traffic stream behavior.

Many researchers have also proposed refinement of cell structure to appropriately represent the smaller vehicles and finer lateral movements observed in no-lane-disciplined heterogeneous traffic streams. Finer cell structure affects the updating procedures and the corresponding parameters, and this need to be thoroughly analyzed.

Data Collection and Analysis

This chapter deals with the microscopic traffic data extraction from the vehicle trajectory data. Details of the video data and the methodology used for extraction of trajectories are discussed in section 3.1. Systematic approaches to smooth the trajectories of vehicles moving in no-lane-disciplined heterogeneous traffic stream are explained in section 3.2. Smoothing of the trajectories using Complete Ensemble Empirical Mode Decomposition with Adaptive Noise (CEEMDAN) is also described in this section. Section 3.3 deals with the estimation of speeds using continuous wavelet transforms (CWT), discrete wavelet transforms (DWT), and numerical differentiation. Internal consistency analyses of the estimated positions and speeds using the basic equations of motion are also discussed in this section. Last section of this chapter summarizes the important conclusions drawn from the analysis.

3.1 Introduction

Traffic stream behavior and vehicular interactions within the traffic stream vary from place to place and section to section. The lateral gap between vehicles moving on two lane roads differ from that of the three lane roads or four lane roads. The driver behavior also differs significantly from one city to the other. The driver from a particular city may be aggressive, whereas, the driver from some other city may be well disciplined. Therefore, it is required to collect the traffic data from different locations and also from road sections of different geometry.

Trajectories of the vehicles are crucial for analyzing the traffic stream behavior. Many microscopic traffic data such as the instantaneous speed, acceleration, headway, lateral gap etc. can be extracted from the vehicle trajectories. Macroscopic data corresponding to a general measurement region can also be extracted using the trajectory data. Various methods are being used to collect the trajectory data, but, video based approaches are useful in detailed analysis of the traffic stream behavior. In this study, vehicular movement has been captured using the cameras focused over the mid block sections of divided multilane roads. Different urban locations of four major cities of India, namely, Delhi, Hyderabad, Bangalore and Kolkata have been considered in

this study. To observe the variability of driver behavior in congested as well as in free flow conditions, the traffic flow data have also been collected in peak and off peak hours. Details of the sites selected for data collection and stream composition corresponding to these locations are discussed in the following subsections.

3.1.1 Site selection

The following criteria were considered in selecting the site for data collection

- ✓ The road stretch under consideration should be straight for at least 50 to 100 m.
- ✓ The road stretch under consideration should not have any potholes or other defects that would affect the driving pattern of the driver.
- ✓ The road stretch should be free from gradients.
- ✓ Availability of suitable vantage point within the vicinity of the proposed data collection site.

Keeping the above criteria in mind, different arterials located in the urban areas of four major cities have been considered for data collection. Foot over bridges are available near all these sites for collecting the video. The video camera was located on the foot over bridge. The camera was positioned in the direction facing the center lane of the road section and incoming traffic. A section length of around sixty meter was covered from the foot over bridge.

3.1.2 Trajectory extraction using TRAZER

In this study, an offline image processing software, named TRAZER, was used to extract the trajectory data from the video films. TRAZER is capable of tracking vehicles even under highly congested traffic conditions. The specific advantage of this software is its ability to capture lateral movements, which is a typical feature of no-lane-disciplined traffic. This software can classify the vehicles in four categories, namely, light motor vehicle (LMV), motorized two wheeler (MTW), motorized three wheeler (MThW) and heavy motor vehicle (HMV). TRAZER collects the trajectory data over 10 to 30 m road length. TRAZER output consists of vehicle id, vehicle type, and its coordinates at all the time frames. From the trajectory data, several microscopic features such as lateral gaps, headways, instantaneous speeds etc. and macroscopic

traffic features such as classified traffic volume, average occupancy, and average speed data, can be collected. Mallikarjuna et al. (2009) have established that TRAZER gives high detection accuracies if the video camera is aligned with the centre line of the road and positioned at a certain altitude. They have reported that TRAZER can detect and identify about 85-90% of the vehicles and in this study also similar results were obtained. TRAZER allows manual intervention and this facilitates the addition of the trajectories corresponding to the unidentified vehicles. The methodology followed in extracting the trajectories using TRAZER is presented in the flow chart shown in Fig. 3.1.

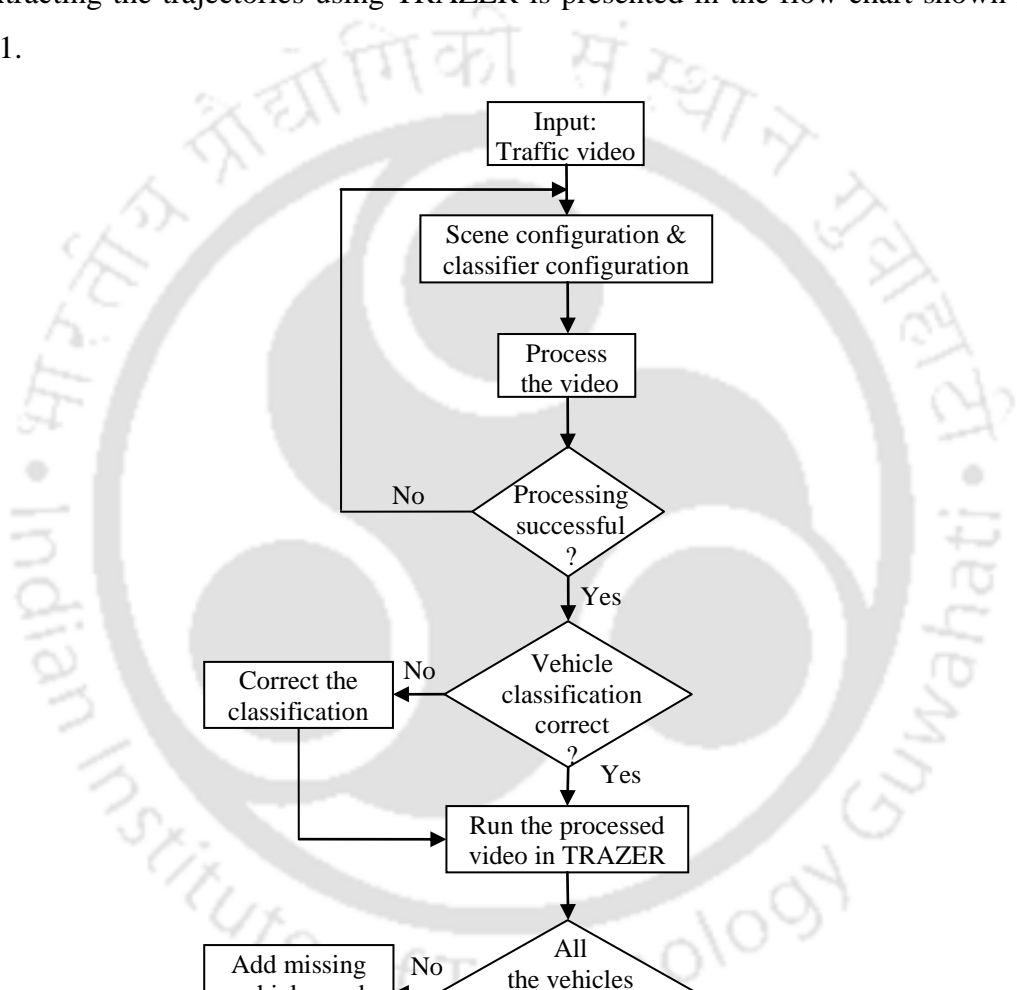


Fig. 3.1 Trajectory data extraction using TRAZER

3.1.3 Details of the traffic data

A total of twenty two hours video data have been collected and processed. Details, such as the road width and time of data collection, variation of hourly flow and vehicle compositions are given in Table 1.1. From the hourly composition it can be observed that LMVs and MTWs are the major constituents of the traffic streams, at all the locations.

Table 3.1 Road geometry and traffic characteristics observed at data collection sites

Location	Road Width (m)	Length of the video (hrs)	Time of data collection (Hrs to Hrs)	Variation of hourly flow (vehicles/hr)	Vehicle composition (%)			
					LMV	MTW	MThW	HMV
VIP Road, Kolkata	10.8	7	9:25 to 16:44	5228 to 2913	59	23	10	8
Salt lake, Kolkata	6.6	4	9:40 to 15:40	3019 to 2799	63	20	13	4
Maharani Bagh, Delhi	12.5	4	13:00 to 17:30	7897 to 6396	48	29	10	13
Kodihalli, Bangalore	8.3	3	11:00 to 14:00	4186 to 3952	34	49	13	4
Indira Nagar, Bangalore	12.0	2	10:50 to 12:50	3771 to 3726	41	47	8	4
Jubilee Hills, Hyderabad	10.0	2	14:42 to 16:42	4550 to 3621	46	43	10	1

3.1.4 Analysis of the raw trajectory extracted using TRAZER

Given the complex nature of vehicular movement in heterogeneous traffic stream, the extracted trajectory data may contain several errors. These errors might be resulting due to the limitations of the software in identifying and tracking the vehicles moving in no-lane-disciplined traffic stream. Lateral movements and closely following vehicles result in temporary partial occlusions. When a vehicle is partially occluded, the tracking ability of the software is reduced and the same position may be tracked over several time instances. These errors, in a way, hinder the applicability of video image processing methods under heterogeneous traffic conditions.

Trajectory of a sample vehicle (Vehicle id_36004) from Jubilee hills, Hyderabad, is shown in Fig. 3.2. It can be seen that, due to various reasons, the position of the vehicle has been tracked to be same in consecutive frames 50-51, 76-77, 82-83, 90-92 and 93-97. It can also be observed from frames 20-21, 32-33, 37-38 and 74-75 that there is a backward movement. At several time steps sudden lateral shifts have also

been observed in lateral positions. These types of problems are to be addressed and the data smoothing techniques can be used for this purpose.

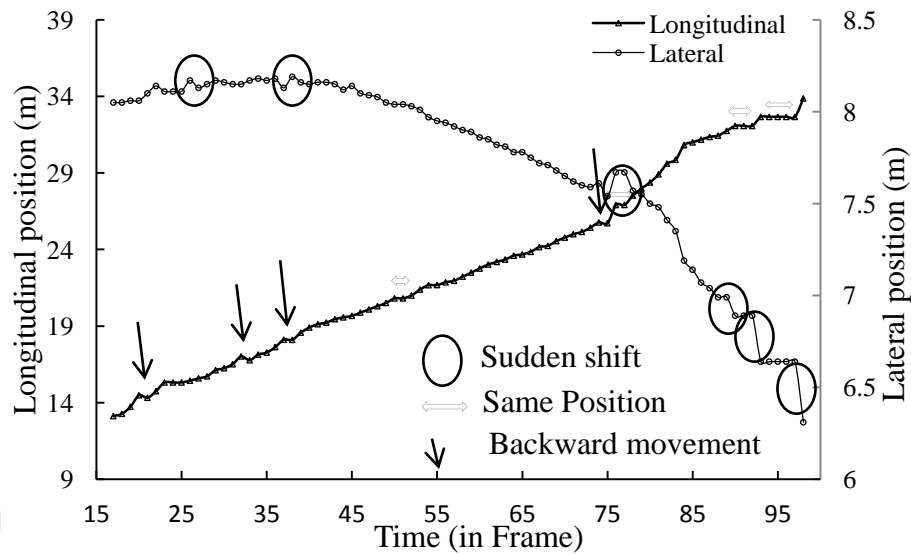


Fig. 3.2 Raw trajectory of Vehicle id_36004 extracted using TRAZER

Various smoothing methods have been suggested in literature (Section 2.5) and it was found that the existing methodologies have certain drawbacks. Considering this, CEEMDAN approach has been used in this study and details of the same are discussed in the following section.

3.2 EMD based Trajectory Smoothing

Yuan (2009) has proposed an Empirical Mode Decomposition (EMD) based trajectory smoothing technique and found that this approach is more convenient compared to the wavelet based techniques. But, this approach is unable to deal with the correction of the positions corresponding to the end points. Wu and Huang (2009) have observed that the mode mixing is a major drawback associated with the original EMD approach. To overcome this problem, they have proposed a noise assisted data analysis (NADA) method termed as Ensemble Empirical Mode Decomposition (EEMD). It performs the EMD over an ensemble of the signal plus white Gaussian noise. The addition of white Gaussian noise solves the mode mixing problem, but, the reconstructed signal includes residual noise and different realizations of signal plus noise may produce different number of modes (Torres et al. 2011). To avoid such problems, Torres et al. (2011) have proposed a Complete Ensemble Empirical Mode Decomposition with Adaptive Noise (CEEMDAN) to smooth the original signal. In this study CEEMDAN approach

has been applied to smooth the trajectories. The EMD and its Noise Assisted Versions are discussed in the following sub-sections.

3.2.1 Empirical Mode Decomposition (EMD) and its Noise Assisted Versions

Huang et al. (1998) have introduced Empirical Mode Decomposition (EMD) method to analyze the non-linear and non-stationary data. Using the EMD method, any complicated data set can be decomposed into a finite and often small number of components which consists of intrinsic mode functions (IMF) and one residue. Huang et al. (1998) have defined an oscillating wave as an IMF, if it satisfies the following criteria:

- ✓ The number of extrema (total number of maxima and minima, refer Fig. 3.3) and the number of zero-crossings must be equal or differ by one
- ✓ At any point, the mean value of the envelope defined by the local maxima and the local minima is zero.

The extracted IMFs, having different amplitudes and frequencies, are complete and adaptive, and reflect the local properties of the signal. Since the decomposition is based on the local characteristic time scale of the data, it can be applied to nonlinear and non-stationary processes. An arbitrary sinusoidal function is shown in Fig. 3.3. For better understanding of the IMF extraction process, various components of the curve (in Fig. 3.3(a)) are shown in Fig. 3.3(b).

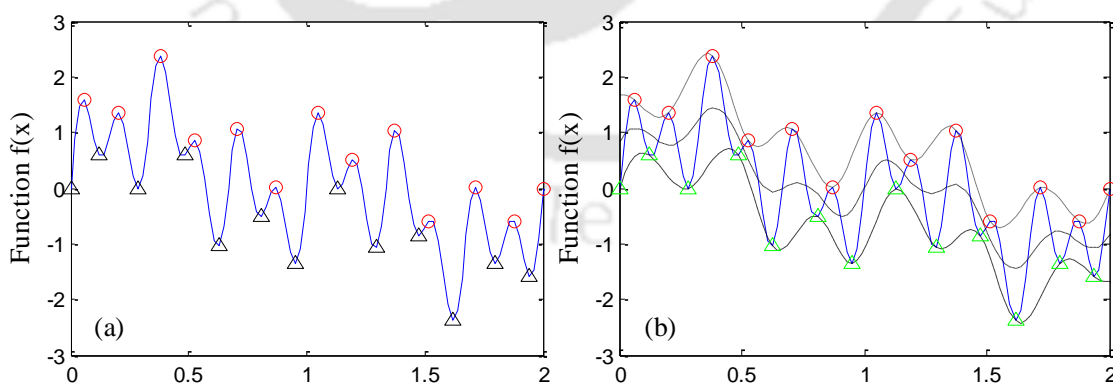


Fig. 3.3 Arbitrary sinusoidal function and IMF extraction process

Solid line in Fig 3.3(a) indicates the original signal $y(t)$, circles indicate local maxima and triangles indicate local minima in Fig. 3.3(a); Dotted line connecting circles and dashed line connecting triangles are upper and lower envelop respectively,

fitted using cubic splines and dash-dot line at middle of upper and lower envelop is the mean envelop in Fig. 3.3(b).

3.2.2 The EMD method

For any signal $y(t)$, the procedure involved in the extraction of IMFs (adopted from Mallikarjuna and Raghukanth 2009) is summarized below:

- (1) Identify the local maxima and minima of the original time series data, $y(t)$, and construct the lower and upper envelopes using cubic splines (Refer Fig. 3.3).
- (2) At every time step, determine the mean of the upper envelop (E^+) and lower envelop (E^-) as,

$$m_0(t) = (E^+(t) + E^-(t))/2 \quad (3.1)$$

- (3) Subtract the average, $m_0(t)$, which is the bias of the data about the zero level, from the original data to get,

$$y_1(t) = y(t) - m_0(t) \quad (3.2)$$

- (4) If the conditions of IMF are not meant by $y_1(t)$ after one iteration, then $y_1(t)$ is required to be sifted again. Hence, in the subsequent processing, $y_1(t)$ is treated as the original signal, the new time series is to be processed using the procedure discussed in steps 1 to 3.

$$y_2(t) = y_1(t) - m_1(t) \quad (3.3)$$

- (5) Repeat the process m times till the sieved data $y_m(t)$ is centered symmetrically such that with every zero only one peak or valley occurs. Now, $y_m(t)$ is the first intrinsic mode function and is denoted as IMF_1 .

- (6) If the remaining signal is still compound of the components with several frequencies, then the next IMF is obtained by taking the residue signal, $r_1(t)=y(t)-y_m(t)$, as a new signal, and repeat the sifting process (steps 1 to 5).

(7) Similarly, $IMF_3, IMF_4, \dots, IMF_n$, are computed until the remaining signal shows no oscillations, i.e., the residue $r_n(t)$ becomes monotonic and no further sifting is possible. Hence, finally with n IMF's, the signal can be expressed as,

$$y(t) = \sum_{i=1}^n IMF_i(t) + r_n(t) \quad (3.4)$$

The number of extrema decreases with hierarchical extraction of IMFs from the data. Thus, long-term trends, centerline drifts, and long-period non-stationary features come out as the residue.

3.2.3 The ensemble EMD method

Wu and Huang (2009) have observed that the mode mixing is the major drawback associated with the original EMD. Mode mixing is a consequence of signal intermittency, defined as either a single IMF consisting of signals with widely disparate scales, or a signal of a similar scale residing in different IMF components. To alleviate such problems, Wu and Huang (2009) have proposed a noise assisted data analysis (NADA) method, termed as the ensemble empirical mode decomposition (EEMD). In this method an ensemble mean is taken over a number of IMFs, extracted from multiple applications of EMD to the original signal each time with the addition of different white noise. The EEMD method is summarized as below.

(1) Different white noise $\omega_m(t)$, with the same amplitude, is added N times to an original signal $y(t)$ to generate N modified signals.

$$y_m(t) = y(t) + \omega_m(t); \quad m = 1, 2, \dots, N \quad (3.5)$$

(2) The EMD decomposition is performed on each modified signal $y_m(t)$. Each signal may be decomposed into n IMFs and one residue as a trend. Then, $y_m(t)$ can be rewritten as,

$$y_m(t) = \sum_{k=1}^n IMF_{mk}(t) + r_{mn}(t); \quad m = 1, 2, \dots, N \quad (3.6)$$

(3) To reduce the mode mixing, the EEMD method averages the result of the IMF set $\widehat{IMF}_k(t)$ and the trend $R(t)$ derived from EMD to produce the final result.

$$\widehat{IMF}_k(t) = \frac{1}{N} \sum_{m=1}^N IMF_{mk}(t) \quad k = 1, 2, \dots, n \quad (3.7)$$

$$R(t) = \frac{1}{N} \sum_{m=1}^N r_{mn}(t) \quad (3.8)$$

The addition of white Gaussian noise solves the mode mixing problem. However, the reconstructed signal includes residual noise and different realizations of signal plus noise may produce different number of modes and the process is also computationally expensive (Torres et al. 2011). To overcome such problems, Torres et al. (2011) have proposed a complete ensemble empirical mode decomposition with adaptive noise (CEEMDAN).

3.2.4 The CEEMDAN method

Let the operator $E_j(\cdot)$ is a function which produces the j^{th} IMF of a given signal obtained by EMD. Let $\omega_m(t)$ be the independent white Gaussian noise with zero mean and unit variance and ε_0 is a noise coefficient. The CEEMDAN method proposed by Torres et al. (2011) is briefly described below.

(1) Generate a collection of noise-added original signal

$$y_m(t) = y(t) + \varepsilon_0 \omega_m(t), m = 1, 2, \dots, N \quad (3.9)$$

(2) The average of the 1st IMF obtained through EMD, corresponding to each $y_m(t)$ gives the first CEEMDAN mode,

$$\overline{IMF}_1(t) = \frac{1}{N} \sum_{m=1}^N IMF_m(t) \quad (3.10)$$

Then the first residue is,

$$r_1(t) = y(t) - \overline{IMF}_1(t) \quad (3.11)$$

(3) Decompose the noise added residue $r_1(t) + \varepsilon_1 E_1(\omega_m(t))$ using EMD mode and define the second CEEMDAN mode as,

$$\overline{IMF}_2(t) = \frac{1}{N} \sum_{m=1}^N E_1(r_1(t) + \varepsilon_1 E_1(\omega_m(t))) \quad (3.12)$$

(4) For $k = 1, 2, \dots, K$ calculate the k^{th} residue:

$$r_k(t) = r_{k-1}(t) - \overline{IMF}_k(t) \quad (3.13)$$

(5) Extract the first mode of $r_k(t) + \varepsilon_k E_k(\omega_m(t))$ by EMD and compute their ensemble average to obtain the $(k + 1)^{th}$ CEEMDAN mode as:

$$\overline{IMF}_{k+1}(t) = \frac{1}{N} \sum_{m=1}^N E_1(r_k(t) + \varepsilon_k E_k(\omega_m(t))) \quad (3.14)$$

The process mentioned in points 4 to 5 continues until the obtained residue cannot be further decomposed using EMD, either because it satisfies IMF conditions or because it does not have more than two local extrema. For a total K number of modes, the final residue can be expressed as,

$$R(t) = y(t) - \sum_{k=1}^K \overline{IMF}_k(t) \quad (3.15)$$

Finally, the target signal can be expressed as,

$$y(t) = \sum_{k=1}^K \overline{IMF}_k(t) + R(t) \quad (3.16)$$

Equation (3.16) makes CEEMDAN a complete decomposition method (Torres et al., 2011). In Comparison with both EMD and EEMD, CEEMDAN not only solves the mode mixing problems, but also provides an exact reconstruction of the original signal. In this study, the trajectory data have been collected with an objective to extract the microscopic data such as the speeds, and lateral gaps maintained by the vehicles when travelling at different speeds. For this purpose, the collected trajectory is represented as two one-dimensional time series data, corresponding to lateral position, $y=y_1, y_2, y_3, \dots, y_n$ and longitudinal position, $x=x_1, x_2, x_3, \dots, x_n$. CEEMDAN has been applied on both the time series data (x, t) and (y, t) . The time series data (x, t) and (y, t) were decomposed into different IMFs and the residuals for both the data were

estimated separately. These residuals are nothing but the smoothed time series of lateral and longitudinal positions of the vehicle.

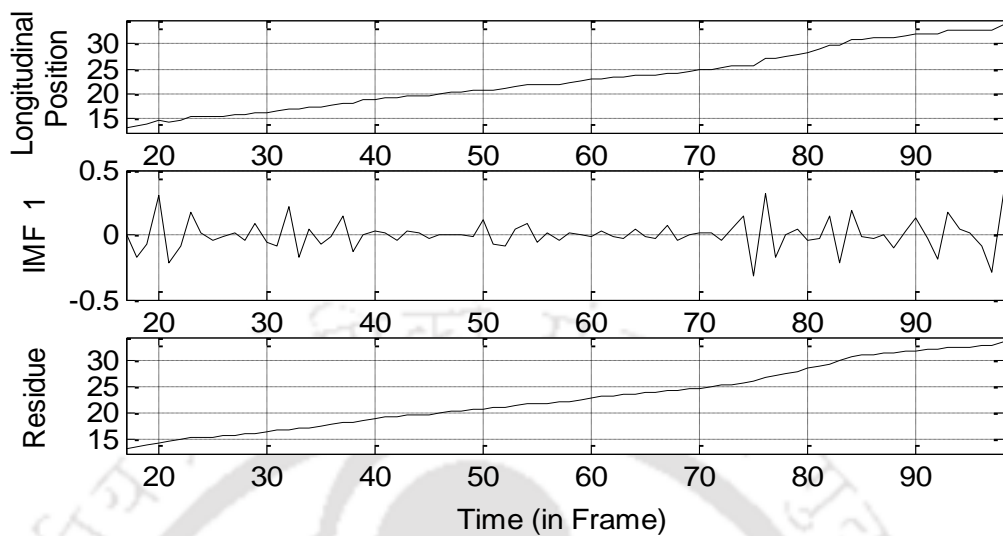


Fig. 3.4 CEEMDAN of longitudinal position (x, t) data of Vehicle id_36004

3.2.5 Trajectory data smoothing using CEEMDAN

The trajectory data shown in Fig. 3.2 have been smoothed using CEEMDAN, EEMD, EMD and locally weighted regression methods. In case of CEEMDAN, the decomposition of the trajectory data corresponding to (x, t) and (y, t) are shown in Figs. 3.4 and 3.5, respectively. It can be seen from Figs. 3.4 and 3.5 that the number of extrema decreases with the hierarchical extraction of IMFs from the original trajectory data. The long-term trends, centerline drifts, and long period non-stationary features come out as the residue; hence further decomposition is not possible.

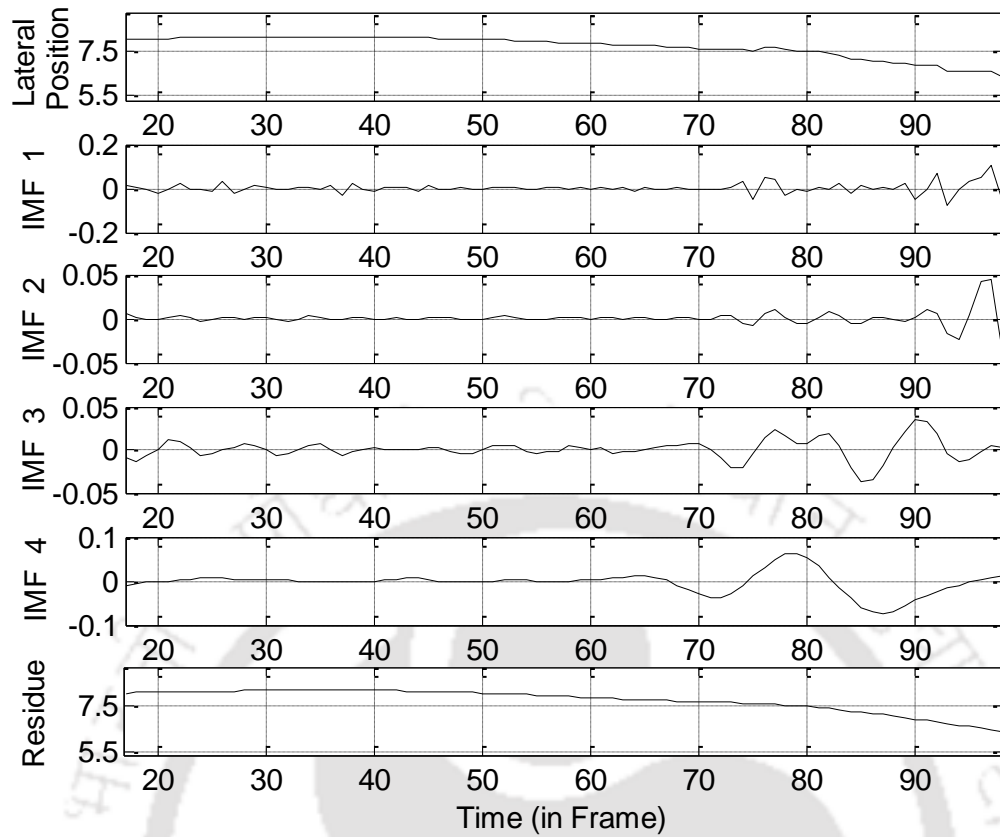


Fig. 3.5 IMF of lateral trajectory data obtained using CEEMDAN

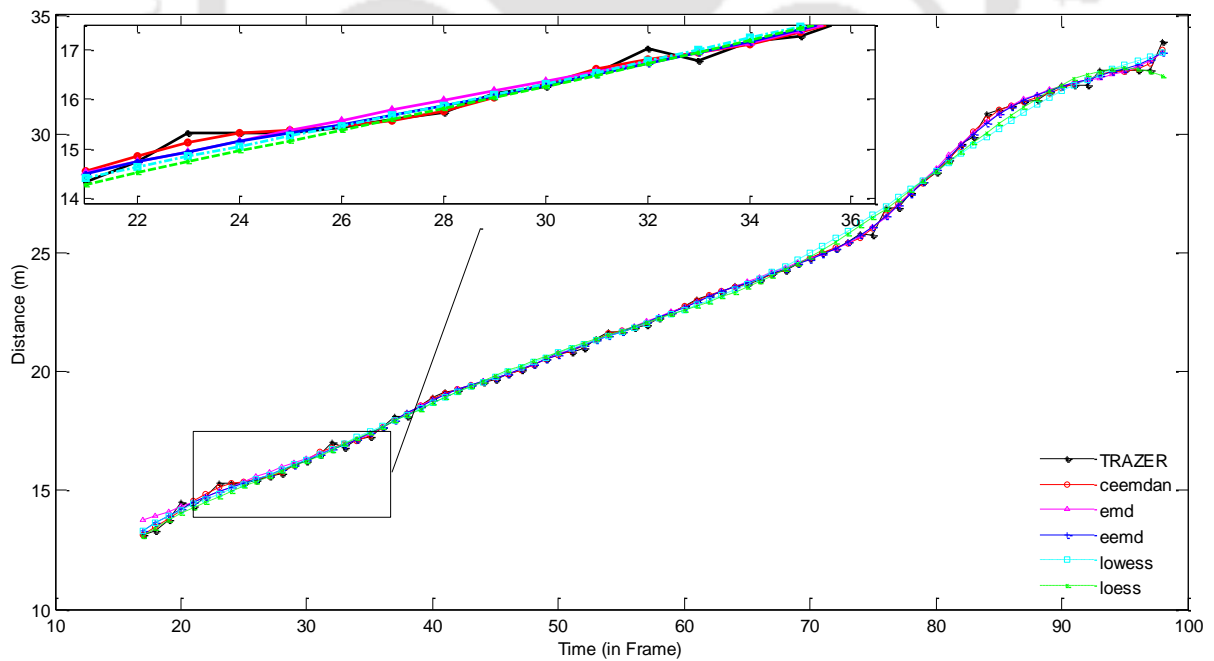


Fig. 3.6 Comparison of trajectories estimated using various methods with the observed trajectory

The residue gives the smoothed trajectory (CEEMDAN in Fig. 3.6). The trajectory has also been smoothed using EEMD and EMD, and the corresponding outputs are shown in Fig. 3.6. Smoothing has also been carried out using the local regression (lowess and loess in Fig. 3.6) method (Toledo et al. 2007; Mallikarjuna et al. 2009).

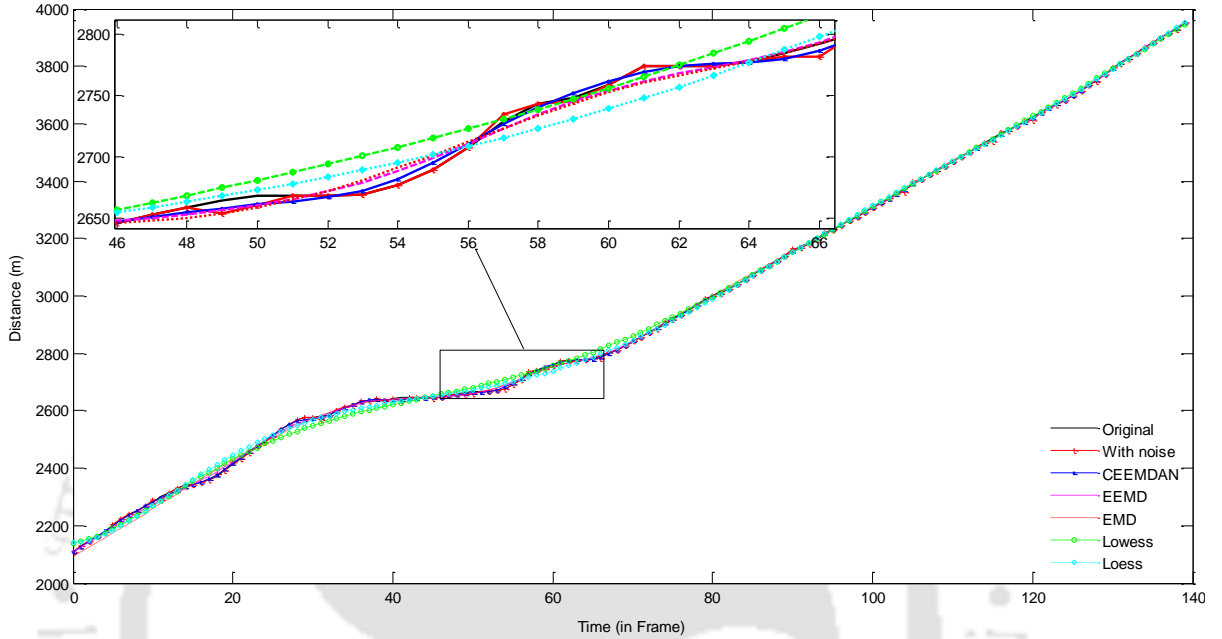


Fig. 3.7 Comparison of smoothed trajectories obtained using various methods

Most of the trajectories extracted using TRAZER are short in length. To further ascertain the suitability of various smoothing techniques a long trajectory obtained from a simulation model has been considered. This hypothetical trajectory was free of any error. Before smoothing this trajectory, white Gaussian noise has been added randomly to make it flawed. The flawed trajectory has been smoothed using various methods, and the outcomes are shown in Fig. 3.7. The result shown in the figure indicates that CEEMDAN, EEMD and EMD can smooth the trajectory efficiently. The differences between the original and the estimated trajectories were quantified using the mean absolute error (MAE) and root mean squared error (RMSE) statistics.

$$MAE = \frac{1}{n} \sum_{i=1}^n |\hat{x}_i - x_i| \quad (3.17)$$

$$RMSE = \sqrt{\frac{1}{n} \sum_{i=1}^n (\hat{x}_i - x_i)^2} \quad (3.18)$$

Where, x_i and \hat{x}_i are the observed and estimated positions for observation i , and, n is the number of observations. The statistical measures corresponding to a trajectory (shown in Fig. 3.2) are shown in Fig. 3.8a. The statistical measures corresponding to the hypothetical trajectory are shown in Fig. 3.8b. From these figures it can be seen that CEEMDAN approach is yielding better results compared to the other approaches. The observed and estimated paths of the vehicle (corresponding to Fig. 3.2) are shown in Fig. 3.9.

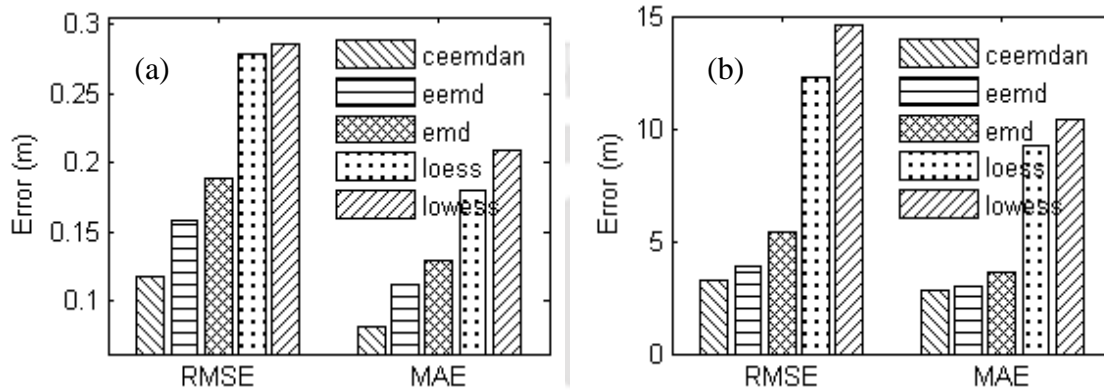


Fig. 3.8 Statistical measures of trajectory corrections for Vehicle id_36004 (a); and arbitrary trajectory(b) by various methods.

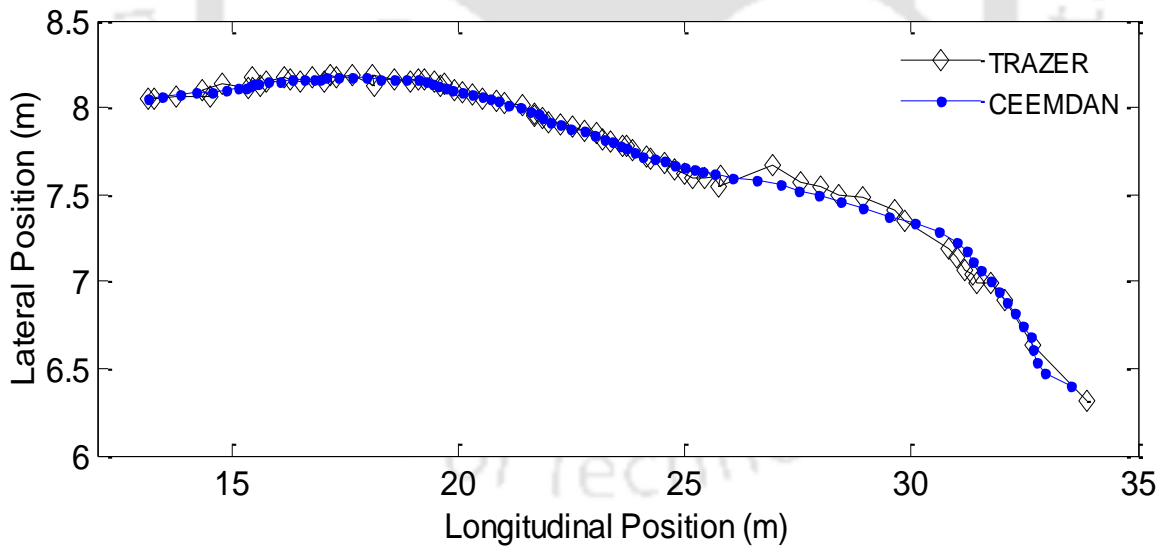


Fig. 3.9 Observed and estimated paths of the vehicle corresponding to Fig. 3.2.

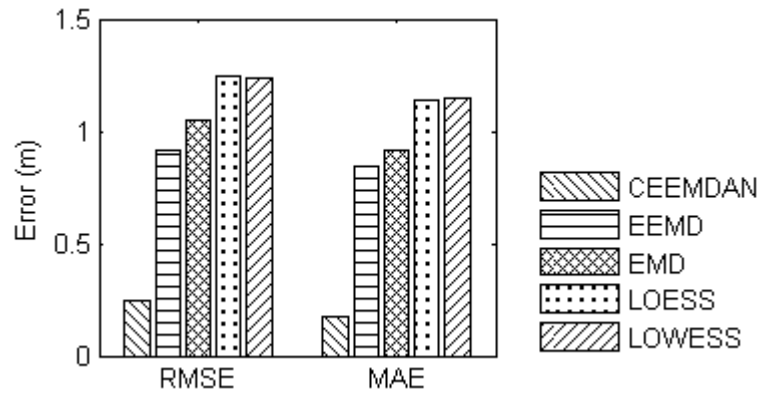


Fig. 3.10 Average RMSE and MAE of the trajectories

The averages of RMSE and MAE for all the vehicle trajectories corresponding to the Jubilee hills road, Hyderabad, are shown in Fig. 3.10. It is evident from the figure that the performance of CEEMDAN technique is better compared to the other techniques. Observed and smoothed (using CEEMDAN) trajectories of vehicles corresponding to the Indiranagar road, Bangalore are shown in Fig. 3.11.

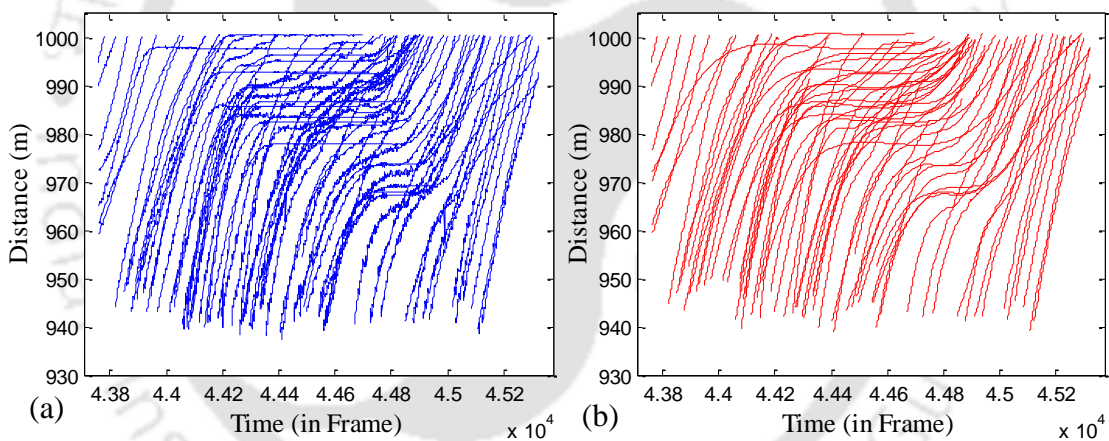


Fig. 3.11 Original (a) and smoothed (b) trajectories of vehicles

3.3 Speed Estimation

The instantaneous speed of the vehicle can be estimated by taking the first derivatives of the smoothed trajectory. The simplest method of derivative calculation is the numerical differentiation. In case of high frequency data, numerical differentiation results in erroneous derivatives (Haswell 1992). To improve the signal-to-noise ratio (SNR) of higher order derivatives, noise reduction is usually performed between the successive derivatives (Antonov and Stoyanov 1996). To handle the data with low SNR, wavelet transforms (Mallat 2008 and Messina 2004), including continuous wavelet transforms (CWTs) and discrete wavelet transforms (DWTs), have been used.

WT, with commonly used wavelet functions, can be regarded as a smoothing and a differentiation process. The order of differentiation is determined by the property of the wavelet function. The calculation of n^{th} order derivative can be achieved by only one transform procedure (Shao et al. 2000). In this study, first derivative of Gaussian function has been used as the wavelet function for CWT and ‘spline’ wavelet function has been used for DWT, to estimate the speed from the smoothed trajectory. Application of WT in derivative calculation is presented in the following sections.

3.3.1 Wavelet Transforms

WT is a useful tool for frequency analysis, with an ability to perform local analysis. It can be used to analyze the time series data that contain non-stationary power at many different frequencies (Daubechies 1990). The wavelet function φ must satisfy the following conditions (Mallat and Hwang 1992):

$$E = \int_{-\infty}^{+\infty} |\varphi(t)|^2 dt < \infty \quad (3.19)$$

$$C_{\varphi} = 2\pi \int_{-\infty}^{+\infty} \frac{|\xi(\omega)|^2}{|\omega|} d\omega < \infty \quad (3.20)$$

Where, E implies the finite energy of the function φ ; ξ is the Fourier transform of φ . C_{φ} , is the admissibility condition which implies that the mean of the function, φ , must be equal to zero. Then the function φ is said to be a mother wavelet or basic wavelet or wavelet function. Mallat (2008) and Messina (2004) have defined the wavelet transform of a real signal $\lambda(t)$ with respect to the wavelet function $\varphi(t)$ as follows,

$$W\{\lambda(v, \rho)\} = \langle \lambda, \varphi_{v,\rho}(t) \rangle = \frac{1}{\sqrt{v}} \int_{-\infty}^{+\infty} \lambda(t) \varphi' \left(\frac{t - \rho}{v} \right) dt, v \neq 0, v, \rho \in R \quad (3.21)$$

Where, v is a scale parameter, used to control the dilation, and ρ is called translation or shift parameter, used to control the translation. φ' denotes the complex conjugate of φ used in case of complex wavelet. The signal energy is normalized at every scale by dividing the wavelet coefficients by \sqrt{v} . The function $\varphi_{v,\rho}(t)$ is derived

from the mother wavelet φ , rescaling by ν and shifting by ρ (Grossmann and Morlet, 1984).

$$\varphi_{\nu,\rho}(t) = \frac{1}{\sqrt{|\nu|}} \varphi\left(\frac{t-\rho}{\nu}\right) \quad (3.22)$$

When the values taken by ν and ρ are continuous, it is called continuous wavelet transform (CWT), and when they are discrete, it is called discrete wavelet transform (DWT). The reproduction property of CWT shows that it is enormously redundant, i.e., the signal is unfolded from one variable t to two variables ν and ρ . Thus, all the information is already contained in a small subset of the $\lambda(\rho, \nu)$ and the result of DWT is much smaller subset of $\lambda(\rho, \nu)$ (Barache et al. 1997). When the function $\varphi(t)$ satisfies the admissibility conditions, as mentioned in equation (3.20), the original signal $\lambda(t)$ can be obtained from the wavelet transform $W\{\lambda(\nu,\rho)\}$ by using the inverse continuous wavelet transform mentioned in the following equation (Mallat 2008);

$$\lambda(t) = \frac{1}{C_\varphi} \int_{-\infty}^{+\infty} \int_{-\infty}^{+\infty} W\{\lambda(\nu,\rho)\} \varphi_{\nu,\rho}(t) d\nu \frac{d\rho}{\nu^2} \quad (3.23)$$

A wavelet function $\varphi(t)$, defined by the m^{th} order derivative of a smoothing function $\theta(t)$ with m vanishing moments, can be written as (Mallat 2008);

$$\varphi(t) = (-1)^m \frac{d^m \theta(t)}{dt^m} \quad (3.24)$$

Where, $\theta(t)$ is fast decaying and a nonzero constant integral as (Mallat 2008 and Messina 2004) shown below

$$\int_{-\infty}^{+\infty} \theta(t) dt = \gamma(\omega)_{\omega=0} = K \neq 0, \quad (3.25)$$

$\gamma(\omega)$ is the Fourier transform of $\theta(t)$. Equation (3.25) establishes that $\varphi(t)$ has no more than m vanishing moments. The CWT, $W\{\lambda(\nu,\rho)\}$ is just the derivative of the signal $\lambda(t)$ smoothed by a weighted average kernel $\theta_s(t)$ which corresponds to the smoothing function $\theta(t)$, dilated using ν , weighed with $\frac{1}{\sqrt{|\nu|}}$ and turned over through $-t$ (Mallat 2008; Messina 2004; Jianwen et al. 2006). As a result, the CWT with the

given wavelet function $\varphi(t)$ has the combined properties of data smoothing and differentiation. Mallat (2008) and Messina (2004) have verified that,

$$\lim_{\nu \rightarrow 0} \frac{W\{\lambda(\nu, \rho)\}}{\nu^{m+1/2}} = K_m \frac{d^m \lambda(t)}{dt^m} \quad (3.26)$$

According to equation (3.26), $\frac{W\{\lambda(\nu, \rho)\}}{K_m \nu^{m+1/2}}$ is used to approximate the derivative.

Messina (2004) has shown that the generating function $\theta(t)$ of the m^{th} Gaussian wavelet behaves as a linear low-pass filter. The wavelet transform as shown in equation (3.21) behaves as a low-pass differentiator filter with the dilation parameter as the cutting frequency (Messina 2004). A small change in dilation leads to high noise sensitivity, while a large value of the dilation is related to a large averaging domain and hence results in strong noise cancellation (Jianwen et al. 2006). The DWT can be also used to calculate the derivatives (Leung et al. 1998; Bruce and Li 2001). Shao and Ma (2003) and Messina (2004) have observed that CWT as well as DWT showed similar characteristics with a given wavelet.

Similar to CWT, the DWT based method uses $\frac{DW\{\lambda(\nu, \rho)\}}{K_m 2^{n(m+1/2)}}$ to approximate the derivative. $DW\{\lambda(\nu, \rho)\}$ is the DWT, i.e., wavelet coefficients or information in the multi resolution signal decomposition (Mallat 2008) of $\lambda(t)$ at the signal decomposition level of n , and the dilation parameter 2^n . Therefore, the m^{th} order derivative calculation of an analytical signal can be obtained through one wavelet transform by using a wavelet function with m vanishing moments. For example, the first and second derivatives can be calculated with Daubechies wavelets db1 and db2, having one and two vanishing moments, respectively (Shao and Ma 2003). A problem that encountered in the WT calculation is the boundary effects. In this study, this is eliminated with the method of symmetric extension (Leung et al. 1998; Chau et al. 1996; Shao and Ma 2003).

3.3.2 Extraction of speed from the smoothed trajectory

CWT, as well as DWT techniques have been applied on smoothed trajectory data to estimate the instantaneous speed. CWT with Gaussian1 wavelet function has been used to estimate the instantaneous speed of the vehicle Wavelet toolbox in MATLAB 2014a was used for this purpose. In case of CWT, the speed of the vehicle was estimated with

different dilation parameters 2, 4, 8, ...up to 32. The dilation parameter has been optimized based on the RMSE of speed consistency. The basic equation of motion is shown below;

$$v_n(t + 1) = v_n(t) + a_n(t) \quad (3.27)$$

The terms $v_n(t)$ and $a_n(t)$ indicates the speed and acceleration estimated for vehicle n at time t . $v_n(t + 1)$ is the speed estimated at time $t + 1$ (next time step) using WT. Difference between the estimated speed at time $t + 1$ and speed resulting from the right-hand side of basic equation of motion is considered as the speed consistency error for calculating the RMSE. The variation of the RMSE for speed consistency with respect to the dilation parameter is shown in Fig. 3.12(a). As can be seen in the figure, the RMSE is decreasing with the increasing dilation parameter and after certain value, there is a marginal change in RMSE. Hence, the ‘gaussian1’ wavelet function with dilataion parameter 16 was chosen for estimating the speed.

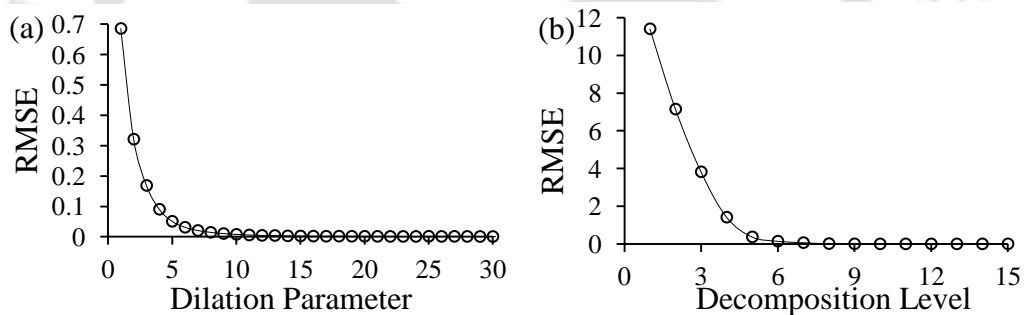


Fig. 3.12 Variation of RMSE with dilation parameter (a), and decomposition level (b)

In case of DWT, speeds have been estimated using spline wavelet function for decomposition level 1,2,3,.. up to 15. Fig. 3.12 (b) shows the variation in RMSE w.r.t. decomposition level and it can be observed that after certain decomposition level (8 in this case) there is only a marginal change in the RMSE. Hence, the speeds have been estimated using ‘spline’ wavelet function with a decomposition level of 8. The speed estimated by numerical differentiation of raw trajectory and speeds from the numerical differentiation of the smoothed trajectory are shown in Fig. 3.13. The difference in estimated and observed speeds are due to numerous errors in raw trajectory data and the error (noise) is magnified due to the differentiation of high frequency data. Speed data estimated using CWT and DWT and using the local regression (Mallikarjuna et al. 2009) are shown in Fig. 3.13. To check the applicability of WT, internal consistency of the trajectory has been verified.

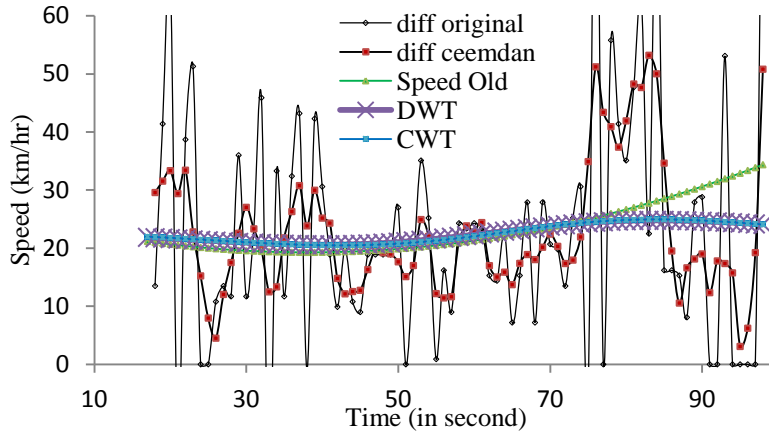


Fig. 3.13 Speed profiles obtained using various techniques

3.3.3 Internal consistency

Toledo et al. (2007) have introduced the internal consistency analysis of positions, speeds and accelerations, estimated from the smoothed trajectory data, using the basic equations of motion as shown below.

$$x_n(t + 1) = x_n(t) + v_n(t) \quad (3.28)$$

$$v_n(t + 1) = v_n(t) + a_n(t) \quad (3.29)$$

The terms $x_n(t)$ and $x_n(t + 1)$ indicates the estimated positions for vehicle n, at time t and t+1 respectively. Consistency error in position is the difference between the present position of the vehicle and the position estimated using the position and the speed of previous time step. If there is any error in estimating the position or speed by various smoothing techniques, then the position of the vehicle in current time step will not be same. Hence, this measure gives an idea about the accuracy of the proposed method. Difference between the estimated position at time t+1 and position resulting from the right-hand side of basic equation of motion (equation 3.28) is considered as the position consistency error. The RMSE and MAE of the consistency errors for the vehicle position with respect to its speed, and vehicle speed with respect to its acceleration are shown in Fig. 3.14. The result indicates that CWT and DWT methods of speed estimation have resulted in relatively low consistency error.

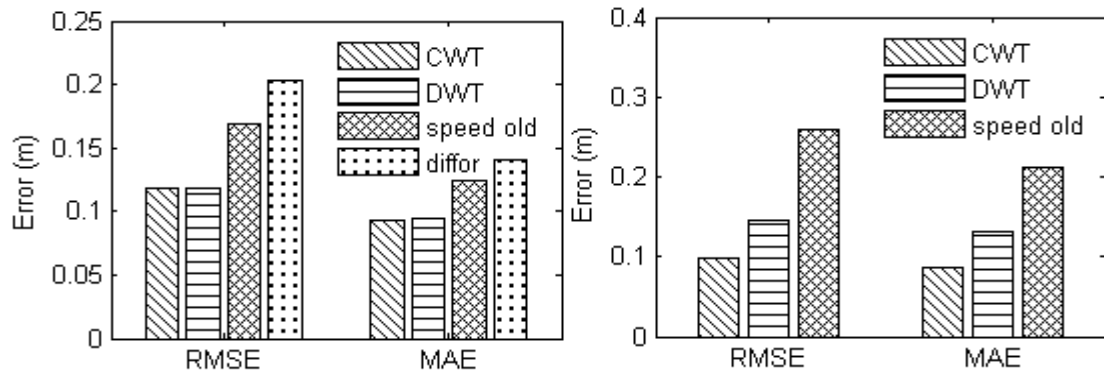


Fig. 3.14 Error measures of the consistency of position(a); and speed (b) estimated using various methods

3.4 Summary and Conclusions

In this study TRAZER has been used to get the vehicular trajectories, ranging from 10 to 30 m. These trajectories were found to have many errors, and need to be smoothed. Commonly used smoothing approaches, such as the local regression methods, were found to be inappropriate for smoothing these trajectories. In this study, a methodology based on complete ensemble empirical mode decomposition with adaptive noise (CEEMDAN) is proposed to smooth the trajectory data. From the error analysis it has been found that the proposed approach is relatively better in smoothing the trajectory. The smoothed trajectory data is further differentiated using wavelet transforms to estimate the instantaneous speed of the vehicle. Relatively more accurate speeds have been estimated by the application of wavelet transforms. Internal consistency analysis of the position and speed also supports the suitability of proposed method for speed correction.



Modeling of Lateral Gap Maintaining Behavior of Vehicles

Analysis and modeling of vehicular lateral gap maintaining behavior under no-lane-disciplined heterogeneous traffic conditions are discussed in this chapter. An inherent characteristic of the vehicle moving in no-lane-disciplined heterogeneous traffic stream is the variability of its lateral gap with the adjacent vehicles. Vehicles in heterogeneous traffic stream with no-lane-disciplined can move anywhere on the available road space and their movement is not only influenced by the characteristics of the leading vehicle but also by the presence of the adjacent vehicles. In such scenario lateral gaps maintained by the vehicles play an important role in the vehicular movement. An overview of such behavior of vehicles is presented in section 4.1. Field data analyses, illustrated in section 4.2, show a wide variation in the total lateral gap, even for a specific combination of passing/overtaking and the corresponding adjacent vehicles. Logistic regression analysis approach is proposed to model the total lateral gaps and the details are provided in section 4.3. Section 4.4 deals with the application of the proposed regression technique to model the total lateral gap data. Analyses of the results are described in section 4.5. The last section of this chapter summarizes the important conclusions drawn from lateral gap analysis and modeling.

4.1 Introduction

Presence of smaller vehicle on traffic stream makes it impractical to enforce the lane discipline. Absent of lane enforcement and the presence of smaller vehicles lead to the variable lateral gap maintaining behavior. In this context the vehicle has the liberty to occupy the free space available on the road depending on its requirement, and the surrounding traffic. Lateral gaps maintained by the vehicles depend on many factors. Fig. 4.1 shows two scenarios, where a MTW maintaining two different total lateral gaps. But it is not exactly clear how the vehicles maintain gaps and what are the factors influencing this behavior. At the same time it is clearly evident that the lateral gap maintaining behavior of vehicles is one of the crucial parameters in developing heterogeneous traffic flow model, and needs to be analyzed.



Fig. 4.1 Variable lateral gap maintained by MTW at two different scenarios

Many researchers have stressed the need to consider the adjacent moving vehicles in modeling the vehicular movement under heterogeneous traffic conditions (Singh 1999; Chakroborty et al. 2004; Gunay 2007; Arasan and Koshy 2005; Mallikarjuna 2007; Dey et al. 2008). Though many have emphasized this requirement, very few attempts were made towards understanding this behavior. Singh (1999) has collected minimum and maximum lateral clearances for different overtaking and overtaken vehicle groups. He has proposed multiple relationships based on speed of overtaking and overtaken vehicle and their lateral clearances. He has also emphasizes on the type of overtaking and overtaken vehicles.

Gunay (2007) has observed that with increasing frictional clearance, speeds of the passing vehicles have increased. The speed of a vehicle moving forward is affected by the effective route width available ahead. In other words it can be said that the vehicle needs certain road width to maintain its speed and if this width is not available it has to slow down. Minh et al. (2006) have observed a linear relationship between passed motorcycle speed and lateral gap. Luo et al. (2013) have observed a linear variation between lateral distance from the surrounding objects and the speed of the passing car. The surrounding objects were shoulder on left side and bicycle on the right side. This study was limited to the lateral interaction of car and bicycle only.

Most of the above referred studies (except Gunay 2007; Minh et al. 2006; Luo et al. 2013) have not clearly differentiated the passing vehicle and the vehicle being passed while modeling the lateral gap maintaining behavior. It can be said that the vehicles which are passing the other vehicles maintain the lateral gaps but not the vice-versa. Many of these studies have emphasized that the lateral gaps maintained by a

vehicle moving in the heterogeneous traffic stream is influenced by several factors but most of these studies have modeled the gaps in terms of the subject vehicle speed.

On wider roads it can be assumed that the movement of passing/overtaking vehicle is influenced by the vehicles moving on either side, and the corresponding lateral gaps are interdependent. Hence, instead of considering the lateral gaps maintained on either side separately it is proposed to study the total lateral gap, which is the summation of both the lateral gaps. Lateral gaps maintained with stationary road features such as the median and kerb have also been considered in this study.

4.2 Data Collection

Traffic data collection methodology has already been explained in chapter 3. Ten hours of video data collected from four different urban road sections (such as, Maharani Bagh, Delhi; Kodihalli, Bangalore; Indira Nagar, Bangalore; Jubilee Hills, Hyderabad) have been utilized to understand the lateral gap maintaining behavior of vehicles. The traffic compositions and road geometry corresponding to these locations are shown in Table 3.1 of chapter 3.

At all the locations about 80% of MTWs and LMVs have been observed. Keeping this in view, in this study lateral gap data have been analyzed mainly for LMV and MTW. Wherever sufficient data were available, lateral gaps have been analyzed for other vehicles also.

Smoothed trajectory data, obtained after application of proposed technique discussed in chapter 3 have been used to identify the left and the right neighboring vehicles of every passing/overtaking vehicle. Passing and overtaking vehicles were identified based on the difference in the speeds of the side-by-side moving vehicles. This has been carried out separately for all the four types of vehicles observed in the traffic stream. Detailed methodology adopted in identifying passing/overtaking vehicles is discussed in the following subsection.

4.2.1 Identification of passing/overtaking vehicles

Fig. 4.2 represents a hypothetical traffic stream and is used in identifying the passing/overtaking vehicles and getting the data on respective total lateral gaps. Five vehicles moving on a road section, at a particular time instance, are shown in this figure.

V_1, V_2, \dots, V_5 are the speeds of the corresponding vehicles and L_1, L_2, \dots, L_7 are the lateral gaps maintained by these vehicles with respect to either the moving adjacent vehicles or with the kerb or median. It was assumed that the speed of vehicle 1 is more than the speed of vehicles 2 and 3, and speed of vehicle 4 is more than the speed of vehicle 5. Hence, vehicles 1 and 4 are considered to be the passing/overtaking vehicles. Total lateral gaps corresponding to these five vehicles are $L_1^T = L_2 + L_3$, $L_2^T = L_3 + L_4$, $L_3^T = L_1 + L_2$, $L_4^T = L_5 + L_6$, $L_5^T = L_6 + L_7$, respectively.

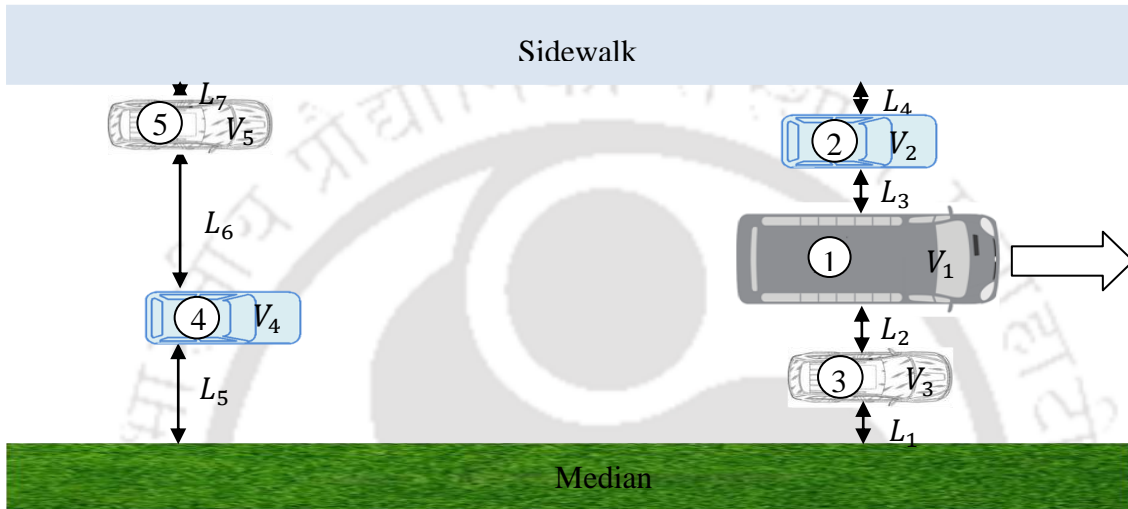


Fig. 4.2 Hypothetical no-lane-disciplined traffic stream with passing/overtaking vehicles and the representation of total lateral gap

It was assumed that the passing/overtaking vehicle can maintain the lateral gap as per its requirement because the driver of this vehicle decides how much lateral gap is to be maintained with respect to the adjacent slow moving vehicles or the median/kerb. Hence, in Fig. 4.2, out of the three data corresponding to vehicles 1, 2 and 3, only the total lateral gap data of vehicle 1 (L_1^T) can be considered for further analysis. Similarly, from vehicles 4 and 5 only total lateral gap data of vehicle 4 (L_4^T) can be considered for analysis. Once the total lateral gaps are extracted, these values are compared with the corresponding total lateral gap threshold values. The reason is that the impact of adjacent vehicles can be neglected when the total lateral gap is found to be beyond certain threshold gap. Hence, if the total lateral gap maintained by vehicle 4 (L_4^T) is larger than the threshold total lateral gap, such data are not considered in further modeling. Therefore, it can be seen that out of five data on total lateral gaps, only one data (L_1^T) is suitable for total lateral gap modeling. Even though vehicles 2, 3, and 5 are maintaining certain lateral gaps while passing the kerb or median, these data are not

considered in further analysis since the present study is dealing with the total lateral gap and not the lateral gap on one side. Table 4.1 shows the total number of passing/overtaking vehicle combinations observed at different data collection sites.

Table 4.1 Number of observations on total lateral gap data

Location	Number of observations on total lateral gap				Number of observations considered in modeling			
	LMV	MTW	MThW	HMV	LMV	MTW	MThW	HMV
Maharani Bagh, Delhi (1 st three hrs)	5293	1647	662	273	191	163	126	74
Kodihalli, Bangalore	885	595	172	90	171	130	--	--
Indira Nagar, Bangalore	458	448	84	25	98	123	--	--
Jubilee Hills, Hyderabad	846	825	176	35	226	227	82	--

4.2.2 Field observations on total lateral gaps

After identifying the passing/overtaking vehicles and the corresponding adjacent vehicles, lateral gaps on either side of these vehicles have been extracted. Total lateral gap maintained by a passing/overtaking vehicle is the summation of the lateral gaps maintained on either side. Fig. 4.3 shows the plot between the observed total lateral gaps and the speed of the passing/overtaking vehicle, corresponding to the data collected from Maharani Bagh, Delhi. From the figure it can be seen that the total lateral gap vary significantly with respect to the speed of the subject vehicle (passing/overtaking vehicle). It can also be observed that the total lateral gap is not constant for a specific speed range of the subject vehicle. There is a significant variation in the total lateral gap data corresponding to a specific speed range. Similar behavior has also been observed in the data corresponding to the other road sections.

4.3 Analysis of the Variations in the Total Lateral Gap

Vehicles moving in lane disciplined traffic stream tend to move on the middle of the lane and the influence of the vehicle moving on a particular lane is negligible on the vehicle moving on the neighboring lane, even during passing/overtaking maneuvers. Lateral gaps between two vehicles moving on adjacent lanes are adequate to maintain their respective speeds and can be assumed that there is no lateral interaction. Total

lateral gap corresponding to this scenario is about 3.5 m (for car) and based on the above discussion the total lateral gaps exceeding this value were excluded from further analysis.

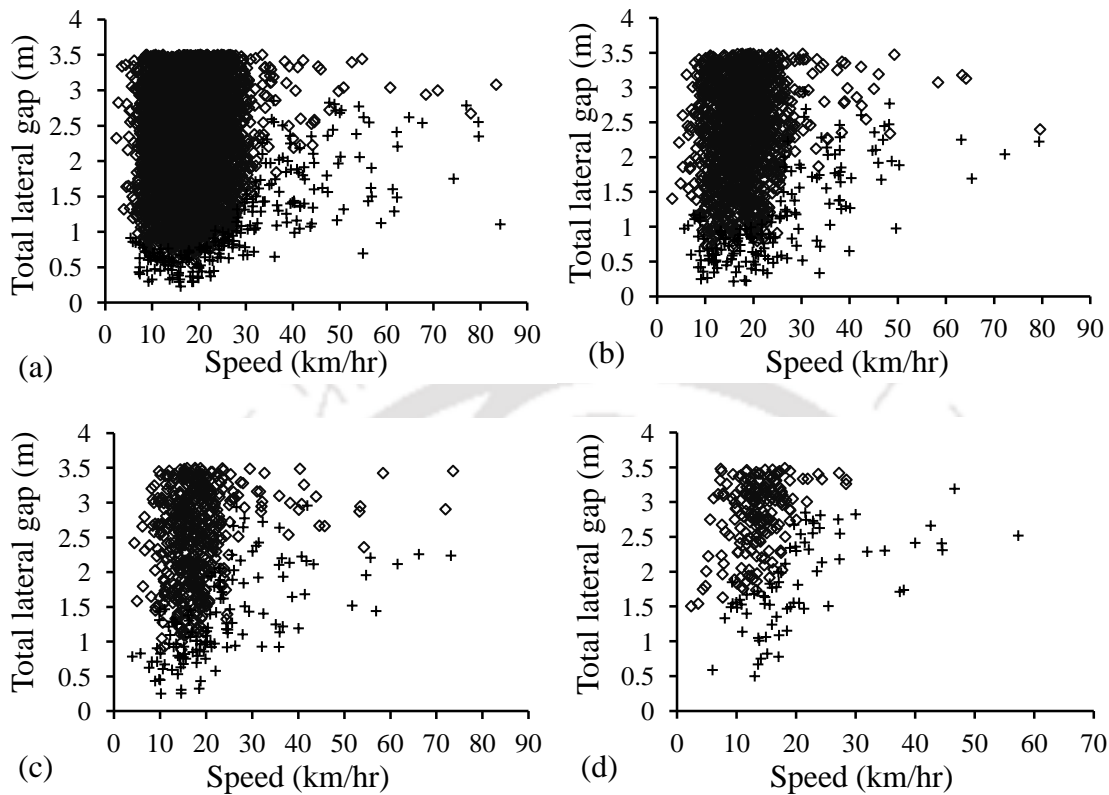


Fig. 4.3 Speed of the passing/overtaking vehicle versus total lateral gap, in case of LMV (a), MTW (b), MThW (c), and H MV (d)

From Fig. 4.3 it can be seen that a passing/overtaking vehicle, moving at certain speed, maintains different total lateral gaps and this may be due to the fact that besides the speed there may be other factors influencing the total lateral gaps. A part of this variation in the total lateral gap may also be attributed to the stochastic nature of the driver behavior. An aggressive driver may drive a vehicle sometimes closer to the vehicle being overtaken/passed, and a timid driver may require a little extra lateral gap. At the same time vehicles may be maintaining variable gaps just by the virtue of no-lane-disciplined. This results in a situation where the entire data corresponding to a specific speed cannot be included in the analysis of gap maintaining behavior. To overcome this difficulty, corresponding to every one kilometer speed range of the passing/overtaking vehicle, five minimum total lateral gap data were considered for the analysis. Data obtained using this approach includes various scenarios such as type of the adjacent vehicle and the speed of the adjacent vehicle. The lower envelop in Fig.

4.3 depicts these data. Trend observed from the data suggests that after certain speed of the passing/overtaking vehicle the total lateral gap remains constant. Also, at even lower speeds the passing/overtaking vehicles maintain certain minimum total lateral gap. This kind of variation can be modeled using the logistic curve and the same is discussed in the following sections.

4.3.1 Logistic curve for modeling the total lateral gaps

The specific form of the logistic curve used in this study is as follows (Button, 2010; Chen et al., 2010);

$$Lg = \frac{L_g^{max}}{1 + e^{-(\alpha_0 + \alpha X)}} \quad (4.1)$$

Where Lg is the total lateral gap, X is the Vector of predictor variables, and α and α_0 are the parameters to be estimated. In this study, L_g^{max} may be perceived as the threshold maximum total lateral gap beyond which the overtaking or passing maneuver is not influenced by the adjacent vehicles. The equation (4.1) can be rewritten as,

$$\ln\left(\frac{Lg}{L_g^{max} - Lg}\right) = \alpha_0 + \alpha X \quad (4.2)$$

Knowing the values of L_g^{max} , Lg and X in equation (4.2), the regression coefficients can be estimated. A non-linear optimization technique, discussed in the following section, has been used to estimate the optimal set of parameters.

4.3.2 Framework for optimization

The parameters of the proposed logistic regression model have been estimated using non-linear optimization. The optimization problem involves the minimization of the sum of the squared errors between the model output and the observed total lateral gap data. The objective function is expressed as,

$$f(X) = \min_{\alpha_0, \alpha} \sum_{i=1}^n \epsilon_i^2 = \min_{\alpha_0, \alpha} \sum_{i=1}^n \left[Lg_i - \frac{L_g^{max}}{1 + e^{-\{\alpha_0 + \alpha_1 v_i + \alpha_2 b_i + \alpha_3 s_i\}}} \right]^2 \quad (4.3)$$

subject to

$$0 \leq L_g^{max} \leq W - w_i - w_{MTW};$$

$$0 \leq v_{tb}^s \leq v_i^m;$$

$$0 \leq v_{tb}^a \leq \text{Max}(v_l^m \text{ or } v_r^m);$$

$$0 \leq v_{ts}^s \leq v_i^m;$$

$$0 \leq v_{ts}^a \leq \text{Max}(v_l^m \text{ or } v_r^m);$$

Where, v_i is the speed of the passing/overtaking (now onwards mentioned as the subject vehicle) vehicle, b_i is a binary variable used to capture the effect of adjacent vehicles' speed, and s_i is also a binary variable used to consider the size effect of the adjacent vehicles. Both these binary variables depend on certain threshold speeds of the subject and the adjacent vehicles and the threshold speeds are obtained while optimizing the parameters. Detailed description on the binary variables is provided in the following section. $\alpha_0, \alpha_1, \alpha_2, \alpha_3$ are the model parameters to be estimated. W, w_i and w_{MTW} are the road width, subject vehicle width and MTW width, respectively. v_i^m, v_l^m and v_r^m are the maximum speeds corresponding to the subject vehicle, left adjacent vehicle and right adjacent vehicle, respectively. v_{tb}^s and v_{tb}^a are the threshold speeds of the subject vehicle and adjacent vehicles, respectively for considering the effect of adjacent vehicles speed. v_{ts}^s and v_{ts}^a are the threshold speeds of the subject vehicle and the adjacent vehicles, respectively, for considering the adjacent vehicles size affect. This kind of problems can be solved numerically either by the gradient-based methods, such as, the iterative gradient search and conjugate gradient method, or by the derivative-free methods, such as, the grid search and genetic algorithm (Jang et al. 1997). In this study 'fmincon' optimization solver of MATLAB with 'interior point' algorithm was used to minimize the objective function and the derivatives were approximated by solver (MATLAB 2014). Constraints on the speed of the subject vehicle, and the adjacent vehicles are explained in the following section.

4.4 Lateral Gap Modeling

Modeling of the total lateral gap data collected from various road stretches is discussed in this section. Three hours of data (13 hrs to 16.30 hrs), collected from the road stretch located in Maharani Bagh, Delhi, were used for total lateral gap modeling. For modeling purpose, several explanatory variables such as the subject vehicle speed, type, adjacent vehicle's speed and type were examined.

Type of the subject vehicle certainly affects the gap maintaining behavior. Hence, the lateral gap modeling is carried out for each vehicle type separately. Speed of the passing vehicle (alternatively referred as subject vehicle) has been directly considered as an explanatory variable. While accounting for the effect of the size of the adjacent vehicle, it was assumed that only a relatively larger or a similar sized adjacent vehicle affects the total lateral gap maintained by the subject vehicle. The size of the adjacent vehicle was assumed to affect the lateral gap only when the speeds of the subject vehicle as well as the adjacent vehicles exceed certain threshold value. Combination of these two assumptions has been incorporated as the size effect of the adjacent vehicles, in terms of a binary variable, s_1 . Effect of the speed of the adjacent vehicle was also included in the model in terms of a binary variable. In this case it was assumed that the speed of the adjacent vehicle influences the total lateral gap only when the subject vehicle and the adjacent vehicles are travelling beyond certain threshold speeds. The details are explained in the following sub-sections.

4.4.1 Effect of the adjacent vehicles' speed

While modeling the total lateral gaps maintained by the subject vehicle, effect of the adjacent vehicles' speed was considered using a binary variable;

$$b_i = if(AND(v_i > v_{tb}^s, or(v_l > v_{tb}^a, v_r > v_{tb}^a)), 1, 0) \quad (4.4)$$

where, v_i , v_l and v_r are the speeds of the subject vehicle, left adjacent vehicle and right adjacent vehicle, respectively; v_{tb}^s and v_{tb}^a are the threshold speeds of the subject vehicle and adjacent vehicles, respectively.

Value taken by the binary variable depends on the following factors:

- (1) If the speed of the subject vehicle is more than v_{tb}^s km/hr, i.e., $v_i > v_{tb}^s$, and
- (2) If there is a moving vehicle on the left side of the subject vehicle with a speed more than v_{tb}^a km/hr, i.e., $v_l > v_{tb}^a$ km/hr, or
- (3) If there is a moving vehicle on the right side of the subject vehicle with a speed more than v_{tb}^a km/hr, i.e., $v_r > v_{tb}^a$ km/hr,

If all the above conditions are satisfied then the binary variable takes a value of 1, i.e., the impact of the speed of the adjacent vehicle is felt on the total lateral gap

maintained by the subject vehicle. Otherwise, the binary variable would be 0, i.e., the impact of the speed of the adjacent vehicle/object is not felt on the subject vehicle's total lateral gap. The threshold values were obtained while minimizing the objective function shown in equation (4.3).

4.4.2 Effect of the adjacent vehicles' size

The size effect of the adjacent vehicles/objects is accounted only when the speeds of the subject vehicle (v_i) as well as the adjacent vehicles exceed certain threshold value;

$$s_i = if \left(AND \left(v_i > v_{ts}^s, or \left(AND(T_l = 1, v_l > v_{ts}^a), \right) \right), 1, 0 \right) \quad (4.5)$$

where, s_i is the binary variable considering the size effect of the adjacent vehicles; v_{ts}^s and v_{ts}^a are the threshold speeds of the subject vehicle and the adjacent vehicles, respectively. T_l and T_r are the binary variables taking a value of either one or zero, based on the width (a proxy to size) of left and right adjacent vehicles, respectively.

$$T_l = if(w_l \geq w_i, 1, 0) \quad (4.6)$$

$$T_r = if(w_r \geq w_i, 1, 0) \quad (4.7)$$

Here, w_i , w_l , w_r are the widths of subject vehicle, left adjacent vehicle and right adjacent vehicle, respectively. Equation (4.5) indicates that when the subject vehicle (v_i) is moving with more than v_{ts}^s km/hr speed, and one of the adjacent vehicle's size is more than or equal to the subject vehicle's size, and speed is more than certain threshold value, then the size effect would be felt by the subject vehicle and the binary variable takes a value of 1.

The objective function shown in equation (4.3) was minimized using the MATLAB function 'fmincon' and the coefficients of all the variables obtained are presented in Table 4.2. The threshold values of L_g^{max} and the variables are shown in Table 4.4.

4.5 Analyses of the Results

The modeled total lateral gap and the observed total lateral gap with respect to the subject vehicle's speed are shown in Fig. 4.4. The total lateral gap model for LMV is,

$$lg_i^{lmv} = \frac{3.03}{1 + e^{(1.904 - 0.039v_i - 0.243b_i)}} \quad (4.8)$$

Here, lg_i^{lmv} is the total lateral gap maintained by i^{th} LMV.

Table 4.2 Parameters of the lateral gap models, for Maharani Bagh road

Vehicle Type	Variable	Coefficients	Standard Error	t Stat	p Value	Regression statistics	Model test
LMV	Constant	1.904	0.105	18.108	4.482×10^{-43}	Observations:191, RMSE:0.36, R-Squared: 0.611, SSE: 24.3651	F statistic vs. zero model: 595, p-value: 1.11×10^{-95}
	v_i	-0.039	0.004	-10.747	2.619×10^{-21}		
	b_i	-0.243	0.107	-2.261	0.02488		
MTW	Constant	1.764	0.151	11.697	3.392×10^{-23}	Observations:163, RMSE:0.434, R-Squared: 0.568, SSE: 30.1232	F statistic vs. zero model: 320, p-value: 6.67×10^{-75}
	v_i	-0.035	0.007	-5.065	1.122×10^{-06}		
	b_i	-0.298	0.122	-2.445	0.015592		
MThW	s_i	-0.421	0.162	-2.603	0.01019	Observations:126, RMSE:0.451, R-Squared: 0.517, SSE: 24.9847	F statistic vs. zero model: 309, p-value: 7.75×10^{-63}
	Constant	0.997	0.149	6.672	7.833×10^{-10}		
	v_i	-0.016	0.008	-1.969	0.051192		
H MV	b_i	-0.370	0.155	-2.383	0.018708	Observations:74, RMSE:0.485, R-Squared: 0.424, SSE: 16.7191	F statistic vs. zero model: 375, p-value: 1.96×10^{-43}
	s_i	-0.763	0.181	-4.215	4.822×10^{-05}		
	Constant	0.829	0.188	4.404	3.677×10^{-05}		
	v_i	-0.043	0.010	-4.242	6.592×10^{-05}		
	b_i	-0.394	0.200	-1.967	0.053085		

The statistical measures of the regression model are shown in Table 4.3. The size effect of the adjacent vehicles is not statistically significant in case of LMVs. Similar exercise has been carried out for MTW, MThW and H MV. Binary variable that considers the effect of the adjacent vehicles' speed and size were assumed to have similar impact in case of the other three types of vehicles also. The parameters of the resulting model and the statistical measures are given in Table 4.2. The threshold values corresponding to the speeds of the subject and adjacent vehicles are listed in Table 4.3. The modeled and the observed total lateral gap with respect to the subject vehicle's speed for MTW, MThW and H MV are shown in Fig. 4.4.

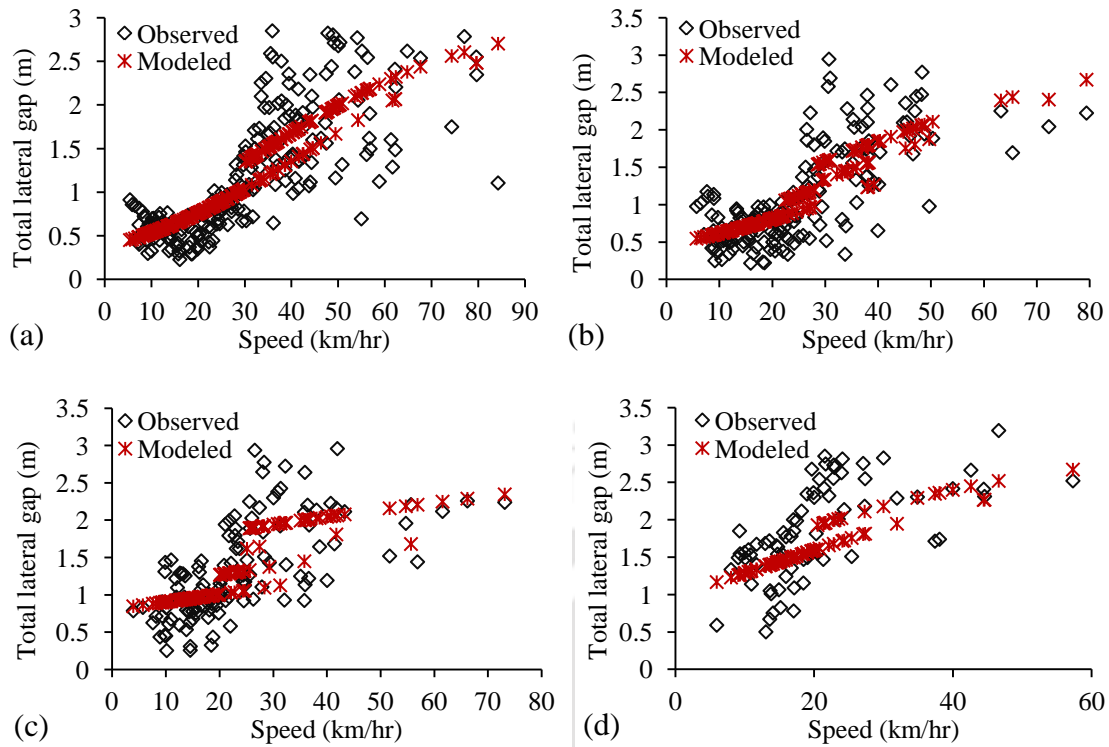


Fig. 4.4 Variation of total lateral gap maintained by the subject vehicle when travelling at different speeds: LMV (a); MTW (b); MThW (c); and HMV (d)

Table 4.3 Threshold values corresponding to the speeds of subject and adjacent vehicles

Location	Vehicle type	Threshold total lateral gap L_g^{max} (m)	Threshold speed values for Speed Effect		Threshold speed values for Size Effect	
			v_{tb}^s (km/hr)	v_{tb}^a (km/hr)	v_{ts}^s (km/hr)	v_{ts}^a (km/hr)
Maharani Bagh, Delhi	LMV	3.03	29.47	15.53	---	---
	MTW	3.15	23.97	15.69	28.08	8.40
	MThW	3.00	20.04	10.33	24.96	7.37
	HMV	3.48	20.00	12.26	---	---
Kodihalli, Bangalore	LMV	3.60	50.50	22.75	---	---
	MTW	3.60	39.97	15.02	49.94	20.01
Indira Nagar, Bangalore	LMV	3.40	32.22	16.02	---	---
	MTW	3.30	20.50	14.50	28.50	11.50
Jubilee Hills, Hyderabad	LMV	3.47	40.98	15.67	---	---
	MTW	3.48	29.97	15.03	38.58	15.03
	MThW	3.06	20.20	10.45	---	---

Similarly, total lateral gap models have been developed using the data collected at the other three locations. Threshold values corresponding to various independent parameters that govern the impact of speed and size of the adjacent vehicles are

summarized in Table 4.3. The estimates for the parameters along with the statistical measures are summarized in Table 4.4.

Table 4.4 Parameters of the lateral gap models, for various other roads

Vehicle Type	Variable	Coefficients	Standard Error	t Stat	p Value	Regression statistics	Model test
Kodihalli, Bangalore							
LMV	Constant	1.179	0.141	8.371	2.144×10^{-14}	Observations:171, RMSE:0.369, R-Squared:0.425, SSE: 22.9289	F statistic vs. zero model: 1.05×10^{03} , p-value: 1.75×10^{-108}
	v_i	-0.022	0.004	-5.829	2.777×10^{-08}		
	b_i	-0.469	0.124	-3.794	0.00020662		
MTW	Constant	1.252	0.25556	4.899	2.899×10^{-06}	Observations:130, RMSE:0.408, R-Squared:0.597, SSE: 21.1317	F-statistic vs. zero model: 732, p-value: 3.77×10^{-86}
	v_i	-0.031	0.008	-3.832	0.000199		
	b_i	-0.295	0.145	-2.044	0.043053		
	s_i	-0.880	0.257	-3.420	0.000843		
Indira Nagar, Bangalore							
LMV	Constant	1.001	0.160	6.271	1.054×10^{-08}	Observations:98, RMSE:0.495, R-Squared:0.518, SSE:23.2959	F-statistic vs. zero model: 336, p-value: 1.87×10^{-50}
	v_i	-0.026	0.007	-3.544	0.0006131		
	b_i	-0.993	0.226	-4.39	2.944×10^{-05}		
MTW	Constant	0.8002	0.166	4.777	5.120×10^{-06}	Observations:123, RMSE:0.458, R-Squared:0.558, SSE:25.1741	F-statistic vs. zero model: 487, p-value: 9.99×10^{-73}
	v_i	-0.028	0.009	-3.131	0.0021902		
	b_i	-0.392	0.141	-2.784	0.0062464		
	s_i	-0.849	0.223	-3.816	0.00021704		
Jubilee Hills, Hyderabad							
LMV	Constant	0.997	0.087	11.477	2.898×10^{-24}	Observations:226, RMSE:0.42, R-Squared:0.635, SSE: 39.413	F-statistic vs. zero model: 1.52×10^{03} , p-value: 3.28×10^{-148}
	v_i	-0.032	0.003	-9.876	5.577×10^{-19}		
	b_i	-0.379	0.122	-3.107	0.002139		
MTW	Constant	1.739	0.131	13.297	4.283×10^{-30}	Observations:227, RMSE:0.498, R-Squared:0.678, SSE: 55.6173	F-statistic vs. zero model: 609, p-value: 9.49×10^{-119}
	v_i	-0.034	0.005	-6.941	4.180×10^{-11}		
	b_i	-0.571	0.125	-4.566	8.226×10^{-06}		
	s_i	-0.388	0.149	-2.605	0.0097986		
MThW	Constant	1.003	0.181	5.542	3.822×10^{-07}	Observations:82, RMSE:0.496, R-Squared:0.549, SSE: 19.4075	F-statistic vs. zero model: 360, p-value: 5.89×10^{-46}
	v_i	-0.039	0.009	-4.332	4.305×10^{-05}		
	b_i	-0.588	0.221	-2.654	0.0096185		

From the developed models it can be seen that the effect of the adjacent vehicle speed is significant only when its own speed and the subject vehicle's speed exceed certain threshold values. As can be seen from the models, in case of LMV (as subject vehicle) it is affected by the speed of the adjacent vehicle only when its speed is more

than 30 km/hr. Whereas the effect of the adjacent vehicle speed is significant when threshold value of the subject vehicle speed is more than 20 km/hr in case of MTW, MThW and HMV. Effect of the adjacent vehicles' speed is significant only when their speeds exceed 10 km/hr and it is true for any type of subject vehicle. Similarly, the size effect of the adjacent vehicles is significant only when the subject vehicle's speed is more than 25 km/hr for all the types of subject vehicles. In case of HMV and LMV, size effect of the adjacent vehicles was found to be negligible.

Model results corresponding to the road sections of various widths have been analyzed to find out whether there is any effect of road geometry on the threshold speeds. Detailed analysis of the variations in the threshold values is presented in the following section.

4.5.1 Effect of the road width on the total lateral gap

Driver's gap maintaining behavior may not be same and road width is found to be having significant impact on the driver's behavior. Variations in the threshold speeds of the subject vehicles (LMV and MTW) and the adjacent vehicles, used to account for the impact of adjacent vehicle's speed and size, with respect to road widths are shown in Fig. 4.5.

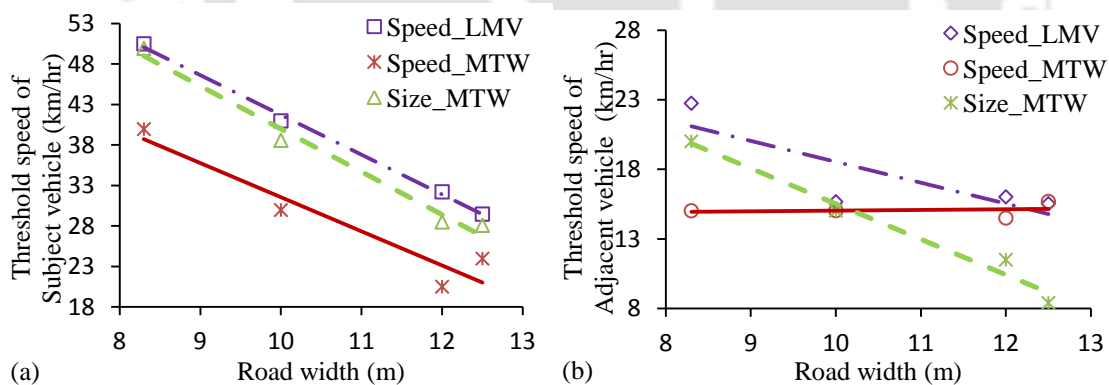


Fig. 4.5 Variation in the threshold values of the subject vehicles' speeds (a); and adjacent vehicles' speeds (b), while assessing the impact of the adjacent vehicle's speed and size

From the figures it can be clearly observed that the impact of the adjacent vehicles' speed and size is not felt at lower speed of the subject vehicle in case of narrow road and as the road width increases the impact of the adjacent vehicle's size and speed is felt even when the speed of the subject vehicle is low. In case of narrow road (e.g. a two lane wide road), most of the cases one side of the subject vehicle is

either median or kerb. The impact of the stationary object on the subject vehicle is less as compared to the moving adjacent vehicle. Hence, the impact of the other moving adjacent vehicle's speed or size is going to affect the movement of subject vehicle only when its speed crosses a higher threshold value as it has more freedom on the other side.

Table 4.5 Parameters for speed and size effects, for different types of vehicles

Vehicle Type	Affect accounted for	Coefficient (β)	Constant (c)
LMV	Threshold speed of the subject vehicle for speed effect on LMV (Speed_LMV in Fig. 4.5a)	-4.9154 (t Stat= -25.399)	90.887 (t Stat= 43.365)
MTW	Threshold speed of the subject vehicle for speed effect on MTW (Speed_MTW in Fig. 4.5a)	-4.2139 (t Stat= -4.491)	73.691 (t Stat= 7.253)
MTW	Threshold speed of the subject vehicle for Size effect on MTW (Size_MTW in Fig. 4.5a)	-5.3013 (t Stat= -10.729)	92.998 (t Stat= 17.379)
LMV	Threshold speed of the adjacent vehicle for speed effect on LMV (Speed_LMV in Fig. 4.5b)	-1.5017 (t Stat= -2.07)	33.561 (t Stat= 4.271)
MTW	Threshold speed of the adjacent vehicle for size effect on MTW (Size_MTW in Fig. 4.5b)	-2.547 (t Stat= -8.547)	40.987 (t Stat= 12.701)

Fig. 4.5(b) also indicates the same trend, except that the impact of the adjacent vehicle's speed on MTW is same across all the road widths. The linear trends, observed between the threshold speed and the road width for different types of vehicles takes the following form;

$$v_j^{th} = \beta W + c \quad (4.9)$$

Where, v_j^{th} is the threshold speed of vehicle type j . β is the coefficient for road width. W is the road width. c is the constant. The parameters obtained for different types of vehicles for speed effect and size effect are listed in Table 4.5.

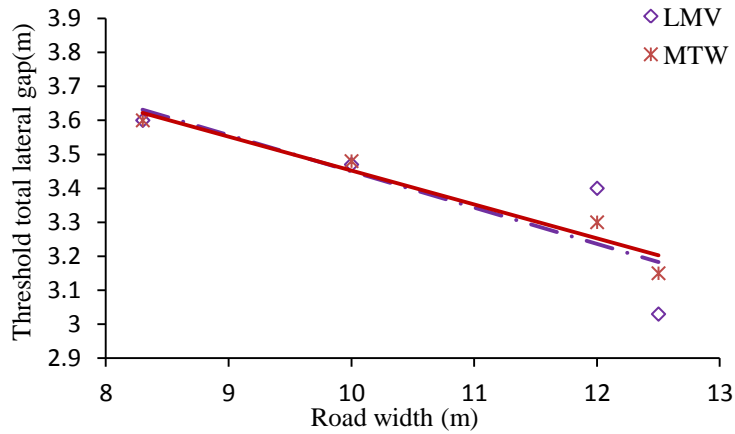


Fig. 4.6 Variation of the threshold total lateral gap with road width

Relationship between threshold total lateral gap with road width for LMV and MTW has been established in Fig. 4.6. It can be observed that in both the cases the threshold total lateral gap is reducing with increasing road width. Linear relationships obtained for LMV and MTW are given in equation (4.10) and equation (4.11).

$$Th_{LMV} = -0.1069xW + 4.5187 \quad (4.10)$$

$$Th_{MTW} = -0.0998xW + 4.4506 \quad (4.11)$$

t-statistics for coefficient of road width and constant are obtained as -2.226 and 8.688 respectively, for LMV, and -5.959 and 24.532 respectively, for MTW. To validate the proposed model data collected from Maharani Bagh road, Delhi, India between 16.30 hrs and 17.30 hrs have been utilized. The variation of observed total lateral gap and estimated total lateral gap data with respect to the subject vehicle speed are shown in Fig. 4.7.

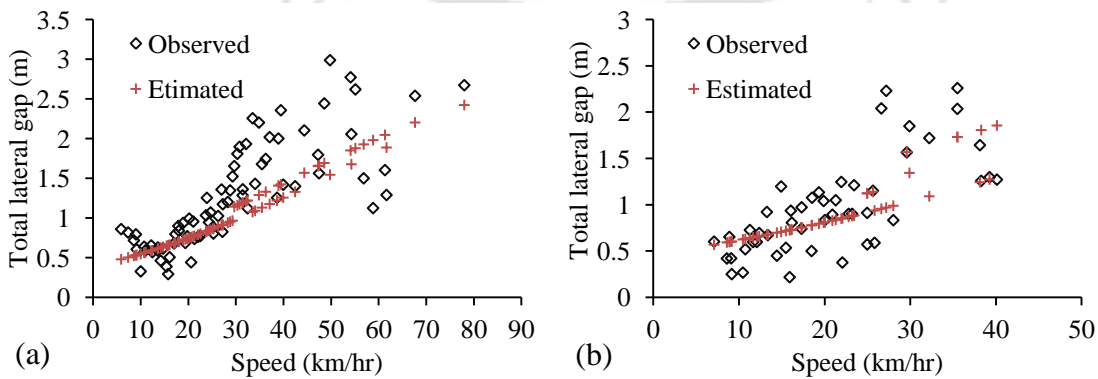


Fig. 4.7 Validation of total lateral gap for LMV (a) and MTW (b)

The validation was carried out using the parameters (Maharani Bagh, Delhi) shown in Table 4.3 and 4.4. R-squared value, SSE and RMSE were found to be 0.6503, 5.618 and 0.2774 respectively for LMV. The validation of total lateral gap for MTW using the data from same road section is also shown in Fig. 4.7. The statistical measures such as, R-squared, SSE and RMSE data were found to be 0.4621, 2.96 and 0.2509 respectively.

4.6 Summary and Conclusions

Lateral gap maintained by a vehicle is an important input for microscopic simulation models dealing with no-lane-disciplined heterogeneous traffic stream. Many researchers have pointed out but very few researchers have analyzed this aspect. In this study the total lateral gap maintaining behavior of vehicles has been analyzed using the trajectory data obtained from video image processing software, TRAZER. Total lateral gaps (gap on both the sides of a vehicle) maintained by four types of vehicles, namely, LMV, MTW, MThW, and HMV have been modeled in this study. Field observations suggest significant variability in the total lateral gaps even when the passing/overtaking vehicle is traveling at a constant speed. Based on this observation, it can be said that many other traffic characteristics influence the total lateral gap maintained by a vehicle moving in the heterogeneous traffic stream. Keeping in view the minimum and maximum lateral gaps, logistic curve has been used to model the total lateral gaps. From the estimated models it has been observed that the speed of the subject vehicle, size and speed of both the adjacent vehicles affect the total lateral gaps. It has been observed that the size and speed of the adjacent vehicles influence the total lateral gap only when the subject vehicle is traveling beyond certain critical speed. This speed is more than 30 km/hr in case of LMV and more than 20 km/hr in case of the other vehicles. The impact of side vehicle has been found to be prominent even at lower speed of the subject vehicle in case of relatively wide road. Linear trends have been observed between various threshold speeds with the road width. Validation of the developed models suggest that these models can be applied for modeling the total lateral gaps maintained by vehicles moving on road sections with widths varying between 8.3 to 12.5 m. Further analysis in this regards, may be carried out on more wider and narrower road sections, specifically for MThW and HMV.



CA Model Development for no-lane-disciplined Traffic

Development of a CA based traffic flow model for no-lane-disciplined heterogeneous traffic stream is described in this chapter. Analysis of the vehicular movement in heterogeneous traffic stream and developing appropriate vehicle updating procedures are the major aspects addressed here. Analysis of the vehicular movements observed in the heterogeneous traffic stream is presented in section 5.1. Section 5.2 illustrates the modified cell structure used to incorporate the variable lateral gap maintaining behavior of vehicles. Vehicle updating procedure used in the modified model is described in section 5.3. Methodologies adopted in collecting the data from the CA model are described in section 5.4. Section 5.5 describes the parameter analysis of the modified model. Salient aspects of the modified model and the important results from the parameter analysis are presented in section 5.6.

5.1 Vehicular Movement in no-lane-disciplined Heterogeneous Traffic Stream

Microscopic observation of no-lane-disciplined heterogeneous traffic stream suggests that the movement of a following vehicle depends not only on the front leading vehicle (FLV) but also on the surrounding vehicles which are within its vicinity (Fig. 5.1). In lane disciplined traffic flow, movement of the subject vehicle (SV) is governed by only one leading vehicle. Hence, the movement of the follower depends on the speed and type of the leading vehicle only.

Fig. 5.1 shows a photograph of no-lane-disciplined traffic stream, taken on the traffic stream moving on VIP road, Kolkata, India. From the photograph it can be seen that the subject vehicle's (SV's) movement in the next time step would be governed by many vehicles. It can be said that the front leading vehicle (LFLV), front leading vehicle (FLV), and right front leading vehicle (RFLV), besides the two back side vehicles may influence the SV's movement. In addition, on wider roads there can be one or more side vehicles which are not there in this case. Depending on the characteristics of the influencing vehicles either the SV move ahead maintaining the same lateral position or it may move ahead by adjusting its lateral position. With its current lateral position if it cannot maintain its desired speed in the next time step, then

only it may adjust its lateral position. This adjustment can be made in either of the directions with respect to its current position. Majority of the times it may shift to right side but on wider roads (3 or more lanes) left shifting are observed. To check whether it can maintain the desired speed with its current lateral position it is necessary to identify the vehicles affecting its movement.

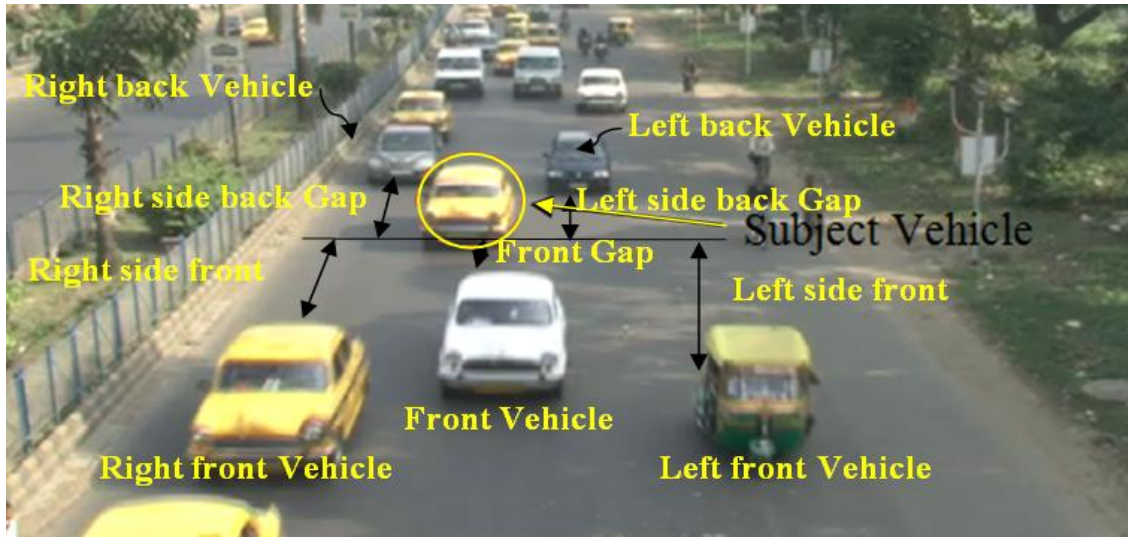


Fig. 5.1 Various vehicles affecting the SV's movement in the heterogeneous traffic stream

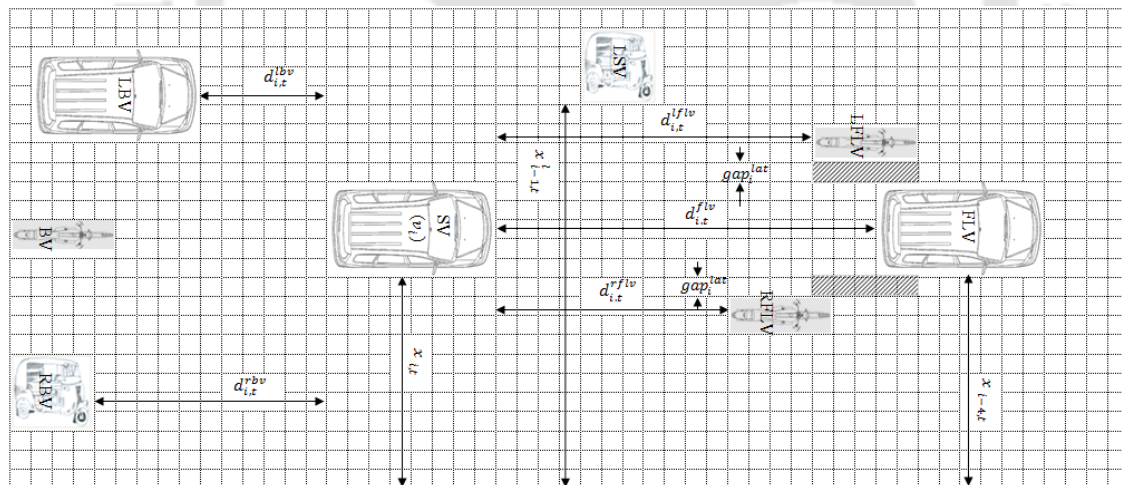


Fig. 5.2 Cell structure of the proposed CA model and the hypothetical representation of vehicles moving in the no-lane-disciplined heterogeneous traffic stream

With reference to Fig. 5.2, it is assumed that the SV's movement is influenced by all the leading vehicles. To know whether there is any effect of the left side vehicle (LSV), it is necessary to understand the lateral gap requirement of the SV. In no-lane-disciplined traffic any moving vehicle has to maintain sufficient lateral and longitudinal gaps with respect to the surrounding vehicles/objects. If the LSV is moving with lesser speed there is a chance of it being overtaken/passed by the SV. Passing is possible only

if there is an adequate lateral gap. According to the discussion in chapter 4, lateral gap requirement is influenced by several factors such as the speed and type of the side vehicle, besides the speed of the subject vehicle. Empirical relations have been proposed between the total lateral gap maintained by a vehicle and the relevant influencing traffic variables.

Based on the speed of the subject vehicle and the corresponding maximum total lateral gap requirement (obtained based on the maximum possible speeds of the subject and the side vehicles, besides assuming that the side vehicles are bigger than the subject vehicle) all the influencing side vehicles can be identified. These vehicles may influence the speed of the subject vehicle, if they are slower than the subject vehicle and consequently the decision of the SV to change the lateral position. If there is no influence and enough longitudinal gap is available to maintain the desired speed the SV may maintain the same lateral position. Otherwise the SV's driver may evaluate all the options available for maintaining the desired speed. These options necessarily include the adjustment of the lateral position.

• With reference to Fig. 5.2, description of the SV's movement when it is maintaining its existing lateral position, and when it is shifting its lateral position, is presented in the subsequent paragraphs. A vehicle moving in the heterogeneous traffic stream can take numerous lateral positions but in this study this is limited to a finite discrete value. This finite number depends on the cell structure of the CA model. As shown in Fig. 5.2 the road width is divided into finite strips and any vehicle may occupy a finite number of these strips thereby limiting the possible lateral positions a vehicle can take. Cell structure adopted in the present study is described in the following section.

5.2 Cell Structure

The presence of vehicles with different physical and mechanical characteristics on the same road section makes it necessary to revise the conventional cell structure. To reproduce the vehicle's mechanical characteristics such as, the acceleration behavior, it is always preferable to have smaller cell length. In this study, the cell length is taken as 0.5 m considering the presence of slow/heavy vehicles in the heterogeneous traffic stream.

Cell width depends on the physical dimension of different vehicles. In addition to this, it also depends on the lateral gaps maintained by vehicles in varying traffic conditions. The cell width needs to be decided in such a way that it can represent the physical width, and the variable lateral gap required by a vehicle. It is also observed that in no-lane-disciplined traffic a vehicle may shift laterally but the shift may be limited to 0.5 m or even less. The cell structure of the model needs to accommodate such smaller lateral shift. Therefore, a finer cell size may represent the actual no-lane-disciplined heterogeneous traffic stream behavior in an appropriate manner. To represent these aspects of heterogeneous traffic stream, a cell width of 0.3 m is considered in this study. This has been decided after analyzing the observed lateral gap maintaining behavior of vehicles.

5.3 Updating rules of the CA Model

The main motivation behind the present work can be directly linked to the drawbacks of the CA model developed by Mallikarjuna (2007). Refined cell structure may address majority of the drawbacks, but, the updating rules are to be modified significantly. Finer cells allow a better representation of the lateral gap maintaining behavior as well as enhanced description of the lateral movements observed in the heterogeneous traffic stream. The modified updating procedures corresponding to the refined cell structure are discussed in the following subsection.

5.3.1 Assumptions used in the updating procedure

The main assumption behind the updating procedures developed in this study is as follows; any vehicle moving in the no-lane-disciplined traffic stream tries to maximize the speed subject to the surrounding constraints, and safety concerns. Within the constraints, a vehicle may be able to achieve the objective by maintaining the same lateral position or by slightly adjusting its lateral position. The following subsection explores the conditions under which a vehicle can maintain its current lateral position. Subsection 5.3.3 explores the possibility of lateral shift, given the current lateral position is not fulfilling the objective.

5.3.2 Decision to maintain the current lateral position

If any vehicle intends to maintain its current lateral position, it has to analyze the characteristics of the effective leading vehicle. With reference to Fig. 5.2, the effective leading vehicle may be one of the vehicles which are directly in front (i.e. FLV) or any one of the side front vehicles (either the LFLV or the RFLV).

5.3.2.1 Detection of the side influencing vehicle

This has been carried out on the basis that any SV may be influenced by the effect of the side vehicles if these are falling within certain lateral distance. These lateral distances are to be found based on the type of the subject vehicle and its anticipated speed in the next time step, besides the characteristics of the side vehicles. It is also to be noted that the side vehicles falling within certain longitudinal distance only can influence the movement of the SV. This longitudinal distance can be decided based on the calibration studies carried out on the model. These distances define the search area for finding out the critical side vehicles on either side. Searching steps (with reference to Fig. 5.2) are given below:

1. The first step is to identify all the vehicles lying within the region of influence on either side and finding the corresponding longitudinal gaps.
2. Find the closest vehicle (in longitudinal direction) on either side of the subject vehicle.
3. Check the lateral gap requirement of the subject vehicle based on its own speed, type, as well as the speed of the side vehicle.
4. If the lateral gap available with respect to the closest side vehicle is more than the lateral gap required by the SV, the next closest side vehicle is identified. This is to be done separately for the left and right side vehicles.
5. The left side influencing vehicle is considered as the left front leading vehicle (LFLV) and the right side influencing vehicle is considered as the right front leading vehicle (RFLV).

5.3.2.2 Detection of effective leading vehicle

Once the influencing side vehicle is detected, the influencing leading vehicle can be detected using the effective longitudinal gap information between the i^{th} vehicle (SV)

and all the leading vehicles. The leading vehicles include the vehicles that are directly in front besides the side influencing vehicles.

With reference to Fig. 5.2, there is one vehicle directly in front of the SV and considering the requirement of lateral gaps, LFLV and RFLV are the side influencing vehicles. One of these three vehicles would be the effective leading vehicles. The position of the right front corner of the front leading vehicle (FLV), at time t , is $(x_{i-4,t}^{lv}, y_{i-4,t}^{lv})$. Similarly the coordinates of the right front corners of the LFLV and RFLV are $(x_{i-3,t}, y_{i-3,t})$ and $(x_{i-2,t}, y_{i-2,t})$ respectively. The longitudinal space headway between the SV and the FLV is $d_{i,t}^{flv}(y_{i-4,t}^{lv} - y_{i,t})$. The headway between the SV and the LFLV is $d_{i,t}^{lflv}(y_{i-3,t}^{lflv} - y_{i,t})$ and between the SV and the RFLV is $d_{i,t}^{rflv}(y_{i-2,t}^{rflv} - y_{i,t})$. It is important to note that the movement of the SV is not only influenced by the above mentioned longitudinal space headways but also by the anticipated distances travelled by all these leading vehicles in the next time step. The anticipated distances travelled by all the leading vehicles are estimated based on their estimated speeds. The expected speeds of the LVs are estimated as:

$$v_{exp}^{flv} = \min(d_{flv}^{lflv}, d_{flv}^{flv}, d_{flv}^{rflv}, v_{flv}) \quad (5.1)$$

$$v_{exp}^{lflv} = \min(d_{lflv}^{lflv}, d_{lflv}^{flv}, d_{lflv}^{rflv}, v_{lflv}) \quad (5.2)$$

$$v_{exp}^{rflv} = \min(d_{rflv}^{lflv}, d_{rflv}^{flv}, d_{rflv}^{rflv}, v_{rflv}) \quad (5.3)$$

Where, v_{exp}^{flv} , v_{exp}^{lflv} and v_{exp}^{rflv} are the expected speeds of FLV, LFLV and RFLV, respectively. d_{flv}^{lflv} , d_{flv}^{flv} and d_{flv}^{rflv} are the headways between the FLV and its corresponding LFLV, FLV and RFLV. Similarly, headways between the LFLV and its corresponding influencing vehicles are measured for estimating v_{exp}^{lflv} . Headway between RFLV and its corresponding influencing vehicles are measured for estimating v_{exp}^{rflv} . v_{flv} , v_{lflv} and v_{rflv} are the speeds of FLV, LFLV and RFLV respectively. Once the expected speeds of the leading vehicles are estimated, the effective gaps available to the SV, with respect to the three leading vehicles can be calculated as follows,

$$d_{flv}^{eff} = d_{i,t}^{flv} - l_{flv} + \max(v_{exp}^{flv} - gap_{security}, 0) \quad (5.4)$$

$$d_{lflv}^{eff} = d_{i,t}^{lflv} - l_{lflv} + \max(v_{exp}^{lflv} - gap_{security}, 0) \quad (5.5)$$

$$d_{rflv}^{eff} = d_{i,t}^{rflv} - l_{rflv} + \max(v_{exp}^{rflv} - gap_{security}, 0) \quad (5.6)$$

Where, d_{flv}^{eff} , d_{lflv}^{eff} and d_{rflv}^{eff} are the effective gaps, with respect to FLV, LFLV and RFLV. l_{flv} , l_{lflv} , l_{rflv} are the length of the FLV, LFLV and RFLV respectively. The parameter $gap_{security}$ can be linked to the effectiveness of the anticipation. Minimum of these three gaps gives the effective longitudinal gap corresponds to the effective leading vehicle. The time headway corresponding to this vehicle is,

$$t_i^t = \frac{d_i^{eff}}{v_i(t)} \quad (5.7)$$

Where, $d_i^{eff} = \min(d_{flv}^{eff}, d_{lflv}^{eff}, d_{rflv}^{eff})$ and $v_i(t)$ is the speed of SV (i^{th} vehicle at time t).

5.3.3 Decision to change the current lateral position

If the effective gap (in terms of the effective time headway) available for the SV is not enough to maintain its desired speed, then it looks for alternate lateral position. Here, the desired speed refers the speed a driver wants to maintain when traveling under given traffic conditions. At the same time the following criteria must be fulfilled.

5.3.3.1 Possible lateral positions for the SV

With reference to Fig 5.2, $(x_{i,t}, y_{i,t})$ are the coordinates of the right front corner of the i^{th} vehicle (of width W_i) at time t . Let $a_lat_{i,t}^{max}(l, v)$ is the maximum lateral acceleration of the i^{th} vehicle given the speed v . $(x_{i-1,t}^l, y_{i-1,t}^l)$ is the position of the left adjacent vehicle of the i^{th} vehicle, at time t . The maximum left lateral movement $l_{lat,gap}^{max}$, for the i^{th} vehicle is limited to either of the following;

$$\begin{cases} (x_{i,t} - x_{i-1,t}^l) - W_i, & \text{if } (x_{i,t} - x_{i-1,t}^l \leq |a_lat_{i,t}^{max}(l, v)|) \\ a_lat_{i,t}^{max}(l, v), & \text{if } (x_{i,t} - x_{i-1,t}^l > |a_lat_{i,t}^{max}(l, v)|) \end{cases} \quad (5.8)$$

The possible range of lateral positions, $x_{i,t+1}$ of i^{th} vehicle towards left direction at time $(t + 1)$ is, $(x_{i,t}, x_{i,t} + l_{lat,gap}^{max})$. Similarly, towards right direction, the

range for lateral shifting is $(x_{i,t}, x_{i,t} - r_{lat, gap}^{max})$. Hence, it is necessary to check for the presence of leading and back vehicles corresponding to all the lateral positions in between $(x_{i,t} + l_{lat, gap}^{max})$ and $(x_{i,t} - r_{lat, gap}^{max})$.

5.3.4 Lateral movement rules

After finding the possible set of lateral positions available for the SV, all the positions are evaluated based on the following two criteria.

5.3.4.1 Incentive criteria

The following incentive criteria insist the subject vehicle to shift laterally.

- a. If the effective front gap corresponding to the intended lateral position is greater than the available effective front gap, then it can shift laterally.
- b. If the effective LV's speed corresponding to the intended lateral position is more than the speed of the effective LV corresponding to the current lateral position, then the SV can shift laterally.
- c. If the effective LV's speed corresponding to the intended lateral position is more than the SV's speed, then it can shift laterally.

5.3.4.2 Safety criteria

The following criteria need to be satisfied for a safe lateral shifting of the subject vehicle.

- a. If the sum of the back gap and back vehicle speed, corresponding to the intended lateral position, is less than the SV's speed, then only it can shift laterally.
- b. If sufficient lateral gap (route width) is available with respect to the intended lateral position, then only it can shift laterally.

5.3.5 Forward movement rules

The forward movement rules are adopted from Mallikarjuna and Rao (2011) with the modifications discussed in section 5.1. The delay in acceleration and delay after braking have been modeled using the slow-to-start (p_0) probability and the brake light probability (p_{bl}), respectively. Slow-to-start probabilities are assumed to be different

for various types of vehicles moving in the heterogeneous traffic stream. Slow down probability (p_{dec}) has been considered to model the random fluctuations in the speeds. Since the cell structure used in the present study is different from the one used in Mallikarjuna and Rao (2011), the values taken by these parameters may also be completely different. This is further explained in parametric analysis of the model. Mathematical formulation of the forward movement rules are shown below:

(1) Randomization parameter:

Randomization parameter P , takes any one of the three probabilities depending on the speed of the subject vehicle, brake light of the effective leading vehicle and the available time headway with respect to the effective leading vehicle.

$$P = P(v_i(t), b_{i+1}(t), t_i^t, t^s) = \begin{cases} p_{bl}, & \text{if } b_{i+1}(t) = 1 \text{ and } t_i^t < t^s \\ P_0, & \text{if } v_i(t) = 0 \\ P_{dec}, & \text{in all other cases} \end{cases} \quad (5.9)$$

(2) Acceleration:

Acceleration of the SV depends on the brake lights of the SV and the effective leading vehicle, and the time headway with respect to the effective leading vehicle.

If $(b_{i+1}(t) = 0 \text{ and } b_i(t) = 0)$ or $(t_i^t \geq t^s)$ then,

$$v_i(t + 1/3) = \min(v_i(t) + a_i(v_i, l_i), v_{max}) \quad (5.10)$$

Else

$$v_i(t + 1/3) = v_i(t) \quad (5.11)$$

$$t_i^t = d_i^{eff} / v_i(t) \quad (5.12)$$

(3) Braking rule:

Braking behavior depends on the effective longitudinal gap and the available route width.

If $(rW_{i,t} \geq W_i + lg_i^l)$ then,

$$v_i(t + 2/3) = \min(v_i(t + 1/3), d_{flv}^{eff}) \quad (5.13)$$

Else

If $(v_i(t + 1/3) > \min(d_{flv}^{eff}, d_{rflv}^{eff}))$

$$v_i(t + 2/3) = \min(\max(v_i^{re}, v_{max}), v_i^{re} \ni \{W_i + lg_i^l < rW_{i,t}\}) \quad (5.14)$$

Else

$$v_i(t + 2/3) = \min(v(t + 1/3), \min(d_{lflv}^{eff}, d_{rflv}^{eff})) \quad (5.15)$$

If $(v_i(t + 2/3) < v_i(t))$ then,

$$b_i(t + 1) = 1 \quad (5.16)$$

(4)Randomization:

Vehicle undergoes random deceleration depending on the randomization probabilities found in step 1.

If $(rand() < p)$ then,

If $(p = p_{bl} \text{ or } p_0)$

$$v_i(t + 1) = \max(v_i(t + 2/3) - \gamma_i(l_i), 0) \quad (5.17)$$

If $(p = p_{dec})$

$$v_i(t + 1) = \max(v_i(t + 2/3) - 1, 0) \quad (5.18)$$

If $(p = p_{bl})$

$$b_i(t + 1) = 1 \quad (5.19)$$

(5)Updating the vehicle position:

$$y_i(t + 1) = y_i(t) + v_i(t + 1). \quad (5.20)$$

Where,

t_i^\dagger is the available time headway for the i^{th} vehicle (SV),

$i + 1$ refers to the effective LV,

t^s is the interaction headway,

$b_i(t)$ is the binary variable denoting brake light's status of the i^{th} vehicle (if equal to 1, brake light is on, if equal to 0 brake light is off),

d_i^{eff} is the effective gap available for the SV after considering the anticipated movement of the effective LV (Equation 5.7),

l_i is the length of the i^{th} vehicle (SV),

$a_i(v_i, l_i)$ is the acceleration of the i^{th} vehicle (SV),

$\gamma_i(l_i)$ is the deceleration of the i^{th} vehicle (SV),

v_i^{re} is the revised speed of the i^{th} vehicle (SV) which is re-evaluated based on the available $rW_{i,t}$,

$rW_{i,t}$ is the effective route width available ahead to the i^{th} vehicle (SV) at time t . The same is illustrated in Fig. 5.3.

v_{max} is the maximum allowable speed,

W_i is the width of the i^{th} vehicle (SV),

lg_i^l is the lateral gap required for the i^{th} vehicle (SV),

$(t+1/3)$ and $(t+2/3)$ denotes various stages at which speed values are updated within each updating step.

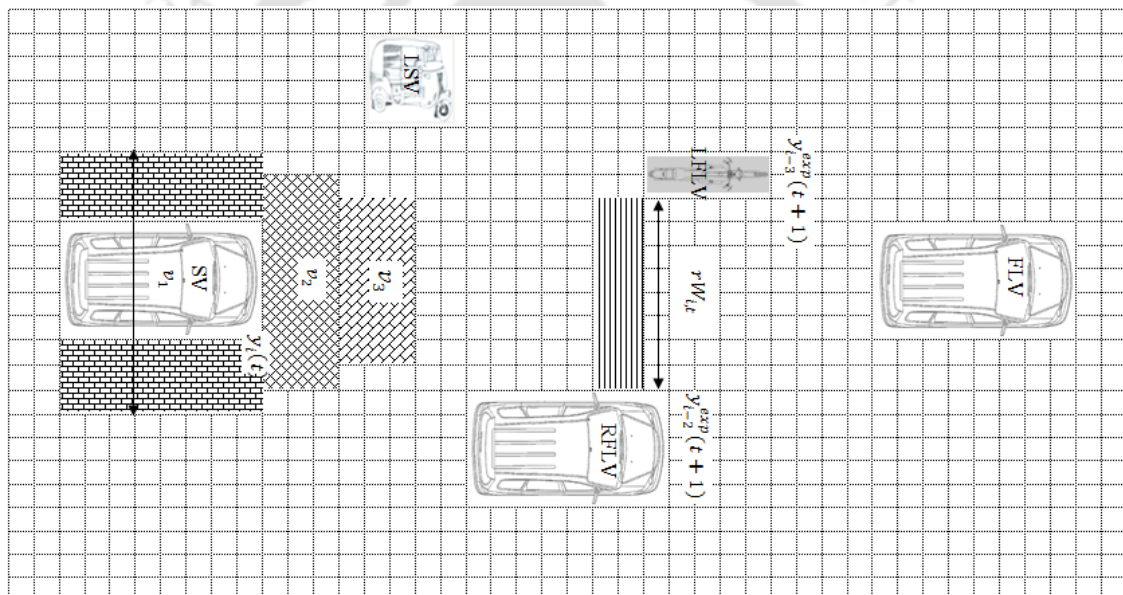


Fig. 5.3 Effective route width available for the SV at various speeds

One of the important changes made in the updating rule is shown graphically in Fig. 5.3. This figure shows the total lateral gap requirement of SV when moving at different speeds. When the SV is moving at speed v_1 , the gap requirements on either side are shown in the figure with hatching on either side of the vehicle. Positions of FLV, LFLV, and RFLV in the next time step $(t+1)$ are also shown in the figure. It can be seen from the figure that the SV has to reduce its speed to v_3 so that it can pass through the gap available between LFLV and RFLV. This aspect is addressed in step 3 and the revised speed is calculated based on the available route width ($rW_{i,t}$).

5.4 Data Collection from the Model

Data from the simulation model are collected using the methodologies adopted from Mallikarjuna (2007). Three different methods (Maerivoet 2006) namely, measurements taken over entire CA lattice, measurements taken over finite area, and measurements taken at a section are used to collect data from the models. All the three methods are briefly summarized in the following sub-sections.

5.4.1 Global measurements

In case of periodic boundaries, since the number of vehicles that are moving on the lattice is constant the global density remains constant during the entire measurement period. This is denoted by the term global occupancy or density and units are cells/unit cell length. Let, N_j is the number of cells in the j^{th} sub-lane that are filled by the vehicles, n is the number of lanes (sub-lanes) and P is the number of cells in all lanes (sub-lanes). Then the global occupancy/density is formulated as follows,

$$k = \sum_{j=1}^n k_j \Rightarrow \sum_{j=1}^n N_j / P \Rightarrow 1/P \sum_{j=1}^n N_j \quad (5.21)$$

Global Flow, in cells/sec is expressed as shown below;

$$q = \frac{1}{T * P} \sum_{t=1}^T \sum_{j=1}^n \sum_{i=1}^N v_{j,i}(t) \quad (5.22)$$

Mean speed in cell length/sec is expressed as shown below;

$$\bar{v}_s(t) = \frac{\sum_{j=1}^n \sum_{i=1}^N v_{j,i}}{\sum_{j=1}^n N_j} \quad (5.23)$$

Mean speed over a time period T is shown below;

$$\bar{v}_s = \frac{1}{T} \sum_{i=1}^T \bar{v}_s(t) \quad (5.24)$$

5.4.2 Local measurements with a detector of finite length

In this case the data are collected using a detector of finite length, typically less than the value taken by v_{max} (in cells). This is similar to the methodology used in data collection with dual loop detectors. Flow and density are measured over this finite measurement region using equations 5.27 and 5.28, and the speed is estimated from the fundamental relationship. Let, $N(t)$ is the number of cells that are filled by the vehicles at time t in the measurement region; v_i is the speed (in cells/sec) attributed to the i^{th} cell and l_d is the finite road length in cells, then,

$$k(t) = \sum_{j=1}^n N(t)/l_d \quad (5.25)$$

$$q(t) = \frac{1}{l_d} \sum_{j=1}^n \sum_{i=1}^{N(t)} v_{j,i}(t) \quad (5.26)$$

The density and flow measurements over consecutive time steps are now temporally averaged over the measurement region.

$$k = \frac{1}{T} \sum_{t=1}^T k(t) = \frac{1}{T * l_d} \sum_{i=1}^T \sum_{j=1}^n N(t) \quad (5.27)$$

$$q = \frac{1}{T} \sum_{t=1}^T q(t) = \frac{1}{T * l_d} \sum_{t=1}^T \sum_{j=1}^n \sum_{i=1}^{N(t)} v_{j,i}(t) \quad (5.28)$$

Based on flow and density, and fundamental relation between traffic characteristics mean speed can be obtained.

5.4.3 Local measurements with a detector of unit length

In case of local measurements with a detector of unit length, the measurements are taken over time. Flow and speed values are measured and density or occupancy is estimated from the fundamental relationship between the traffic characteristics.

$$q = N/T \quad (5.29)$$

$$\bar{v}_s = \frac{1}{\frac{1}{N} \sum_{i=1}^N 1/v_i} \quad (5.30)$$

Where N is the number of cells (constituting the vehicle) crossing the detector during the observation period T .

5.5 Parameter Analysis

Updating procedure discussed in the previous section involve several parameters. These parameters may be classified into two groups, such as, parameters used for forward movement rules and parameters used for lateral movement rules. Important parameters used for forward movement rules are interaction headway (h), security distance (SD), slow down probability (p_{dec}), slow-to-start probability (p_0), break light probability (p_{bl}), lateral gap and longitudinal acceleration. Some of the important parameters used in the lateral movement rules are probability of lateral movement (p) and look back distance (β). Details of the parameter analysis carried out in this study are presented in the following sub-sections.

5.5.1 Parameters of forward movement rules

Parameters used for updating the vehicle's longitudinal positions are analyzed and presented below.

5.5.1.1 Interaction headway (h)

In lane based traffic effect of the LV is felt on the FV only when the time headway between these vehicles is less than certain threshold headway, termed as the interaction headway. In case of no-lane-disciplined traffic, any vehicle is influenced by the vehicle downstream, irrespective of the lateral positions of the vehicles, if the time headway (measured across the road width) is less than the interaction headway. From previous studies (meant for lane based traffic), it has found that this parameter varies from 6 to 11 seconds. But this may not be true for no-lane-disciplined heterogeneous traffic. In every time step there is a possibility of lateral movement in heterogeneous traffic, hence, the SV may not be influenced by the downstream vehicles unless they are really close. Possibility of lateral position adjustment gives more flexibility to the SV and it can maintain relatively higher speeds even when the downstream (leading) vehicles are

closer. Fig. 5.4 shows the global flow-occupancy relationships for various values of interaction headways. With higher interaction headways, flow in the congested branch is less compared to lesser interaction headways. It may be due to the reason that in heterogeneous traffic vehicles always looks for the opportunity to overtake/pass. When the interaction headway is high, the SV may react to the presence of a downstream slower vehicle even when the distance between these vehicles is relatively high. Since the SV has freedom to move laterally, it may not react to the presence of slower vehicle unless both are really close; hence higher flows are resulting at lower interaction headways.

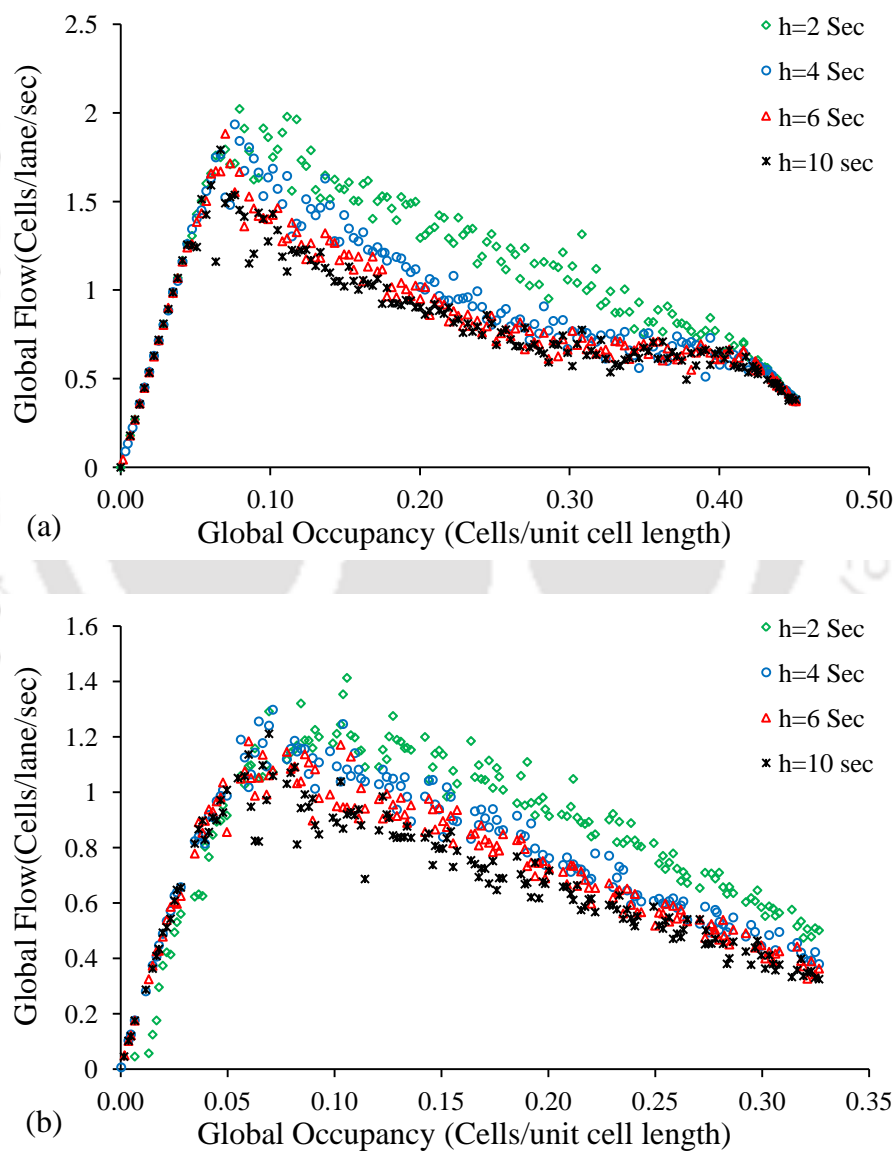


Fig. 5.4 Relationship between global flow and global occupancy for various interaction headways for homogeneous traffic, consisting of only cars (a); and heterogeneous traffic (b)

5.5.1.2 Security distance (SD)

Security distance is another important parameter used in vehicle updating procedure. Vehicles moving in the traffic stream anticipate the movement of the LV in order to update its own speed. This anticipation depends on driver/vehicle combination and accurate estimation of the front vehicle speed may not be possible. The parameter SD is used to offset the anticipated movement of the LV. This parameter can be associated to the safety perception of the following vehicle's driver. Aggressive drivers' behavior can be represented with less SD compared to that of a timid driver. This may be influenced by the type of vehicle as well. Flow-occupancy relationships corresponding to various values of SD are shown in Fig. 5.5. From the figure it can be seen that as the SD is decreasing flow values are increasing. This is reflecting the scenario where the traffic stream contains more aggressive drivers. Also, the drivers of the heavy vehicles are attributed with higher SD to reflect the difficulty in maneuvering heavy vehicles.

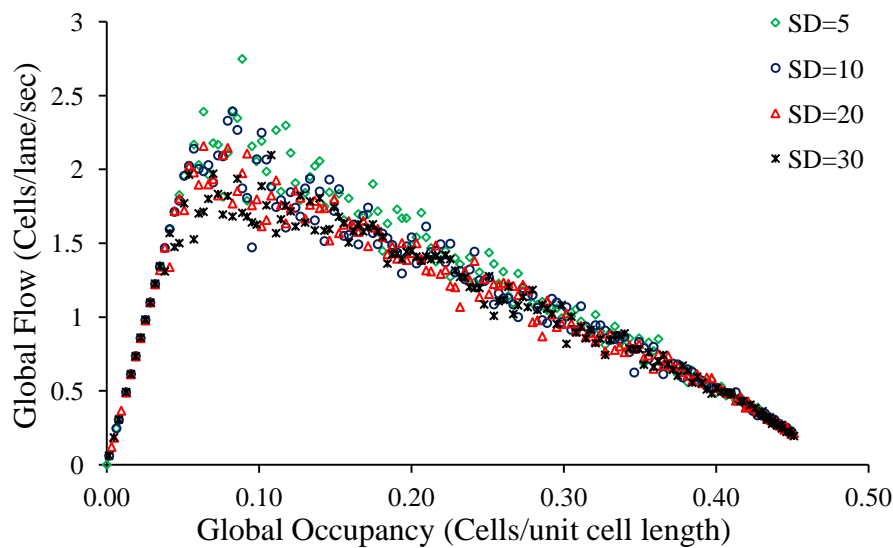


Fig. 5.5 Relationship between global flow and global occupancy for various security distances for homogeneous traffic, consisting of only cars

5.5.1.3 Slow down probability (p_{dec})

This parameter is used to simulate the random fluctuations in the vehicular speed resulting due to the driver behavior. Random fluctuations in speeds of free moving vehicles may lead to break down of the free flow conditions leading to congestion. Flow-occupancy relations corresponding to various values taken by this parameter are shown in Fig. 5.6. From the figure it can be seen that as the value taken by this

parameter is increasing, the maximum flow is decreasing. Results shown in the figure corresponds to no-lane-disciplined heterogeneous traffic stream and due to the inherent flexibility of the vehicles to adjust the lateral position, nullified the effect of p_{dec} . In case of lane based homogeneous traffic, this parameter may have significant impact on the breakdown of free flow branch.

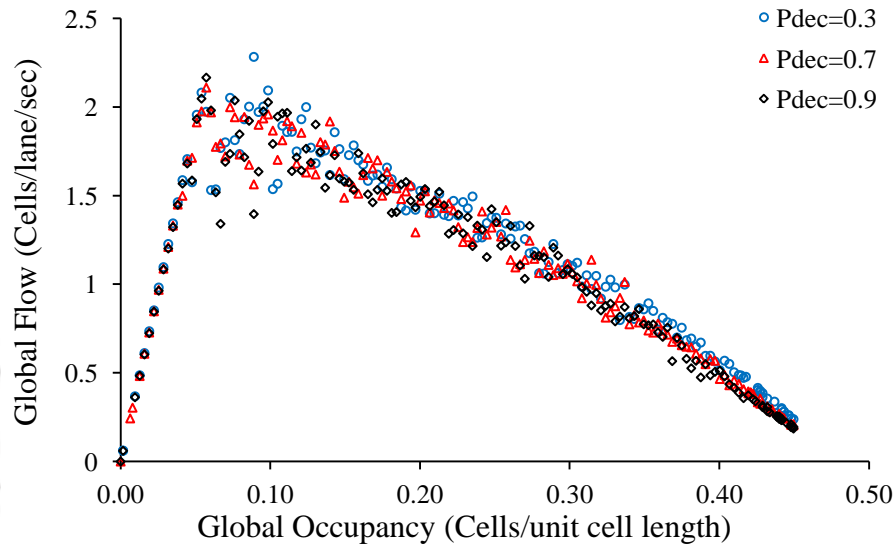


Fig. 5.6 Relationship between global flow and global occupancy for various values taken by p_{dec} , for homogeneous traffic, consists of only cars

5.5.1.4 Slow-to-start probability (P_0)

A vehicle in stationary condition takes some time before accelerating. A small vehicle such as MTW may start quickly whereas an HVM may take longer time to accelerate. This delay in acceleration varies from vehicle to vehicle because of its acceleration characteristics. There may be some additional delay in acceleration due to the relaxation behavior of the driver. The effect of slow-to-start parameter is trend to be significant on the congested branch (Fig. 5.7). It can be clearly seen from the figure that there is a change in the slope of the congested branch. Mallikarjuna (2007) has shown similar parameter analysis and the results are significantly different compared to the result from present study. This difference can be attributed to the better refined cell structure adopted in the present study.

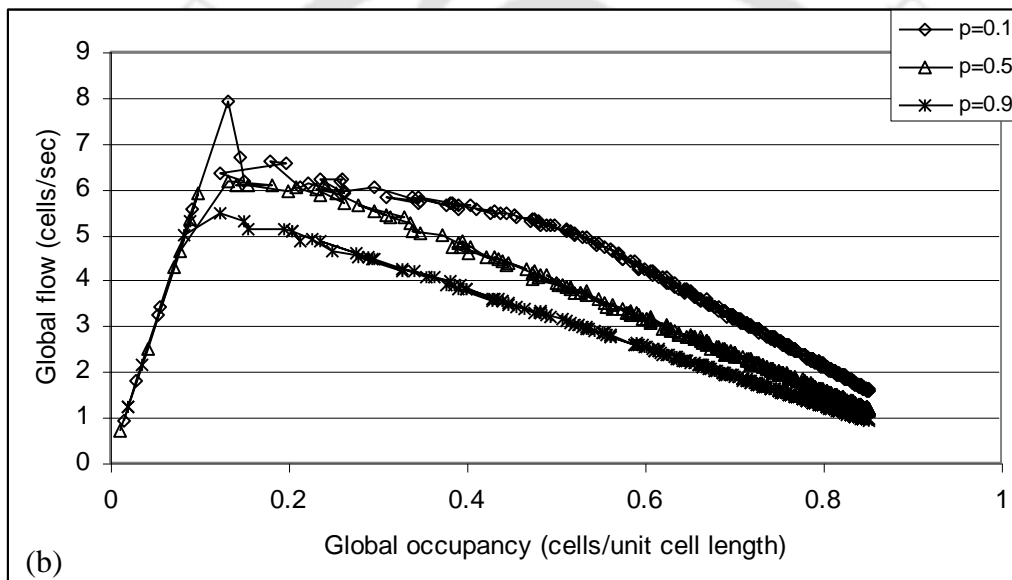
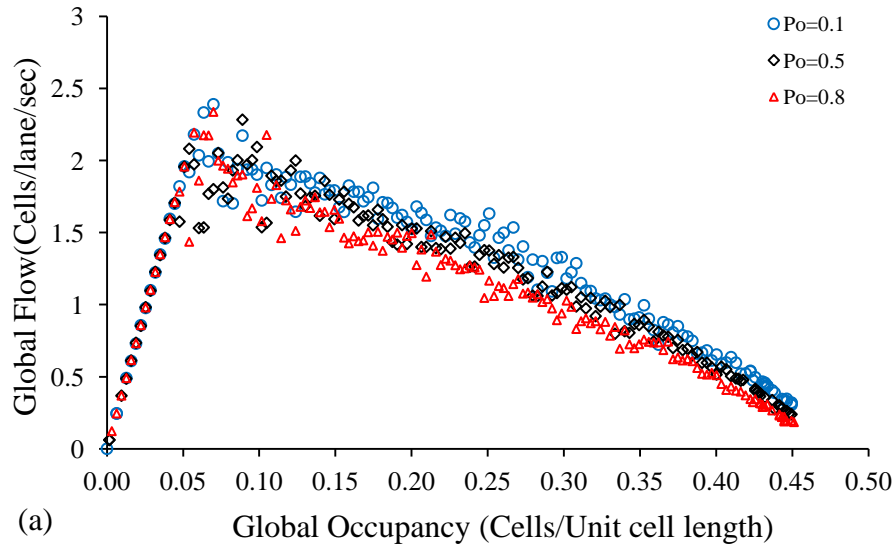


Fig. 5.7 Relationship between global flow and global occupancy for various slow-to-start parameters for homogeneous traffic consists of only cars; current model (a); results from Mallikarjuna (2007) (b)

5.5.1.5 Lateral gap

Lateral gaps maintained with the adjacent vehicles or with the median or kerb significantly influence the no-lane-disciplined traffic stream behavior. Some of the past researchers have considered this parameter, but the lateral gap was assumed to be constant irrespective of the traffic state. In this study a suitable methodology has been developed to find the total lateral gap requirement of a particular type of vehicle based on its own speed, and speed and type of the adjacent vehicles. The details of the approach were described in chapter four. The variable lateral gap is incorporated

explicitly, i.e., the lateral gap is not included in the vehicle width. The influence of the variable lateral gap and the constant lateral gap on traffic flow is examined. The global flow-occupancy relationships corresponding to constant and variable lateral gaps are shown in Fig. 5.8. From the figure it can be seen that gap maintaining behavior affects the flows significantly.

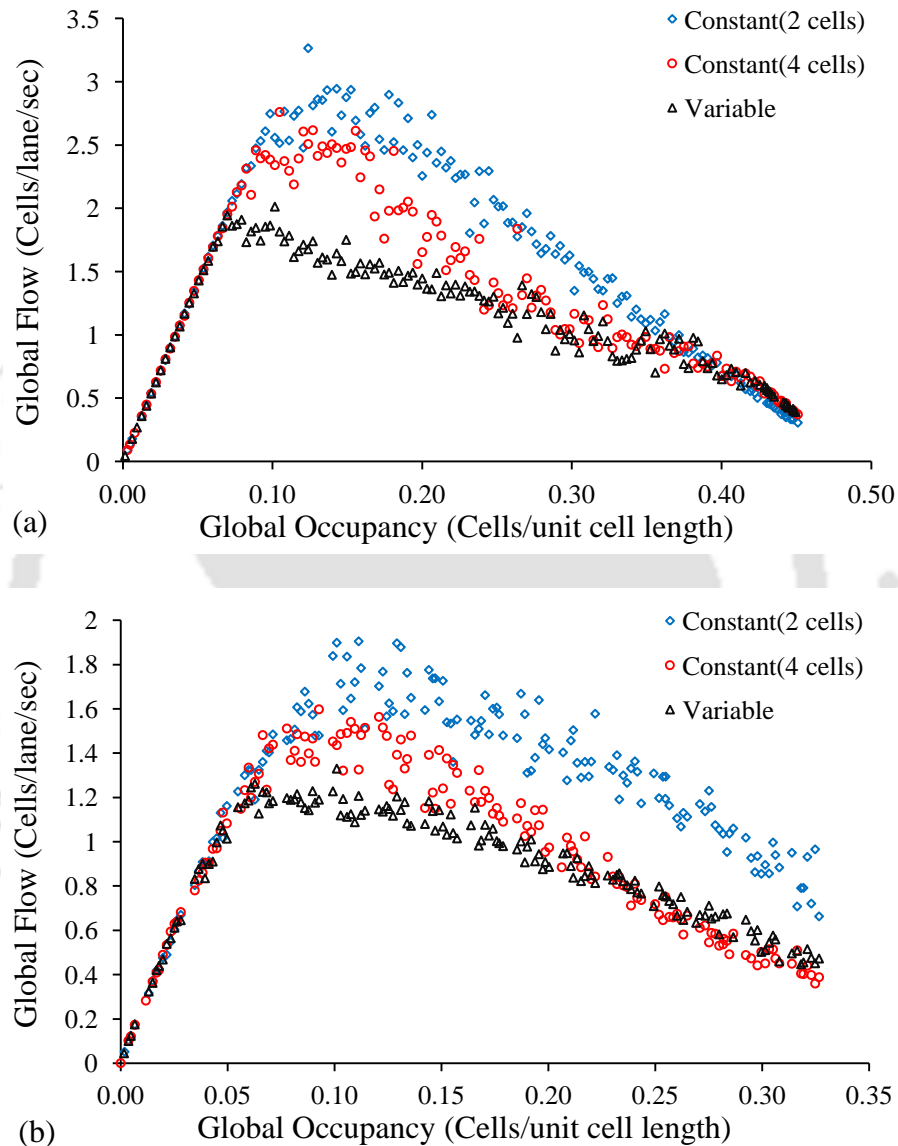


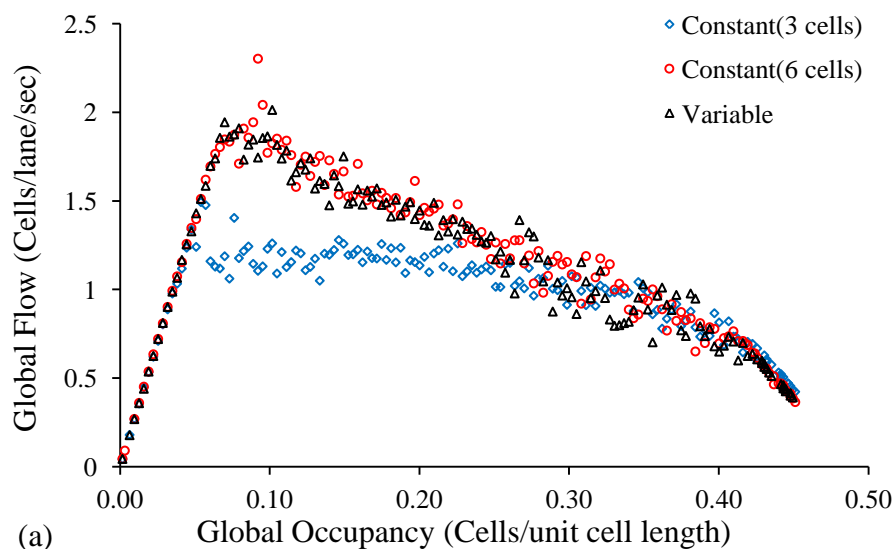
Fig. 5.8 Relationship between global flow and global occupancy for constant and variable total lateral gap for homogeneous traffic consists of only cars (a); and heterogeneous traffic (b)

The gaps shown in the legend of the figure denotes the total lateral gap maintained by a vehicle. Total lateral gap of 2 cells refers to a vehicle maintaining a gap of one cell on either side. Constant gap of 2 cells implies that irrespective of the speed and other factors this gap will not change. Variable gaps referred to the actual

gap maintaining behavior of LMV observed in the field. From the figure it can be seen that the gap maintaining behavior significantly affects the breakdown of the free flow conditions. Up to certain occupancy levels, free flow branch corresponding to all the three lateral gaps remain same. Corresponding to the constant gap of 2 cells, free flow conditions were observed beyond the occupancy of 0.1. Similarly, the congested branch is also significantly affected by the gap maintaining behavior. Overlapping congested branch corresponds to the constant gap of 4 cells and the variable lateral gaps implies that the vehicles need to maintain a total lateral gap of 4 cells in the congested conditions (when occupancy is greater than 0.25). Flow values corresponding to the occupancy levels 0.1 to 0.2 significantly differ depending on the gap maintaining behavior. From the figure it can be said that the constant lateral gaps of lesser magnitude (2 to 4 cells or 0.6 to 1.2 m) results in over estimation of the capacity values.

5.5.1.6 Acceleration characteristics

In this study, variable acceleration values are considered against the constant value generally used in the CA based models. It is known that, depending on the speed the acceleration capability of a vehicle will change. The refined cell structure used in the present study can accommodate the variable accelerations. From Fig. 5.9 it can be seen that the variable acceleration affects the free as well as the congested branches.



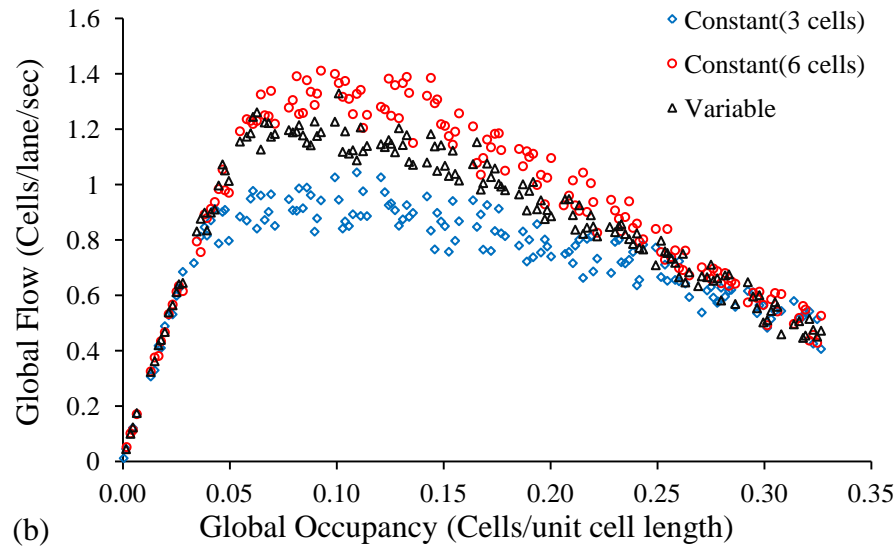


Fig. 5.9 Relationship between global flow and global occupancy for constant and variable acceleration for homogeneous traffic consists of only cars (a); and heterogeneous traffic (b)

5.5.2 Parameters of lateral movement rules

Parameters used for updating the vehicle's lateral positions are analyzed and presented in the following sub-sections.

5.5.2.1 Probability of lateral movement (p)

Vehicles moving in the no-lane-disciplined heterogeneous traffic stream have the flexibility to adjust the lateral positions. Many vehicles moving in the stream may compete for the same space and driver's behavior play major role in utilizing the road space. To account for the timid driver's reluctance to move on to the new lateral position certain probability is associated to lateral movement even when all the safety criteria are satisfied. Results related to various values taken by this parameter are shown in Fig. 5.10. From the results it can be seen that as the probability of lateral movement is decreasing the maximum flow is decreasing. It is logical since the reduced probability restrains the vehicle to take up the new lateral position, thereby causing speed reduction. The probability values may also depend on the vehicle type. The lighter vehicles have the tendency to utilize all the opportunities whereas the heavy vehicles have lesser tendency to take up the new lateral position.

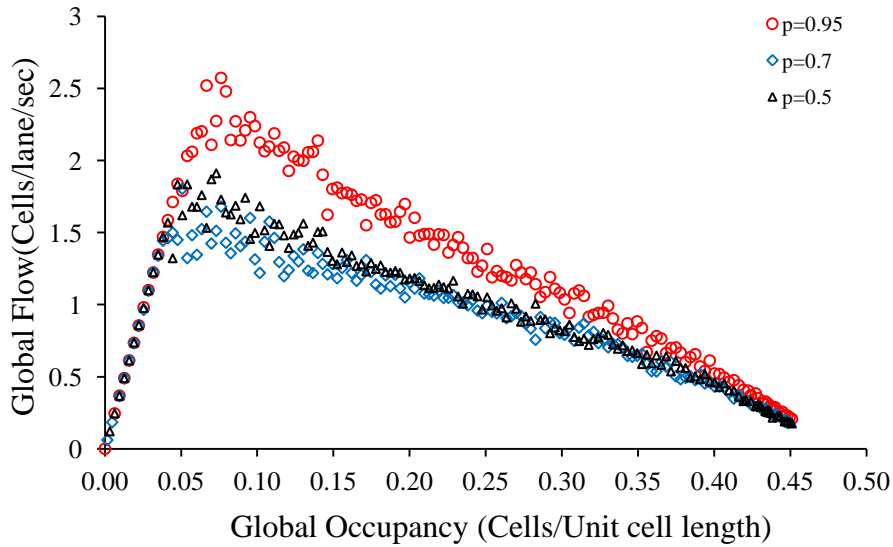


Fig. 5.10 Relationship between global flow and global occupancy for different probability of lateral movement (p) for homogeneous traffic consists of only cars

5.5.2.2 Look back distance

When a vehicle intends to move laterally the driver needs to evaluate the safety aspects corresponding to the new lateral position. One of the major concerns is the vehicles coming from back and the driver of the SV needs to judge the position of the back vehicle.

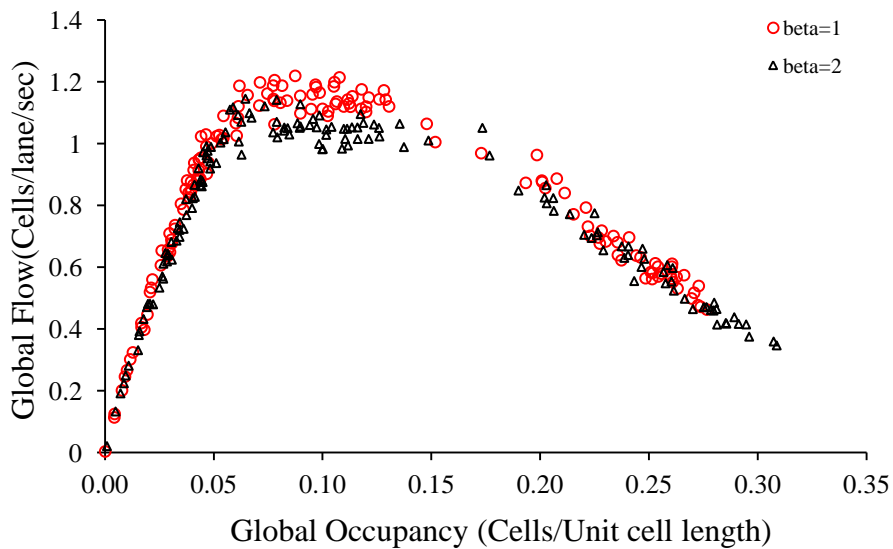


Fig. 5.11 Global flow-occupancy relationship of heterogeneous traffic for various beta (β) values

Look back distance parameter models the ability of the driver in judging the position of the back vehicle. Look back distance is considered in terms of the back

vehicle speed. The results shown in Fig. 5.11 correspond to the multiplication factor associated to the back vehicle speed. From the results it can be seen that when the factor takes higher value owing to safety concerns the SV cannot move laterally, hence the drop in the speed.

5.5.3 Effect of traffic composition

Effect of traffic composition on global flow–density relationships are shown in Fig. 5.12. From the figure it can be seen that in case of 100% LMV the maximum flow is 3200 vehicles/hr. It can also be seen from the figure that at the same proportion of HMV and MThW, the variation in MTW proportion affects the maximum flow. Due to the increased proportion of MTW the maximum flow has increased significantly. As expected, increased proportions of MThW and HMV resulted in lesser maximum flows. This behavior can be attributed to the maneuverability of various types of vehicles.

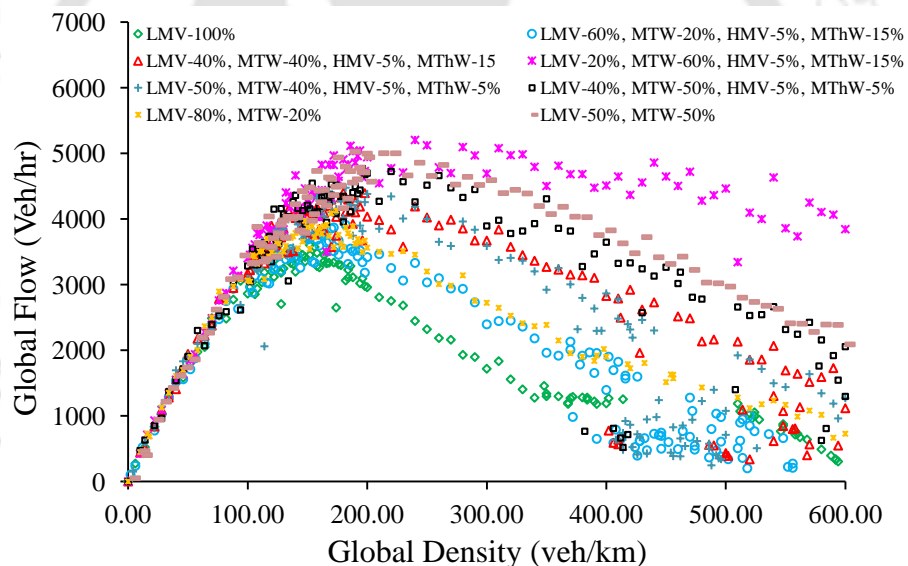


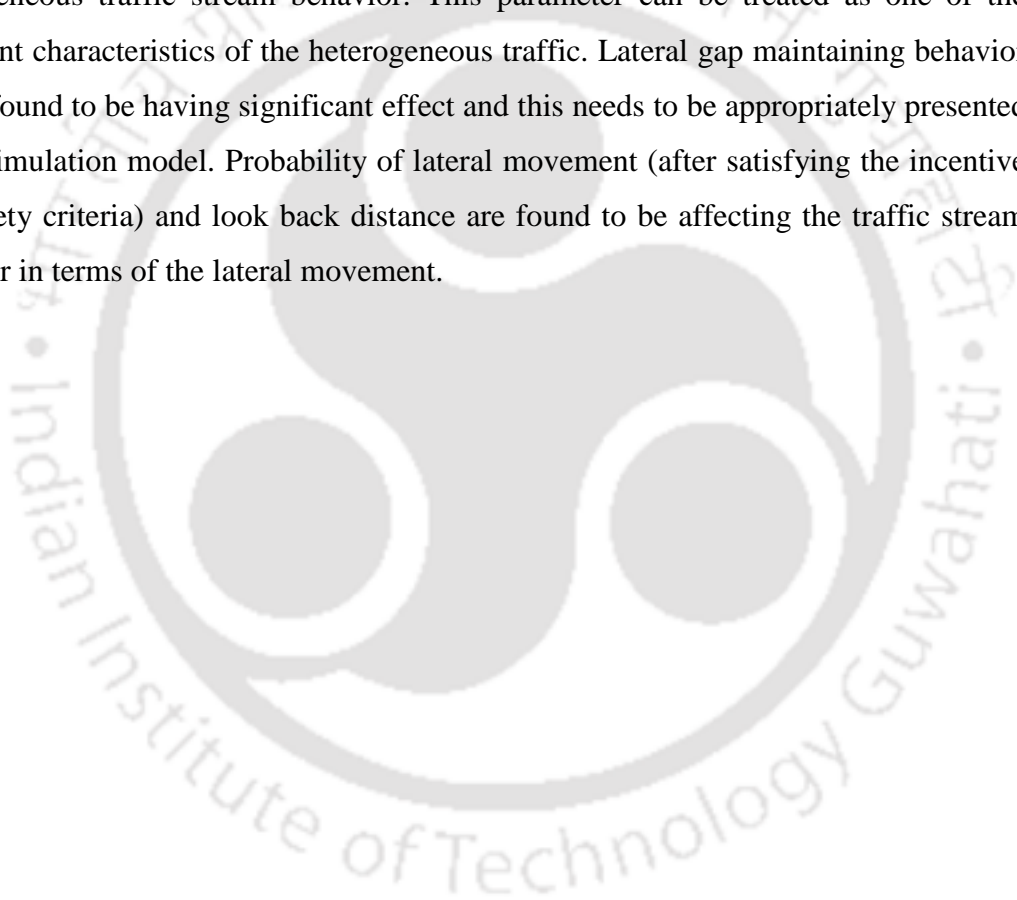
Fig. 5.12 Effect of traffic composition on Global flow-density relationships

5.6 Summary and Conclusions

Vehicular movement in no-lane-disciplined heterogeneous traffic stream is different from that of the lane based homogeneous or heterogeneous traffic. Vehicle moving in this traffic stream is influenced by all the surrounding vehicles. Longitudinal movement of the subject vehicle is influenced by more than one leading vehicle. Effective LV is the closest vehicle that is influencing the movement of the subject vehicle. This closest

vehicle may not be directly in front and by virtue of the lateral gap requirement (of the SV to maintain its speed) it is influencing the SV's movement.

To incorporate the variability of lateral gap maintained by the vehicles, the cell structure of the present CA model is modified, and a finer cell width of 0.3m is proposed. This finer cell width gives the vehicles flexibility to adjust their lateral positions. Refined cell structure was found to be affecting many of the CA parameters. Parameters such as the interaction headway, slowdown probability, slow-to-start probability, lateral gaps have been evaluated in terms of flow-occupancy relationships. Interaction headway is found to be having significant impact on the no-lane-disciplined heterogeneous traffic stream behavior. This parameter can be treated as one of the important characteristics of the heterogeneous traffic. Lateral gap maintaining behavior is also found to be having significant effect and this needs to be appropriately presented in the simulation model. Probability of lateral movement (after satisfying the incentive and safety criteria) and look back distance are found to be affecting the traffic stream behavior in terms of the lateral movement.



Model Validation and Application

Validation of the microscopic simulation model and some of its applications are presented in this chapter. The model has been validated for traffic stream moving on the road sections with widths 8.3 m and 10 m. The model is validated at microscopic as well as macroscopic levels. Queue formation and dissipation behavior obtained from simulation model is compared with the corresponding field data. Validated model is used to study the impact of minor variations in the width of a typical two-lane road observed in Indian cities. Simulation model set-up is presented in section 6.1. Section 6.2 describes the validation of the CA model. Inferences on global measurements are discussed in section 6.3. Application of the developed CA model to analyze the effect of road width is presented in section 6.4. The last section of this chapter describes the important conclusions drawn from the validation of simulation model and its application.

6.1 Simulation Model Set-up

Important parameters of the simulation model such as, warm up time, data extraction time, boundary conditions (periodic or open), length of the road section to be simulated, stretches of the road section to be selected for data extraction need to be finalized for validation of the developed model. Warm up time is the time elapsed to set the vehicles in equilibrium conditions i.e., it is the time to be elapsed before extracting the simulation result from the model so that the initial vehicle generation impact is minimized. A warm up time of 480 seconds is used for the present study (Mallikarjuna 2007). Data extraction time or measurement time is the time for which the data are collected from the model. Data on all the macroscopic variables are collected over a period of 60 seconds. Length of the road stretch is kept as 2 km i.e., lattice length of 4000 cells. Requisite data have been collected when the vehicles are crossing a road section as well as over the entire road stretch (global measurements).

Since periodic boundary conditions are used in the present CA model, by controlling the density/occupancy, it is easy to simulate different traffic scenarios such as free flow and congested flow. Local and global measurements can be made from the

CA model with periodic boundaries. Field observations are not possible either at global level or even on a finite road area. Hence, local measurements are made from the simulation model to compare with the observed data.

6.2 Validation of the CA Model

The CA model is validated at microscopic level as well as at macroscopic level. In this study the developed model has been validated at microscopic level for free and congested conditions separately. Macroscopic data such as flow, speed, and occupancy measured at a road section (equivalent to the detector of unit length in the simulation model) is available for two different locations. All these data have been collected in terms of vehicles instead of equivalent number of cars which is the normal procedure under heterogeneous traffic conditions. Similar data have been collected from the simulation model using a detector of unit cell length. Validation of the simulation model using these data sets has been presented in the following subsections. Two dimensional Kolmogorov-Smirnov (2D-KS) test (Peacock 1983) has been conducted to check the closeness of the observed and simulated macroscopic relationships. From the microscopic simulation models it is possible to collect different microscopic data, but, the same is difficult to obtain from field. Microscopic validation of the simulation model for free flow condition has been carried out in terms of observed and simulated cumulative distribution of free flow speed data (FFS). The model has been validated for congested conditions in terms of the simulated queue formation and dissipation. Queue formation and dissipation speeds are comparable to that of the field observed values.

6.2.1 Traffic stream moving on 10 m wide road

Observed traffic composition and free flow speeds are the key inputs to the simulation model. Other important aspect is the road width to be used in the simulation model. To validate the present CA model, two hour data have been collected from Jubilee Hills, Hyderabad, India. The width of the road section is 10.0m. In the CA model, the road width is divided into 34 sub-lanes. Majority of the vehicles plying on this road section were LMV and MTW. Around 10% MThWs and 1% HMTVs were also observed. Traffic composition details corresponding to this road stretch are presented in Table 6.1. Mean and standard deviations of the observed free flow speeds of different types

of vehicles are also presented in Table 6.1. Other relevant traffic characteristics and CA parameters corresponding to each vehicle type are shown in Table 6.3.

Table 6.1 Representation of 10 m wide road (Jubilee hills, Hyderabad) and the corresponding vehicles related parameters used in the simulation model

Road Characteristics					
Cell width (m)		0.3			
Cell length (m)		0.5			
Road Width (Cells)		34			
Road length (Cells)(Periodic Boundary)		4000			
Warm up time (Sec)		480			
Data extraction time (Sec)		60			
Total run time (Sec)		540			
Vehicle Compositions					
LMV	44.30%	HMV	1.20%		
MThW	10.00%	MTW	44.50%		
Vehicle Characteristics					
Parameter	LMV	HMV	MThW	MTW	
Length (Cell)	9	21	6	4	
Width (Cell)	6	8	5	2	
Mean desired speed (Cell/sec)	26	18	17	23	
Standard deviation of the maximum speed (Cell/sec)	5	4	2	3	
Acceleration (Cell/sec ²) (Mallikarjuna, 2007)	$v_i \leq 5.5$	4	2	2	5
	$5.5 < v_i < 11$	3	1	2	4
	$v_i \geq 11$	2	1	1	3
Deceleration (Cell/sec ²)	4	3	3	2	
Maximum lateral gap (Cells)	7	7	5	1	
Lateral gap *	Variable based on speed and type of subject vehicle as well as adjacent vehicles.				

Note: v_i is SV's speed in Cells/sec

*Total lateral gap for different types of vehicles are estimated using the methodology proposed in chapter 4, and is shown below;

$$lg_i^l = \frac{L_g^{max}}{1 + e^{-\{\alpha_0 + \alpha_1 v_i + \alpha_2 b_i + \alpha_3 s_i\}}} \quad (6.1)$$

Here, lg_i^l is the total lateral gap required by vehicle i of type l . The coefficients used for validating the simulation model are taken from chapter 4 and are shown in Table 6.2. All the symbols have usual meaning as described in chapter 4.

Table 6.2 Coefficients and threshold total lateral gap for 10 m wide road

Vehicle type	Coefficients				L_g^{max} (m)	Threshold speed values for Speed		Threshold speed values for Size	
	α_0	α_1	α_2	α_3		v_{tb}^s (km/hr)	v_{tb}^a (km/hr)	v_{ts}^s (km/hr)	v_{ts}^a (km/hr)
LMV	0.997	-0.032	-0.379	---	3.47	40.98	15.67	---	---
MTW	1.739	-0.034	-0.571	-0.388	3.48	29.97	15.03	38.58	15.03
MThW	1.003	-0.039	-0.588	---	3.06	20.20	10.45	---	---
HMV	0.829	-0.043	-0.394	---	3.48	20.00	12.26	---	---

Table 6.3 CA model Parameters corresponding to validated model (10 m wide road)

Updating Model				
Slow down probability (p_{dec})	0.3	0.1	0.3	0.1
Slow-to-start probability (P_o)	0.2	0.5	0.5	0.1
Break light probability (P_{bl})	0.94	0.94	0.94	0.94
Minimum gap (Cells)	4	4	4	4
Interaction headway (t^h) (Sec)	4	5	4	3
Security distance ($gap_{security}$) (Cells)	10	12	12	10
Lane Change Model				
Probability of lateral movement (P)	0.90	0.60	0.70	0.95
Multiplication parameter (α)	1.0	1.1	1.2	1.0
Back gap ($\beta * v_t^b + \Delta$) factor (β)	1.0	1.0	1.0	1.0

Note: v_t^b is back vehicle speed; Δ is a constant.

6.2.1.1 Macroscopic validation

Flow, speed, and occupancy obtained from Jubilee hills road for each one minute interval, collected over a period of two hours, have been utilized to validate the CA model. Simulated and observed flow-occupancy relationships are shown in Fig. 6.1. Observed and simulated speed-occupancy and flow-speed relationships are shown in Fig. 6.2 and 6.3 respectively. From these three relationships it can be seen that the observed and simulated data are fairly matching.

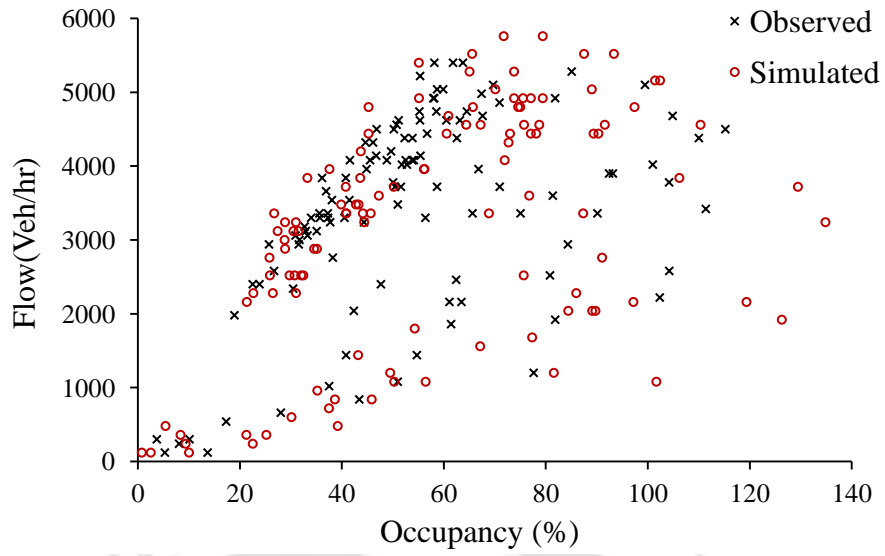


Fig. 6.1 Observed and simulated Flow-Occupancy relationship for Jubilee hills Road

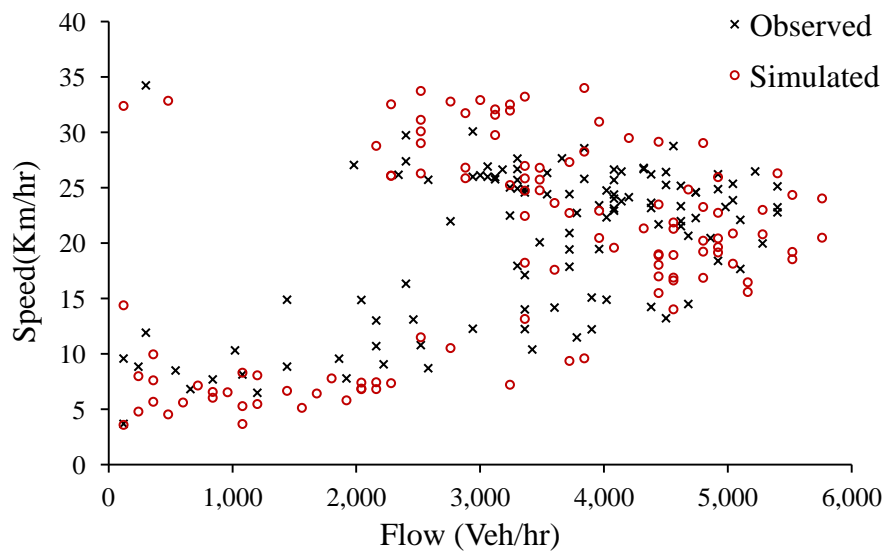


Fig. 6.2 Observed and simulated Speed-Flow relationship for Jubilee hills Road

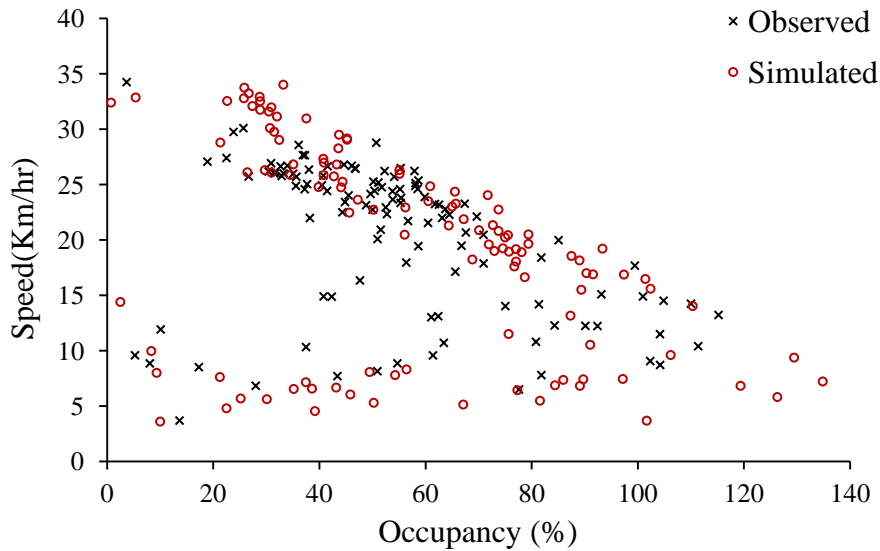


Fig. 6.3 Observed and simulated Speed-Occupancy relationship for Jubilee hills Road

The 2D-KS test has been performed to ensure that the distribution of the simulation results represent the real traffic conditions. A comparison has been made between the observed and simulated data distributions. The 2D-KS test statistics for flow-occupancy, speed-occupancy and speed-flow distributions are found to be 0.2494, 0.2579 and 0.2507, respectively. Corresponding p-values are found to be 0.0368, 0.0252 and 0.0347, respectively. The result indicates that there is no statistically significant difference between the observed and simulated joint distributions.

6.2.1.2 Microscopic validation

Microscopic validation of the model output for free flow traffic has been carried out using the observed and simulated FFS distributions corresponding to different types of vehicles. Free flow speed parameters for the observed and simulated data are given in Table 6.4. Cumulative distributions of observed and simulated FFS for different types of vehicles are compared and are shown in Fig. 6.4. The results indicate that the distributions of both the data for all types of vehicles are matching fairly. The FFS simulated by the model were statistically compared with observed FFS values. A paired F-test null hypothesis of no variance difference was performed to check the closeness between simulated and observed FFS of vehicles. At the same time a paired t-test of null hypothesis of no mean difference was performed to check the closeness of the simulated and observed FFS of vehicles. Statistical comparison of the parameters of observed and simulated cumulative distribution of FFS data shows that these

parameters are not different at 5% level of significance. The statistical measures are shown in Table 6.4.

Table 6.4 Statistical comparison of observed and simulated free flow speeds of various types of vehicles

Vehicle Type	Observed		Simulated		F-test (for variance)		t-test (for mean)	
	μ	σ	μ	σ	$F_{\text{statistical}}$	F_{critical}	$t_{\text{statistical}}$	t_{critical}
LMV	47.42	8.73	48.36	8.53	1.04819	1.40909	0.70342	1.98729
MTW	42.42	6.00	42.87	6.91	1.32828	1.36672	0.53474	1.97066
MThW	30.18	4.51	29.18	4.57	1.02715	1.58520	1.17445	1.98552
HMV	33.40	6.80	32.43	5.88	1.33793	1.56939	0.76916	1.99125

μ -Mean (Km/hr); σ -Standard deviation (Km/hr)

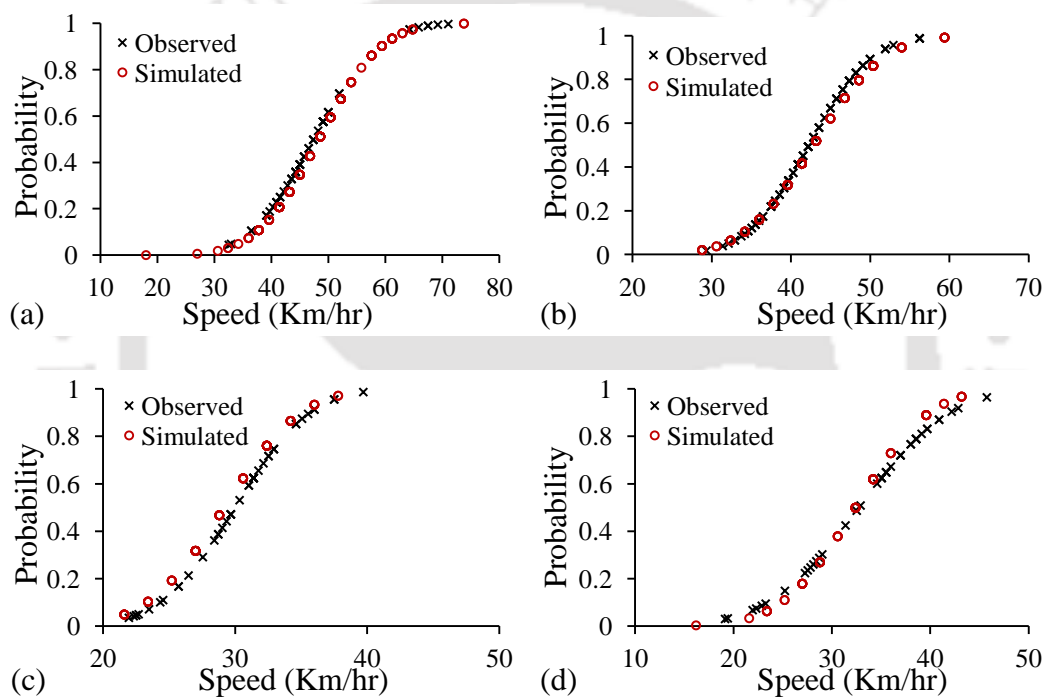


Fig. 6.4 Comparison of observed and simulated cumulative distributions of FFS for LMV (a); MTW (b); MThW(c); HMV(d)

6.2.2 Traffic stream moving on 8.3 m wide road

A two lane road section located at Kodihalli, Bengalore, India, has been chosen to further validate the developed CA model. This road section is of 8.3 m, and the majority of the vehicles are MTW and LMV. Representation of road and traffic characteristics in terms of cells is shown in Table 6.5. Other parameters of the CA model are listed in Table 6.7.

Table 6.5 Representation of 8.3 m wide road (Kodihalli, Bangalore) and the corresponding vehicles related parameters used in the simulation model

Road Characteristics					
Cell width (m)		0.3			
Cell length (m)		0.5			
Road Width (m)		8.30			
Road Width (Cells)		28			
Road length (Cells) (Periodic boundary)		4000			
Warm up time (Sec)		480			
Data collection time (Sec)		60			
Total run time (Sec)		540			
Vehicle Compositions					
LMV	33.62%	HMV	3.90%		
MThW	12.65%	MTW	49.83%		
Vehicle Characteristics					
Parameter	LMV	HMV	MThW	MTW	
Length (Cell)	9	21	6	4	
Width (Cell)	6	8	5	2	
Mean maximum speed (Cell/sec)	26	21	21	24	
Standard deviation of the maximum speed (Cell/sec)	5	3	4	4	
Acceleration (Cell/sec ²)	$v_i \leq 5.5$	4	2	2	5
	$5.5 < v_i < 11$	3	1	2	4
	$v_i \geq 11$	2	1	1	3
Deceleration (Cell/sec ²)	4	3	3	2	
Maximum lateral gap (Cells)	7	7	5	1	
Lateral gap**	Variable based on speed and type of subject vehicle as well as adjacent vehicles.				

Note: v_i is SV's speed in Cells/Sec

**Total lateral gap for different types of vehicles are estimated using the methodology proposed in chapter 4, and is shown below;

$$lg_i^l = \frac{L_g^{max}}{1 + e^{-\{\alpha_0 + \alpha_1 v_i + \alpha_2 b_i + \alpha_3 s_i\}}} \quad (6.2)$$

Here, lg_i^l is the total lateral gap required by vehicle i of type l . The coefficients used for validating the simulation model are taken from chapter 4 and are shown in Table 6.6. All the symbols have usual meaning as described in chapter 4.

Table 6.6 Coefficients and threshold total lateral gap for 8.3 m wide road

Vehicle type	Coefficients				L_g^{max} (m)	Threshold speed values for Speed		Threshold speed values for Size	
	α_0	α_1	α_2	α_3		v_{tb}^s (km/hr)	v_{tb}^a (km/hr)	v_{ts}^s (km/hr)	v_{ts}^a (km/hr)
LMV	1.179	-0.022	-0.469	---	3.60	50.50	22.75	---	---
MTW	1.252	-0.031	-0.295	-0.880	3.60	39.97	15.02	49.94	20.01
MThW	1.003	-0.039	-0.588	---	3.06	20.20	10.45	---	---
HMV	0.829	-0.043	-0.394	---	3.48	20.00	12.26	---	---

Table 6.7 CA parameters corresponding to the validated model (8.3 m wide road)

Updating Model				
Slow down probability (p_{dec})	0.3	0.1	0.3	0.1
Slow-to-start probability (P_o)	0.1	0.5	0.5	0.1
Break light probability (P_{bl})	0.94	0.94	0.94	0.94
Minimum Gap (Cells)	4	4	4	4
Interaction Headway (t^h) (Sec)	2	3	3	2
Security distance ($d_{security}$) (Cells)	10	12	12	10
Lane Change Model				
Probability in lane change (P)	0.95	0.6	0.6	0.95
Multiplication parameter (α)	1.0	1.1	1.0	1.0
Back gap ($\beta * v_t^b + \Delta$) factor (β)	1.0	1.0	1.0	1.0

Note: v_t^b is back vehicle speed

6.2.2.1 Macroscopic validation

Flow, speed and occupancy data obtained from Kodihalli, Bangalore, over a period of two hours have been utilized to validate the model on traffic stream moving on 8.3 m wide road. The field data are mostly corresponding to free flow conditions and this is also evident from the Global flow-occupancy relationship (Fig. 6.11). Simulated and observed flow-occupancy relationships are shown in Fig. 6.5. Similarly, observed and simulated speed-occupancy and flow-speed relationships are shown in Fig. 6.6 and 6.7, respectively.

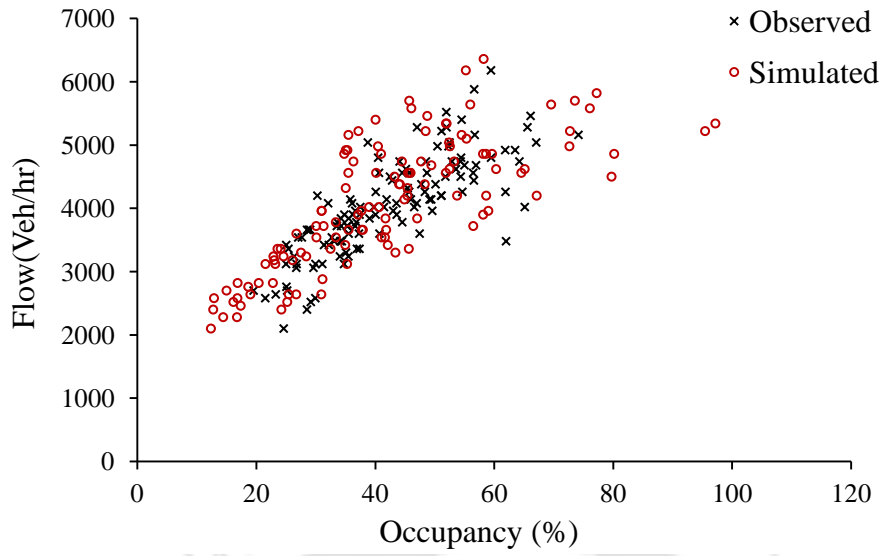


Fig. 6.5 Observed and simulated Flow-Occupancy relationship for Kodihalli Road

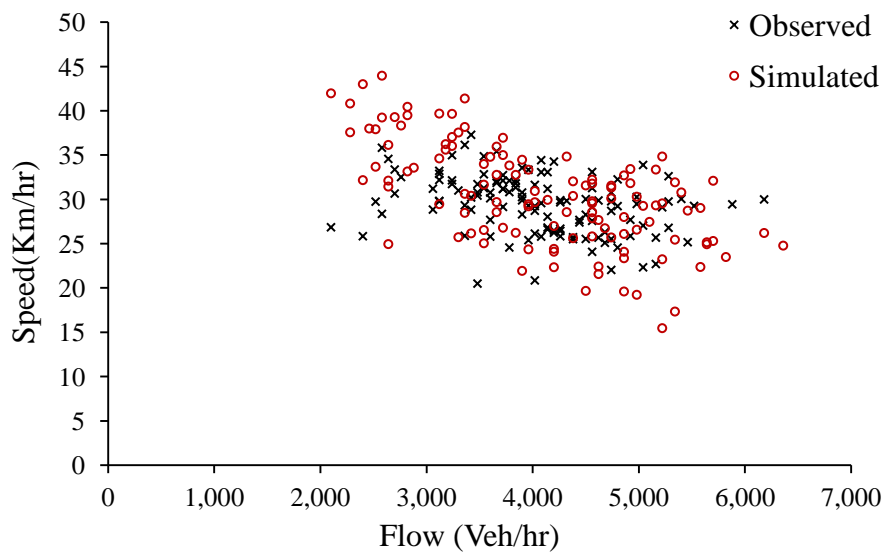


Fig. 6.6 Observed and simulated Speed-Flow relationship for Kodihalli Road

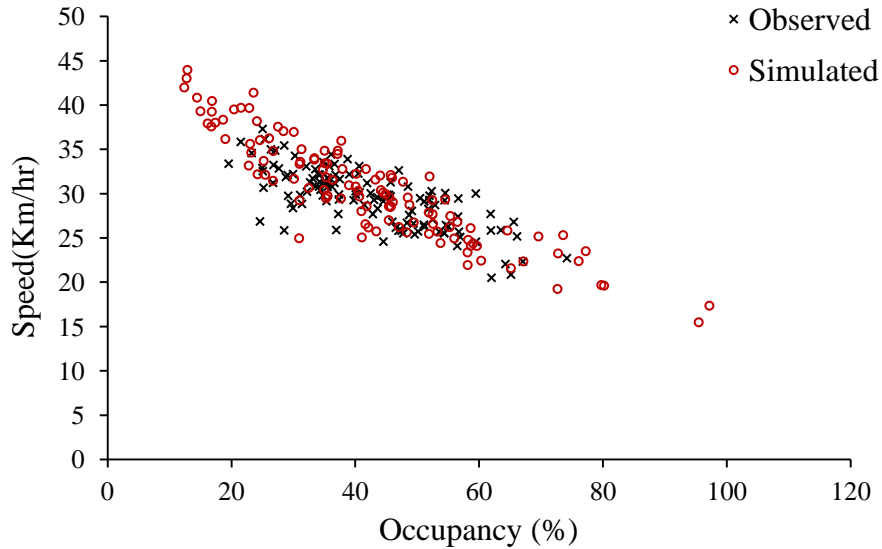


Fig. 6.7 Observed and simulated Speed-Occupancy relationship for Kodihalli Road

The 2D-KS test has been performed to ensure that the distribution of the simulation results represent the real traffic conditions. A comparison has been made between the observed and simulated data distributions. The 2D-KS test statistics for flow-occupancy, speed-occupancy and speed-flow distributions are found to be 0.1709, 0.3154 and 0.2140, respectively. Corresponding p-values are found to be 0.1039, 0.0002 and 0.0176, respectively. The result indicates that there is no statistically significant difference between the observed and simulated joint distributions.

6.2.2.2 Microscopic validation

Similar to the 10 m wide road, microscopic validation of the model for free flow condition has been carried out using the FFS data collected on different types of vehicles. Parameters corresponding to the observed and simulated FFS data are shown in Table 6.8. Comparisons of cumulative distributions of the observed and simulated FFS for different types of vehicles are shown in Fig. 6.8. The simulated FFS values were also statistically compared with the observed FFS values. A paired F-test, with null hypothesis of no variance difference was performed to check the closeness between simulated and observed FFS of vehicles. At the same time a paired t-test of null hypothesis of no mean difference was performed to check the closeness of the simulated and observed FFS of vehicles. The statistical tests on means and variances are shown in Table 6.8. The results indicate that the distributions of both the data, for all types of vehicles, are statistically similar.

Table 6.8 Statistical comparison of observed and simulated free flow speeds of various types of vehicles

Vehicle Type	Observed		Simulated		F-test (for variance)		t-test (for mean)	
	μ	σ	μ	σ	$F_{\text{statistical}}$	F_{critical}	$t_{\text{statistical}}$	t_{critical}
LMV	45.62	7.97	46.52	8.21	1.05979	1.43296	0.76594	1.97993
MTW	43.88	7.90	44.38	7.86	1.01116	1.38914	0.42731	1.98667
MThW	37.00	6.61	35.66	6.80	1.05849	1.43690	1.83280	1.97944
HMV	36.00	6.50	35.07	6.61	1.03387	1.53547	1.17053	1.97993

μ -Mean (Km/hr); σ -Standard deviation (Km/hr)

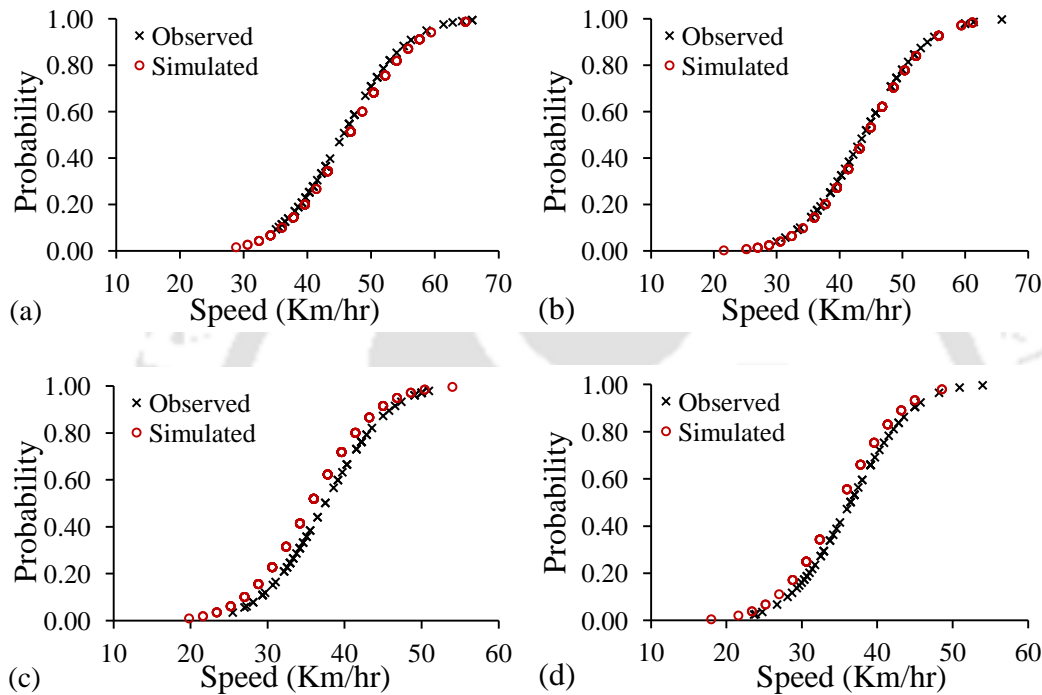


Fig. 6.8 Comparison of observed and simulated cumulative distributions of FFS for LMV (a); MTW (b); MThW(c); HMV(d)

6.3 Microscopic Validation of Queue Formation and Dissipation

Microscopic validation of the model for congested conditions is carried out in terms of the queue formation and dissipation. Data collected from Indira Nagar, Bangalore, have been used for this purpose. Fig. 6.9(b) shows the observed trajectories of the vehicles passing through a queue that was built up due to the downstream traffic conditions. The speed of queue formation and dissipation from field is calculated as 4.11 km/hr and 14.40 km/hr. Similar conditions have been recreated in the model by blocking the traffic across the road widths. Trajectories corresponding to the queue built up and dissipation in the model are shown in Fig. 6.9(a). From the simulated trajectories, the queue formation and dissipation speeds are calculated as 8.25 km/hr and 22 km/hr,

respectively. A close look on both the trajectory data shows that fairly the queue formation in field and simulation model is matching. The estimated formation and dissipation speeds of queue are also fairly matching.

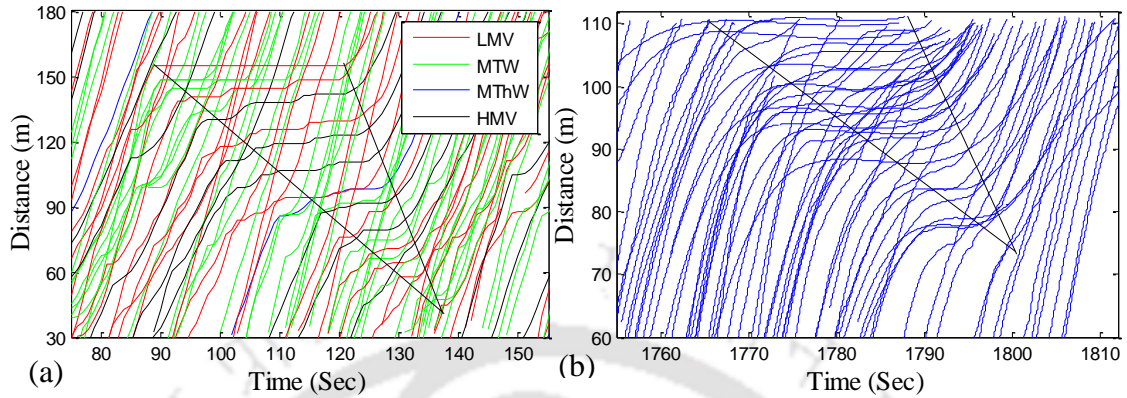


Fig. 6.9 Comparison of the simulated (a) and observed (b) queue formation and dissipation

6.4 Analysis of the Global Measurements

From the simulation model it is possible to collect the data over the entire CA lattice (or the data collected over general measurement region) and such observations are called, global measurements or the measurements made over a general measurement region. When each sub lane is considered as a lane and each cell (filled with the vehicles) is considered as a vehicle, it can be said that the cells (filled with the vehicles) are following lane discipline. In this scenario, heterogeneous traffic is converted into equivalent homogeneous traffic where traffic is composed of cells of identical size. Under these conditions, macroscopic measurements made in terms of cell, adhere to the fundamental relationships among the macroscopic traffic variables. Since all the vehicles are composed of cells and number of cells composing each vehicle type is clearly known, it is easy to convert all the variables in terms of vehicles. This information is utilized in finding the capacities of three lane and two lane road sections in terms of cells. Simulation runs are made for the similar traffic characteristics and CA parameters shown in Tables 6.1-6.3, and 6.5-6.7, respectively, for 10 m and 8.3m wide road sections. Analysis of the global measurements obtained for both the road sections is presented in the following two subsections.

6.4.1 Global flow-occupancy relation for the 10 m wide road

For the conditions presented in Table 6.1, global measurements are taken from the simulation model and the relationship between the global flow and global occupancy (area occupancy) are shown in Fig. 6.10. These global measurements correspond to the general measurement region of 2 km road length and 60 second observation period. It is to be noted that when measurements are taken at global level in terms of cells, global occupancy and area occupancy are the same. The global flow is observed and expressed in terms of number of cells and global occupancy is expressed in percentage of cells in the CA lattice filled with the vehicles. It can be observed that a maximum flow of 1.24 cells/sub-lane/sec is occurring at a global occupancy of 11.5%. Converting flow values from cells/sub-lane/sec to vehicles/hr is described in Table 6.9.

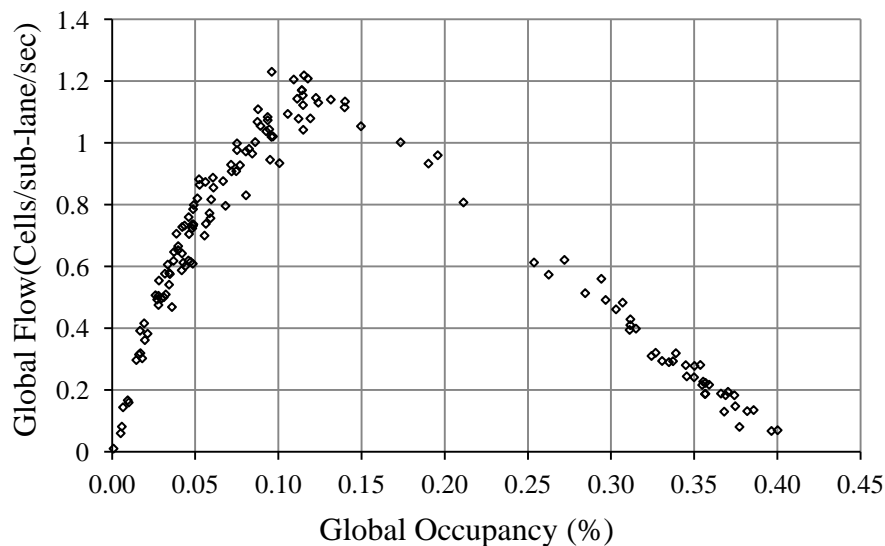


Fig. 6.10 Simulated global flow and global occupancy relationship for 10 m wide road

Flow value in cells/hr comes out to be 146880 cells and the percentage cells related to different vehicles is given in this table. From this information and the corresponding vehicle area, in cells, it is possible to get the flow value corresponding to each vehicle type. When this flow is converted into vehicles, it comes out to be 4669 vehicles/hr and it consists of 2069 LMV, 56 H MV, 467 MThW and 2077 MTW. The maximum flow of 4669 vehicles is corresponding to the vehicle composition given in Table 6.1. This methodology of collecting flow data in cells is very useful when flow is composed of different vehicles, which is the case with heterogeneous traffic.

Table 6.9 Conversion of global flows obtained in cells /sub-lane/sec to vehicles/hr, in case of three lane road

Vehicle Type	Percentage	Length (cells)	Width (cells)	Vehicle Area (cells)	Composition (cells)	% Cells	Flow (cells/hr)	Flow (Veh/hr)
LMV	44.30	9	6	54	2392.20	73.61	111722	2069
MTW	44.50	4	2	8	356.00	10.95	16619	2077
HMV	1.20	21	8	168	201.60	6.20	9410	56
MThW	10.00	6	5	30	300.00	9.23	14009	467
TOTAL							151760	4669

6.4.2 Global flow-occupancy relation for the 8.3 m wide road

The methodology explained in the previous subsection holds good for this road as well. Simulated global flow and global occupancy relationship for two lane roads is shown in Fig. 6.11. The maximum flow comes out to be 1.68 cells/sub-lane/sec corresponding to occupancy of 13%.

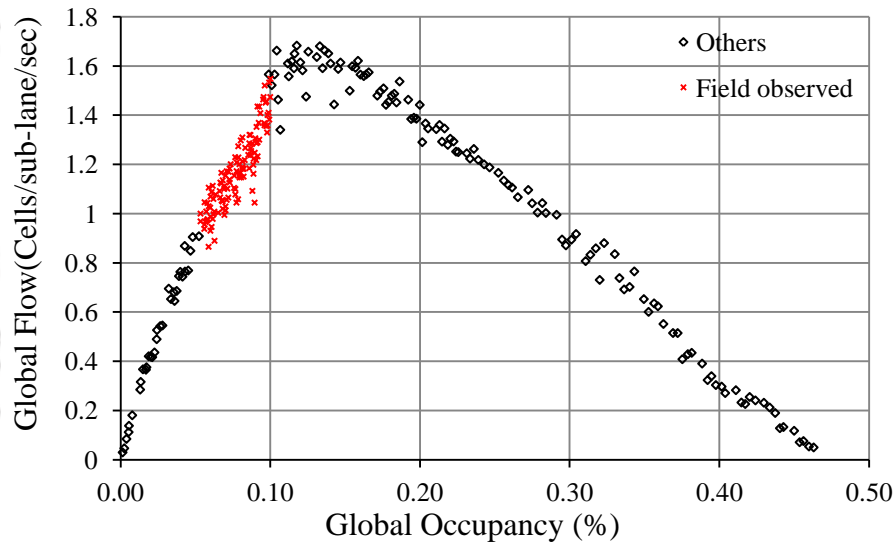


Fig. 6.11 Simulated global flow and global occupancy relationship for 8.3 m wide road

Converting flow values from cells/sub-lane/sec to vehicles/hr is described in Table 6.10. The maximum flow in terms of vehicles is 5211 and it consists 1752 LMVs, 2597 MTWs, 203 HMVs, and 659 MThWs. This maximum flow is true only for the traffic characteristics and CA parameters given in Table 6.5. It can also be observed that the maximum flow produced by 8.3 m wide road is higher than the maximum flow produced by 10 m wide road. This is due to the reason that the FFS of different types of vehicles corresponding to 10 m wide road are low compared to the

FFS of vehicles moving in 8.3 m wide road. Also the composition of MTWs is relatively high compared to the 10 m wide road.

Table 6.10 Conversion of global flows obtained in cells /sub-lane/sec to vehicles/hr, in case of two lane road

Vehicle Type	Percentage	Length (cells)	Width (cells)	Vehicle Area (cells)	Composition (cells)	% Cells	Flow (cells/hr)	Flow (Veh/hr)
LMV	33.62	9	6	54	1815.48	55.88	94629	1752
MTW	49.83	4	2	8	398.64	12.27	20779	2597
HMV	3.90	21	8	168	655.20	20.17	34157	203
MThW	12.65	6	5	30	379.50	11.68	19779	659
TOTAL							169361	5211

6.5 Effect of Road Width on Maximum Flow

Width of two-lane urban roads considered in Indian cities varies between 6.9 to 8.4 m. Given the no-lane-disciplined traffic moving on these roads the traffic flows corresponding to these road widths are expected to be different. The model developed in the present study has been utilized to study the effect of road width (of two-lane roads) on the traffic characteristics. Different simulation runs were carried out by altering the two-lane road width between 6.9 to 8.4 m. The global flow-occupancy relationships for homogeneous (considering only cars but without lane discipline) traffic and heterogeneous traffic corresponding to different road widths are shown in Fig. 6.12. It can be seen from Fig. 6.13 that widening the two-lane road of 6.9 m (23 cells) to 8.4 m (28 cells) increases the maximum flow values in both the cases. When the width was increased from 6.9 m to 7.2 m the maximum flow increment is marginal in case of cars only traffic but it is significant in case of heterogeneous traffic. When the road width is further increased more or less same growth in the maximum flow can be seen in case of heterogeneous traffic. In case of cars only traffic, the growth is nominal up to 7.5 m and there is a significant change between 7.5 m to 8.1 m. Beyond 8.1 m the increment is again marginal. But the difference in flows corresponding to the congested conditions is quite significant in case of cars only traffic. From Fig 6.12 (a) it can be seen that the flows seen in the congested conditions on 6.9 m wide road are considerably low compared to the road widths ranging from 7.2 to 8.4 m. When the global occupancy exceeds 300 vehicles/km there was no difference between the flows corresponding to 7.2 to 8.4 m road widths.

Figure 6.13 (b) shows the global flow-occupancy relationships corresponding to heterogeneous traffic stream moving on road widths ranging from 6.9 to 8.4 m. From the figure it can be seen that the flows in congested conditions were increasing with the increasing road width. The difference in the congested flows was marginal in between 7.2 to 7.5 m and 7.8 to 8.1 m. Significant difference in congested flows can be seen when the road width is changed from 6.9 to 7.2 m and 7.5 to 7.8 m. Presence of smaller sized vehicles in the heterogeneous traffic stream was the main reason behind this difference.

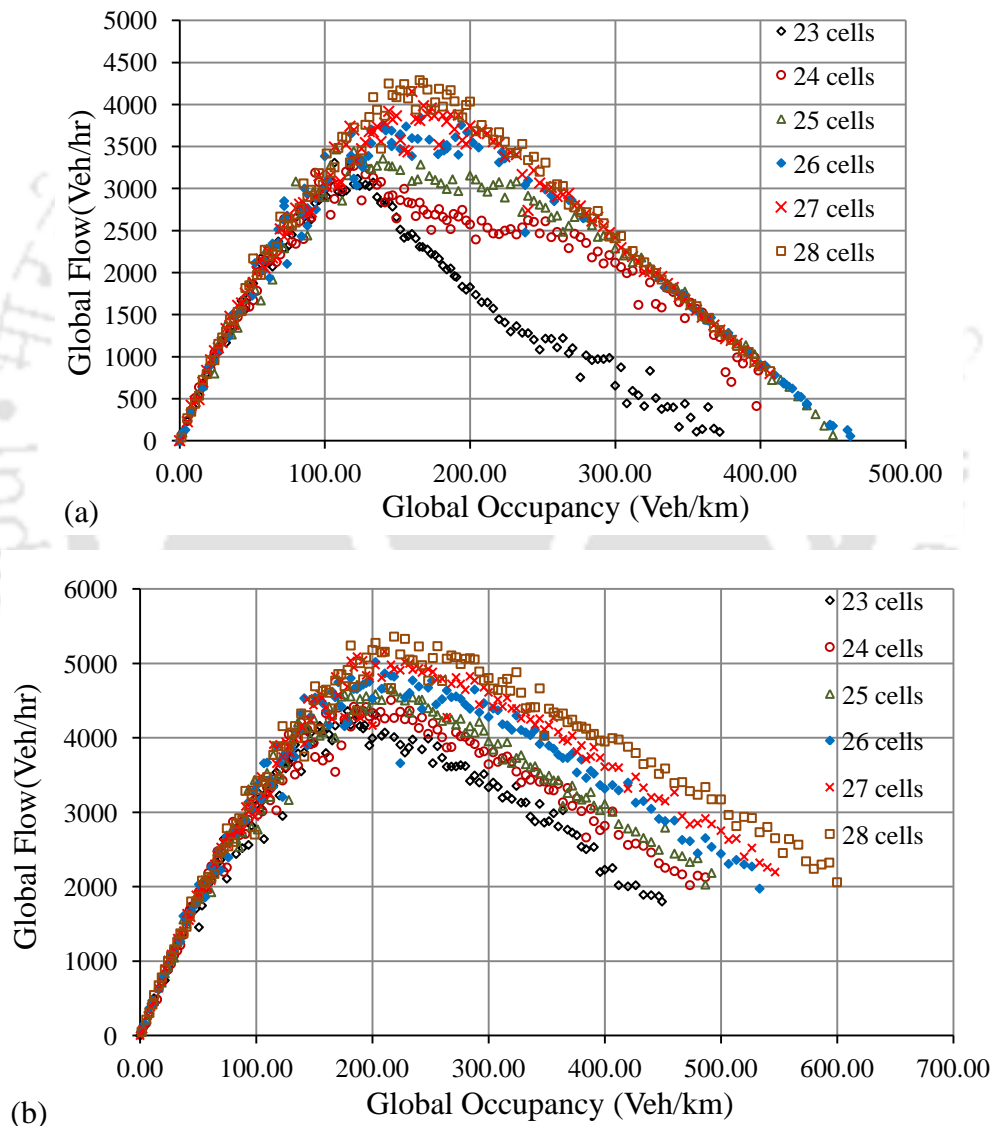


Fig. 6.12 Variation of Global flow-occupancy relationships for homogeneous traffic (a); and heterogeneous traffic (b), with changing two-lane road width

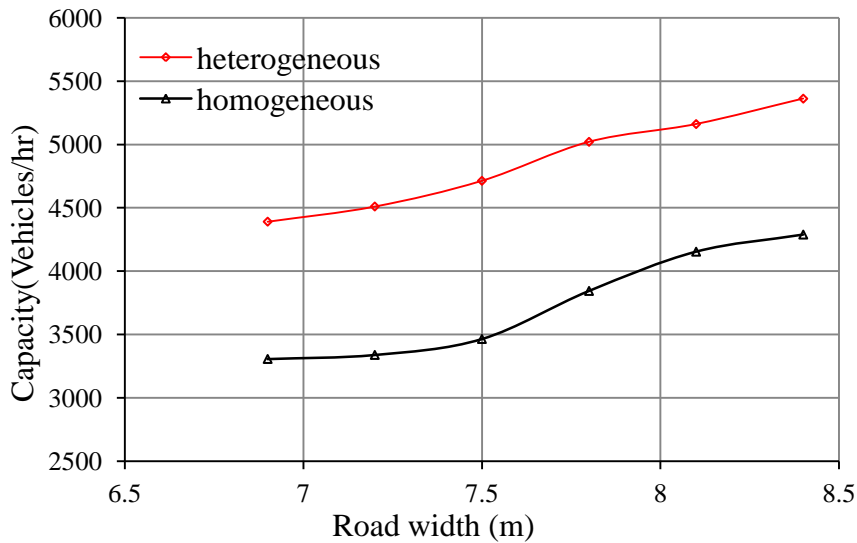


Fig. 6.13 Variation of capacity on slight changes in the width of a two lane road

6.6 Summary and Conclusions

Microscopic model developed in this study has been validated using the data collected at multiple road sections. Model has been validated at macroscopic level in terms of the observed and simulated macroscopic relations. It was observed that the observed and simulated macroscopic relations were statistically similar. The model has been validated at microscopic level in terms of the free flow speed distributions and the formation and dissipation of queues in congested conditions. The validated model has been utilized in studying the effect of two-lane road widths, presently being used in urban regions in India, on the traffic flow behavior. It was observed that changing the road width from 6.9 m to 7.2 or 7.5 m has marginal effect on the maximum flows crossing the road section, in case of both heterogeneous traffic and cars only traffic. The change in the maximum flow of heterogeneous traffic stream was significant in case of road width increasing from 7.5 to 7.8 m.

Summary and Conclusions

7.1 Summary

Understanding the behavior of vehicles moving in no-lane-disciplined heterogeneous traffic stream is essential in developing the simulation model. Based on the empirical observations it has been found that one of the important characteristics of no-lane-disciplined heterogeneous traffic is the variable lateral gap maintaining behavior of different types of vehicles. In this study the total lateral gap maintaining behavior of vehicles has been analyzed using the trajectory data obtained from the video image processing software, TRAZER. Total minimum lateral gap (gap on both the sides of vehicle) maintained by four types of vehicles, namely, LMV, MTW, MThW, and HMV has been modeled in this study. Field observations suggest significant variability in the lateral gaps even when the passing/overtaking vehicle was traveling at more or less constant speed. Logistic model has been used to model the total lateral gaps. From the estimated models it was observed that the speed of the subject vehicle, size and speed of both the adjacent vehicles affect the lateral gaps. It has also been observed that the size and speed of the adjacent vehicles influence the lateral gap only when the subject vehicle's speed is more than certain critical speed. The impact of side vehicle has been found to be prominent even at lower speed of the subject vehicle in case of a relatively wide road. This lateral gap maintaining behavior of vehicles of no-lane-disciplined heterogeneous traffic has been incorporated in the present CA based simulation model. The cell structure of the present CA model has been modified to adequately represent the lateral gap maintaining behavior.

In no-lane-disciplined heterogeneous traffic stream, following vehicle encounters multiple leading vehicles. In this study, FLV, LFLV and RFLV have been considered as the leading vehicles and the closest among these vehicles would be the effective leading vehicle. The movement of the following vehicle was considered to be depending on the effective leading vehicle. The impact of side vehicles has also been considered in indentifying the effective leading vehicle. The road section was divided into multiple numbers of sub-lanes in terms of finer cell size. The movement of vehicles in no-lane-disciplined heterogeneous traffic stream is governed by the finer

lateral movements. Gradual lateral shifting has been introduced, unlike the instantaneous lane change observed in homogeneous traffic.

Updating procedures and the corresponding parameters depend on the cell structure of the CA model. Since the cell structure was changed in this study, its effect on the updating procedures and the corresponding parameters was thoroughly analyzed. The parameters of the present CA model have been arrived at based on the previous researches, field observations, and parametric analysis. Based on the parametric analysis, some of the parameters have been modified. The impact of variable lateral gap and interaction headways were found to be prominent. The developed model has been macroscopically validated using the field observed speed, flow, and occupancy data of two different road sections. The macroscopic relations of the observed and simulated data were matching fairly. Simulated free flow conditions are further validated by comparing the observed and simulated free flow speed distributions. Model's ability to simulate the congested traffic conditions has also been validated by comparing the observed and simulated queue formation and dissipation characteristics. The queue formation and dissipation speeds obtained from the simulation model were comparable to the field observed values.

The developed model was used to analyze the effect of road width (specifically two lane roads) being used in urban regions. It has been observed that slight changes in the road width, between 6.9 to 8.4 m, significantly influence the traffic stream characteristics.

7.2 Conclusions

7.2.1 Trajectory correction

Empirical observations are crucial in understanding and modeling the traffic behavior. Analysis of the vehicular trajectories leads to a fair understanding of the traffic behavior and for this to be successful trajectory data need to be fairly accurate. Trajectories obtained from TRAZER were found to be erroneous and need to be corrected before proceeding to data analyses.

1. In this study, a methodology based on complete ensemble empirical mode decomposition with adaptive noise (CEEMDAN) is proposed to smooth the trajectory data.

2. From the error analysis it has been found that the CEEMDAN approach was relatively better compared to the existing approaches in smoothing the trajectory.
3. It was found that successive smoothing is essential to estimate the accurate speed and acceleration from the smoothed trajectories.
4. Wavelet Transform(WT) using 'gaussian' wavelet function (for CWT) and 'spline' wavelet function(for DWT) were found to be more accurate in estimating the instantaneous speed and acceleration from the smoothed trajectories.
5. Internal consistency analysis of the position and speed also proved the suitability of proposed method (WT) for speed estimation.

7.2.2 Lateral gap model

Lateral gap maintaining behavior of vehicles moving in no-lane-disciplined heterogeneous traffic depends on several factors. Total lateral gaps (gap on both the sides of a passing/overtaking vehicle) maintained by four types of vehicles, namely, LMV, MTW, MThW, and HMV have been modeled in this study.

1. Field observations suggest significant variability in the total lateral gaps even when the passing/overtaking vehicle is traveling at a constant speed.
2. A vehicle maintains a minimum lateral gap with its adjacent vehicle at zero speed and a maximum lateral gap beyond certain speed limit. Keeping in view the minimum and maximum lateral gaps, Logistic curve model was found to be more suitable in representing the vehicular total lateral gap maintaining behavior.
3. It has been observed that the speed of the subject vehicle, size, and the speeds of both the adjacent vehicles affect the total lateral gaps.
4. It was also found that the size and speed of the adjacent vehicles influence the total lateral gap only when the subject vehicle is traveling beyond certain critical speed. This speed is more than 30 km/hr in case of LMV and more than 20 km/hr in case of the other vehicles.

5. In case of relatively wide roads, the impact of side vehicles was found to be prominent even at lower speeds of the subject vehicle.
6. Linear trends have been observed between various threshold speeds and the road width.

7.2.3 Traffic characteristics

1. It has been observed that in no-lane-disciplined heterogeneous traffic the following vehicle is not only influenced by the LV, but, also by the other vehicles such as, LFLV and RFLV.
2. Effective LV is the closest longitudinal vehicle among FLV, LFLV and RFLV.
3. Lateral shifting of a vehicle depends on the availability of lateral gap considering the impact of side vehicles in addition to the other safety criteria based on available back vehicle.

7.2.4 Simulation model

Cell width of the present CA model is modified based on the minimum lateral gap requirement of vehicles and the physical width of smaller sized vehicles such as MTW and MThW. Cell length of the CA model was decided based on the mechanical characteristics of vehicles, such as accelerations etc. Lateral gaps were represented explicitly, i.e., the lateral gap required by a vehicle is not included in the physical width of the vehicles.

1. It was found that even the LFLV or RFLV, if longitudinally closer to the SV compared to the LV, sometimes hamper the movement of SV. In this case one of these two vehicles would be the effective leading vehicle. In this scenario the SV may reduce the speed based on the available road width ahead and pass the LFLV or RFLV rather than following the LFLV or RFLV.
2. The interaction headway was found to be significantly influencing the traffic stream behavior. Increasing interaction headway reduces the maximum flow. It indicates that, in no-lane-disciplined heterogeneous traffic, the effect of the

leading vehicle is not felt on the following vehicle unless both the vehicles are longitudinally closer. This may be due to the reason that the freedom available for the following vehicle to adjust its lateral position. It can be in the form of completely shifting to the other available part of the road or veering away slightly.

3. Results obtained based on the various lateral gap models indicate that the gap maintaining behavior has significant impact on the macroscopic relations. Constant (but low) lateral gap model results in overestimated capacity flows.
4. The final simulation model has been validated for two different road sections. The simulated macroscopic relationships were found to be statistically matching with the observed macroscopic relationships.
5. Two-dimensional Kolmogorov-Smirnov (2D-KS) test between observed and simulated distributions indicates that the simulated distributions of flow-occupancy and speed-occupancy are statistically similar to that of the observed joint distributions.
6. Model results have also been validated at microscopic level in terms of comparisons between the observed and simulated FFS distributions corresponding to various vehicle types.
7. Ability of the model to replicate the congested conditions has been verified in terms of queue formation and dissipation. Queue formation and dissipation speeds obtained from the model were similar to that of the field observed values.

7.2.5 Effect of road width

The simulation model developed in this study has been utilized in studying the effect of two-lane road widths, presently being used in urban regions in India, on the traffic flow behavior.

1. It was observed that changing the road width from 6.9 m to 7.2 or 7.5 m has marginal effect on the maximum flows crossing the road section, in case of both heterogeneous traffic and cars only traffic.

2. The change in the maximum flow of heterogeneous traffic stream was significant in case of road width increasing from 7.5 to 7.8 m.
3. Increasing road width from 6.9 to 7.2 m or 7.5 to 7.8 m has significant effect on the congested flows of heterogeneous traffic stream. The difference in the congested flows was marginal in between 7.2 to 7.5 m and 7.8 to 8.1 m.

7.3 Contributions

The goal of this research effort was to develop an adaptable no-lane-disciplined heterogeneous traffic flow model. This thesis contributes to this objective in the following aspects;

- A systematic methodology for the correction of erroneous trajectory, such as CEEMDAN is proposed.
- A framework for extraction of vehicle speed using Wavelet Transforms is proposed.
- Logistic curve model is proposed to model the variable total lateral gap maintaining behavior of vehicles moving in no-lane-disciplined heterogeneous traffic stream considering the impact of side vehicles speed and size.
- Cell structure of the cellular automata model is modified to represent the variable lateral gap maintaining behavior of vehicles.
- Updating procedures of the CA model are modified based on the impact of effective leading vehicle.
- Forward movement and lateral movement rules of CA model are adapted in accordance with effective route width, effective leading vehicles, and safety criteria.

7.4 Further Scope

The proposed method of speed estimation from the smoothed trajectories may be further checked using various other wavelet functions. The estimation of total lateral gap, specifically for HMV and MThW, may further be investigated for various road widths. More data on this aspect may reveal further better interrelations between the

total lateral gap and the traffic stream characteristics. The cell structure and cell width can be further refined to check its effect on the model output. More field data related to the congested branch can help in further fine tuning of various CA parameters. The CA model developed in this study can be extended to simulate the traffic flows near intersections. This model can be used in analyzing the impact of various traffic control measures.





REFERENCES

- Adeli, H., and Ghosh-Dastidar, S., 2004. Mesoscopic-wavelet freeway work zone flow and congestion feature extraction model. *Journal of Transportation Engineering*, 130 (1), 94–103.
- Adeli, H., and Samant, A., 2000. An adaptive conjugate gradient neural network-wavelet model for traffic incident detection. *Computer-Aided Civil and Infrastructure Engineering*, 15 (4), 251–260.
- Adnan, M.A., Zainuddin, N.I., Sulaiman, N., and Besar, T.B.H.T., 2013. Vehicle Speed Measurement Technique using Various Speed Detection Instrumentation. *IEEE Business Engineering and Industrial Applications Colloquium*, 7-9, April 2013, 668-672.
- Antonov, L., and Stoyanov, S., 1996. Step by step filter - an approach for noise reduction in the derivative UV-visible spectra. *Analytical Chimica Acta*, 324, 77-83.
- Arasan, V.T., and Koshy, R. Z., 2005. Methodology for Modeling Highly Heterogeneous Traffic Flow. *Journal of Transportation Engineering*, 131(7), 544-551.
- Barache, D., Antoine, J. P., and Dereppe, J. M., 1997. The Continuous Wavelet Transform, an Analysis Tool for NMR Spectroscopy. *Journal of Magnetic Resonance*, 128, 1–11.
- Barak, P., 1995. Smoothing and Differentiation by an Adaptive-Degree Polynomial Filter. *Anal Chem.*, 67, 2758-2762.
- Barlovic, R., Santen, L., Schadschneider, A., and Schreckenberg, M., 1998. Metastable states in cellular automata for traffic flow. *European Physical Journal B*, 5, 793-800.
- Benjamin, S. C., Johnson, N. F., and Hui, P. M., 1996. Cellular automata models of traffic flow along a highway containing a junction. *Journal of Physics A, Mathematical and General*, 29(12), 3119-3127.
- Blue, V. J., and Adler, J. L., 2001. Cellular automata micro simulation for modeling bidirectional pedestrian walkways. *Transportation Research Part B*, 35, 293–312
- Brackstone, M., McDonald, M. and Wu, J., 1998. Lane changing on the motorway: Factors affecting its occurrence, and their implications. *Proc. 9th International Conference Road Transport Inform. Control*, London (Inspect/Iee, London, UK), 160–164.
- Bruce, L.M., and Li, J., 2001. Wavelets for computationally efficient hyperspectral derivative analysis. *IEEE Transactions on geosciences and remote sensing*, 39(7), 1540-1546.
- Burstedde, C., Kirchner, A., Klauck, K., Schadschneider, A., and Zittartz, J., 2001. Cellular automaton approach to pedestrian dynamics—applications. M. Schreckenberg, S. Sharma (Eds.), *Pedestrian and Evacuation Dynamics*, Springer, Berlin (2001), 87.
- Button, K., 2010. *Transport Economics*, 3rd Ed., Edward Elgar Publishing Limited, UK.

- Cameron, D.G., and Moffatt, D.J., 1987. A Generalized Approach to Derivative Spectroscopy. *Applied Spectroscopy*, 41, 539-534.
- Chakroborty, P., Agrawal, S., and Vasishta, K., 2004. Microscopic Modeling of Driver Behavior in Uninterrupted Traffic Flow. *Journal of Transportation Engineering*, 130(4), 438-451.
- Chandler, R. E., Herman, R., and Montroll, E. W., 1958. Traffic dynamics: studies in car following. *Operations Research*, 6, 165-184.
- Chau, F.T., Shih, T.M., Gao, J.B., Chan C.K., 1996. Application of the Fast Wavelet Transform Method to Compress Ultraviolet-Visible Spectra. *Applied Spectroscopy*, 50, 339-348.
- Chen, Y., Qin, X., Noyce, A. D., and Lee, C., 2010. Interactive Process of Microsimulation and Logistic Regression for Short-Term Work Zone Traffic Diversion. *Journal of Transportation Engineering*, 136(3), 243-254.
- Choudhury, C., Ben-Akiva, M., Rao, A., Lee, G., Toledo, T. 2007. State dependence in lane changing models. Allsop RE, Bell MGH, Heydecker BG, eds. *Proc. 17th Internat. Sympos. Transportation and Traffic Theory*, London, 711-733.
- Chowdhury, D., Santen, L., and Schadschneider, A., 2000. Statistical Physics of Vehicular Traffic and Some Related Systems. *Physics Reports*, 329(4), 199-329.
- Chowdhury, D., Wolf, D. E., and Schreckenberg, M., 1997. Particle hopping models for two-lane traffic with two kinds of vehicles: Effects of lane-changing rules. *Physica A: Statistical and Theoretical Physics*, 235(3-4), 417-439.
- Cremer, M., and Ludwig, J., 1986. A fast simulation model for traffic flow on the basis of Boolean operations. *Mathematics and Computers in Simulation*, 28 (4), 297-303.
- Daganzo, C. F., 2006. In traffic flow, cellular automata = kinematic waves. *Transportation Research Part B: Methodological*, 40(5), 396-403.
- Das, S., Gupta, V.K., 2008. Wavelet-based simulation of spectrum-compatible aftershock accelerograms. *Earthquake Engng Struct. Dyn.*, 37, 1333-1348.
- Daubechies, I., 1990. The wavelet transforms time-frequency localization and signal analysis. *IEEE Trans. Inform. Theory*, 36, 961-1004.
- Dey, P.P., Chandra, S., and Gangopadhyay, S., 2008. Simulation of Mixed Traffic Flow on Two-Lane Roads. *Journal of Transportation Engineering*, 134(9), 361-369.
- Duell, M., Levin, M., Waller, S.T., 2014. On estimating vehicle energy consumption using dynamic traffic assignment vehicle trajectories. 5th International symposium on dynamic traffic assignment, June 17-19, Salerno, Italy.
- Emmerich, H., and Rank, E., 1997. An improved cellular automaton model for traffic flow simulation. *Physica A: Statistical and Theoretical Physics*, 234 (3-4), 676-686.
- Ervin, R. D., MacAdam, C. C., Gilbert, K., Tchoryk, Jr. P., 1991. Quantitative characterization of the vehicle motion environment (VME). In: *Proceedings of 2nd Vehicle Navigation and Information Systems Conference*, 1991, 1011-1029.
- Gazis, D. C., Herman, R., and Rothery, R. W., 1961. Nonlinear follow the leader models of traffic flow. *Operations Research*, 9, 545-567.

- Gentile, A., and Messina, A., 2003. On the continuous wavelet transforms applied to discrete vibrational data for detecting open cracks in damaged beams, *International Journal of Solids and Structures*, 40, 295–315.
- Gipps, P. G., 1981. A behavioural car following model for computer simulation. *Transportation Research B*, 15, 105-111.
- Gorry, P. A., 1990. General least-squares smoothing and differentiation by the convolution (Savitzky-Golay) method. *Anal. Chem.*, 62(6), 570–573.
- Greaves, S., and Figliozzi, M., 2008. Urban Commercial Vehicle Tour Data Collection Using Passive GPS Technology: Issues and Potential Applications. Proceeding of the 87th Transportation Research Board Annual Meeting CD rom - Washington DC. USA.
- Grossmann, A., and Morlet, J., 1984. Decomposition of hardy functions into square integrable wavelets of constant shape. *Siam J Math Anal*, 15(4), 723–736.
- Gunay, B., 2007. Car following theory with lateral discomfort. *Transportation Research Part B: Methodological*, 41(7), 722-735.
- Gundaliya, P.J., 2005. Heterogeneous Traffic Flow Modelling for an Arterial Road using Cellular Automata. Ph D thesis, IIT Bombay.
- Haswell, S.J., 1992. *Practical Guide to Chemometrics*, Marcel Dekker, New York, 264–267.
- Hsu, C. C., Lin, Z. S., Chiou, Y. C., and Lan, L. W., 2007. Exploring Traffic Features with Stationary and Moving Bottlenecks Using Refined Cellular Automata. *Journal of the Eastern Asia Society for Transportation Studies*, 7, 2502-2516.
- Huang, N. E., Shen, Z., Long, S. R., Wu, C. M., Shih, H. H., Zheng, Q., Yen, N. C., Tung, C. C., and Liu, H. H., 1998. The empirical mode decomposition and the Hilbert spectrum for nonlinear and non-stationary time series analysis. *Proc. R. Soc. London, A* 454, 903–995.
- Jang, J. S. R., Sun, C. T., and Mizutani, E., 1997. *Neuro-Fuzzy and Soft Computing: A Computational Approach to Learning and Machine Intelligence*. Prentice Hall, New Jersey.
- Jiang, X., and Adeli, H., 2004. Wavelet packet-autocorrelation function method for traffic flow pattern analysis. *Computer-Aided Civil and Infrastructure Engineering* 19 (5), 324–337.
- Jiang, X., and Adeli, H., 2005. Dynamic wavelet neural network model for traffic flow forecasting. *Journal of Transportation Engineering* 131 (10), 771–779.
- Jianwen, L., Jing, B., and Jinhua, S., 2006. Application of the wavelet transforms on axial calculation in ultrasound elastography. *Progress in Natural Science*, 16(9), 942-947.
- Jin, W.L., 2010. A kinematic wave theory of lane-changing traffic flow. *Transportation Res. Part B*, 44(8–9), 1001–1021.

- Kanagaraj, V., Asaithambi, G., Toledo, T., and Lee, T-C., 2015. Trajectory data and flow characteristics of mixed traffic. Presented at the 94th Transportation Research Board Annual Meeting (TRB), Washington D.C., USA.
- Kauppinen, J.K., Moffatt, D.J., Mantsch, H.H., and Cameron, D.G., 1981. Fourier transforms in the computation of self-deconvoluted and first-order derivative spectra of overlapped band contours. *Anal. Chem.* 53(9), 1454–1457.
- Kerner, B. S. and Rehborn, H., 1996. Experimental properties of complexity in traffic flow. *Physical Review E.*, 53(5), 4275-4278.
- Kerner, B. S., Klenov, S. L., and Wolf, D. E., 2002. Cellular automata approach to three-phase traffic theory. *Journal of Physics A, Mathematical and General*, 35, 9971-10013.
- Kesting, A., Treiber, M., and Helbing, D., 2007. General lane-changing model MOBIL for car-following models. *Transportation Research Record: Journal of the Transportation Research Board* 1999, 86–94.
- Knospe, W., Santen, L., Schadschneider, A., and Schreckenberg, M., 2000. Towards a realistic microscopic description of highway traffic. *Journal of Physics A, Mathematical and General*, 33(48), L477-L485.
- Kovvali, V. G., Alexiadis, V., and Zhang, P. E., 2007. Video-Based Vehicle Trajectory Data Collection. 72nd Annual Meeting, Transportation Research Board, Washington D.C.
- Lan, L. W., Chiou, Y. C., Lin, Z. S., and Hsu, C. C., 2009. A refined cellular automaton model to rectify impractical vehicular movement behavior. *Physica A*, 388 (18) (2009), pp. 3917–3930
- Lan, L. W., and Chang, C. W., 2003. Motorbike's moving behavior in mixed traffic: particle-hopping model with Cellular Automata. *Journal of the Eastern Asia Society for Transportation Studies* 5, 23–37.
- Lan, L. W., Chiou, Y. C., Lin, Z. H., and Hsu, C. C., 2010. Cellular automaton simulations for mixed traffic with erratic motorcycles' behaviours. *Physica A*, 389, 2077–2089.
- Lan, W. L. and Chang, C. W., 2005. Inhomogeneous Cellular Automata modelling for mixed traffic with cars and motorcycles. *Journal of Advanced Transportation*, 39, 323-349.
- Lan, W. L. and Hsu, C., 2006. Formation of Spatiotemporal Traffic patterns with Cellular Automaton Simulation. TRB 2006 Annual Meeting CD-ROM.
- Laval, J. A., and Daganzo, C. F., 2006. Lane-changing in traffic streams. *Transportation Res. Part B*, 40(3), 251–264.
- Laval, J. A., and Leclercq, L., 2008. Microscopic modeling of the relaxation phenomenon using a macroscopic lane-changing model. *Transportation Res. Part B*, 42(6), 511–522.

- Lee, T. C., Polak, J. W. and Bell, M. G. H., 2008, Trajectory Extractor User Manual Version 1.0, Technical Report, Centre for Transport Studies, Imperial College London, UK.
- Leung, A. K. M., Chau, F. T., and Gao, J. B., 1998. Wavelet Transform: a method for derivative calculation in analytical chemistry. *Anal chem.*, 70(24), 5222-5229.
- Li, K. P., Gao, Z. Y., and Ning, B., 2005. Cellular automaton model for railway traffic, *Journal of Computational Physics* 209 (1), 179-192.
- Lin, Z-S., Hsu, C-C., Chiou, Y-C., and Lan, L. W., 2013. Exploring Traffic Patterns and Phase Transitions with Cellular Automaton. *Asian Transport Studies*, 2(4), 395-410.
- Luo, Y., Jia, B., Liu, J., Lam, H. K. W., Li, X., and Gao, Z., 2013. Modeling the interactions between car and bicycle in heterogeneous traffic. *Journal of Advanced Transportation*, DOI: 10.1002/atr.1257.
- Maerivoet, S., and De Moor, B., 2005. Cellular automata models of road traffic. *Physics Reports*, 419(1), 1-64.
- Maerivoet, S., 2006. Modelling Traffic on Motorways: State-of-the-Art, Numerical Data Analysis, and Dynamic Traffic Assignment. PhD Thesis, Faculty of Engineering, K. U. Leuven, Leuven, Belgium.
- Mallat, S., 2008. *A Wavelet Tour of Signal Processing*, Academic Press, New York.
- Mallat, S., and Hwang, W. L., 1992. Singularity detection and processing with wavelets. *IEEE Transactions on information theory*, 38(2), 617-643.
- Mallikarjuna C., and Raghukanth, S. T. G., 2009. Forecasting the air traffic for North-East Indian cities. *Advances in Adaptive Data Analysis*, 2(1), 1-16.
- Mallikarjuna, C., 2007. *Analysis and Modeling of Heterogeneous Traffic*. Ph.D thesis, IIT Delhi, India.
- Mallikarjuna, C., and Ramachandra Rao, K., 2009. Cellular automata model for heterogeneous traffic. *Journal of Advanced Transportation*, 43(3), 321-345.
- Mallikarjuna, C., and Ramachandra Rao, K., 2011. Heterogeneous traffic flow modelling: a complete methodology. *Transportmetrica*, 7(5). 321-345.
- Mallikarjuna, C., Phanindra, A., and Ramachandra Rao, K., 2009. Traffic Data Collection under Mixed Traffic Conditions Using Video Image Processing. *Journal of Transportation Engineering*, 135(4). 174-182.
- Mathew, T. V., Gundaliya, P., and Dhingra, S. L., 2006. "Heterogeneous Traffic Flow Modeling and Simulation Using Cellular Automata." 9th International conference on Applications of Advanced Technology in Transportation, Chicago, Illinois, USA, 492-497.
- Mathew, T. V., Munigety, C. R., and Bajpai, A., 2013. Strip-Based Approach for the Simulation of Mixed Traffic Conditions, *Journal of Computing in Civil Engineering*, 29(5), 04014069.

- Messina, A., 2004. Detecting damage in beams through digital differentiator filters and continuous wavelet transforms. *Journal of Sound and Vibration*, Elsevier, 272, 385-412.
- Michaels, R. M., 1965. Perceptual factors in car following. In *Proceedings of the 2nd international symposium on the theory of traffic flow*, 1963, 44–59.
- Minh, C. C., Matsumoto, S., and Sano, K., 2005. Characteristics of passing and paired riding maneuvers of motorcycle. *Journal of the Eastern Asia Society for Transportation Studies*, 6, 186-197.
- Mittermayr, C. R., Nokolov, S. G., Hutter, H., and Grasserbauer, M., 1996. Wavelet denoising of Gaussian peaks: a comparative study. *Chemometrics and Intelligent Laboratory Systems*, 34, 187–202.
- Montanino, M. and Punzo, V., 2013. Making NGSIM Data Usable for Studies on Traffic Flow Theory: A Multistep Method for Vehicle Trajectory Reconstruction. *Transportation Research Record*, No. 2390, TRB, Washington, D.C., 99-111.
- Moridpour, S., Rose, G., and Sarvi, M., 2010. Effect of Surrounding Traffic Characteristics on Lane Changing Behavior. *J. Transp. Eng.*, 136(11), 973–985.
- Munigety, C. R., Vicraman, V., and Mathew, T. V., 2014. Semiautomated Tool for Extraction of Microlevel Traffic Data from Videographic Survey. *Transportation Research Record: Journal of the Transportation Research Board*, No. 2443, Transportation Research Board of the National Academies, Washington, D.C., 88–95.
- Nagaraj, B. N., George, K. J., and John, P. K., 1990. A Study of Linear and Lateral Placement of Vehicles in Mixed Traffic Environment through Video-Recording. *Highway Res. Bulletin*, 42, Indian Roads Congress, New Delhi, India, 105– 136.
- Nagatani, T., 1993. Self-organization and phase transition in traffic-flow model of a two-lane roadway, *J. Phys. A: Math. Gen.*, 26, 781.
- Nagel, K. and Schreckenberg, M., 1992. A cellular automaton model for freeway traffic. *Journal de Physique I*, 2(12), 2221-2229.
- Nagel, K., 1995. Particle hopping vs. fluid dynamic models for traffic flow. In: Wolf, D.E., Schreckenberg, M., Bachem, A. (Eds.), *Workshop on Traffic and Granular Flow*. World Scientific Publishers, 41–56.
- Nagel, K., Wolf, D. E., Wagner, P., and Simon, P., 1998. Two-lane traffic rules for cellular automata: A systematic approach. *Physical Review E*, 58(2), 1425-1437.
- Nassab, K., Schreckenberg, M., Boulmakoul, A., and Ouaskit, S., 2006. Effect of the lane reduction in the cellular automata models applied to the two-lane traffic. *Physica A* 369(2), 841-852.
- Newell, G. F., 1961. Nonlinear effects in the dynamics of car following. *Operations Research*, 9(2), 209–229.
- Ossen, S., and Hoogendoorn, S. P., 2008. Validity of trajectory-based calibration approach of car-following models in the presence of measurement errors.

- Transportation Research Record: Journal of the Transportation Research Board, 2088, 117–125.
- Pal, D., and Mallikarjuna, C., 2010. Cellular Automata Cell Structure for Modeling Heterogeneous Traffic. *European Transport*, 45, 50-63.
- Palaniswamy, S. P., Gynnerstedt, G., and Phull, Y. R., 1985. Indo-Swedish Road Traffic Simulation Model: Generalized Traffic System Simulator. *Transportation Research Record: Journal of Transportation Research Board*, 1005, 72-80.
- Peacock, J. A., 1983. Two-dimensional goodness-of-fit testing in astronomy. *Month. Not. Roy. Astron. Soc.*, 202, 615–627.
- Pipes, L. A., 1953. An operational analysis of traffic dynamics. *Journal of Applied Physics*, 24, 274-281.
- Punzo, V., Borzacchiello, M. T., and Ciuffo, B., 2011. On the assessment of vehicle trajectory data accuracy and application to the Next Generation SIMulation (NGSIM) program data. *Transportation Research Part C*, 19, 1243-1262.
- Punzo, V., Formisano, D. J., and Torrieri, V., 2005. Nonstationary Kalman filter for estimation of accurate and consistent car-following data. *Transportation Research Record: Journal of the Transportation Research Board*, 1934, 3–12.
- Ramanayya, T. V., 1988. Highway capacity under mixed traffic conditions. *Traffic engineering and control*, 19(5), 284-287.
- Ravishankar, K. V. R., and Mathew, T. V., 2011. Vehicle-Type Dependent Car-Following Model for Heterogeneous Traffic Conditions. *J. Transp. Eng.*, 137(11), 775–781.
- Rickert, M., Nagel, K., Schreckenberg, M., and Latour, A., 1996. Two lane traffic simulations using cellular automata. *Physica A: Statistical and Theoretical Physics*, 231(4), 534-550.
- Savitzky, A., and Golay, M. J. E., 1964. Smoothing and Differentiation of Data by Simplified Least Squares Procedures. *Anal. Chem.*, 36 (8), 1627– 1638.
- Schadschneider, A. and Schreckenberg, M., 1997. Traffic flow models with 'slow-to-start' rules. *Annalen der Physik*, 509(7), 541-551.
- Shao, X., and Ma, C., 2003. A general approach to derivative calculation using wavelet transform. *Chemometrics and Intelligent Laboratory Systems*, 69, 157– 165.
- Shao, X., Pang, C., and Su, Q., 2000. A novel method to calculate the approximate derivative photoacoustic spectrum using continuous wavelet transform. *Fresenius J Anal. Chem.*, 367, 525-529.
- Singh, B., 1999. Simulation and Animation of Heterogeneous Traffic on Urban Roads. Ph.D. thesis, IIT Kanpur, India.
- Sun, D., and Elefteriadou, L., 2014. A Driver Behavior-Based Lane-Changing Model for Urban Arterial Streets, *Transportation Science*, 48(2), 184-205.
- Takayasu, M. and Takayasu, H., 1993. 1/f noise in a traffic model. *Fractals*, 1(4), 860-866.

- Thiemann, C., Treiber, M. and Kesting, A., 2008. Estimating Acceleration and Lane-Changing Dynamics from Next Generation Simulation Trajectory Data, *Transportation Research Record*, No. 2088, TRB, Washington, D.C., 90–101.
- Toledo, T., Koutsopoulos, H. N., and Ahmed, K. I., 2007. Estimation of vehicle trajectories with locally weighted regression. *Transportation Research Record: Journal of the Transportation Research Board*, 1999, 161-169.
- Torres, M. E., Colominas, M. A., Schlotthauer, G., and Flandrin, P., 2011. A complete ensemble empirical mode decomposition with adaptive noise, in: *Proc. 36th IEEE Int. Conf. on Acoust., Speech and Signal Process, ICASSP 2011*, May 22-27, Prague, Czech Republic, 4144–4147.
- Treiber, M., Kesting, A., and Helbing, D., 2010. Three-phase traffic theory and two-phase models with a fundamental diagram in the light of empirical stylized facts. *Transportation Res. Part B*, 44(8–9), 983–1000.
- Wagner, P., Nagel, K., and Wolf, D. E., 1997. Realistic multi-lane traffic rules for cellular automata. *Physica A: Statistical and Theoretical Physics*, 234(3-4), 687-698.
- Wei, H., Feng, C. Meyer, E. and Lee, J., 2005. Video-Capture-Based Approach to Extract Multiple Vehicular Trajectory Data for Traffic Modeling, *Journal of Transportation Engineering*, 131(7), 496-505.
- Wiedemann, R., 1974. *Simulation des straenverkehrsflusses*. Schriftenreihe des Instituts fur Verkehrswesen der Universitat Karlsruhe, Karlsruhe, Germany.
- Wolfram, S., 1986. Cellular Automaton Fluids 1: Basic Theory. *J. Stat. Phys.* 45, 471.
- Wu, Z., and Huang, N. E., 2009. Ensemble empirical mode decomposition: a noise-assisted data analysis method. *Advances in Adaptive Data Analysis*, 1(1), 1–41.
- Yang, D., Qiu, X., Yua, D., Suna, R., and Pu, Y., 2015. A cellular automata model for car–truck heterogeneous traffic flow considering the car–truck following combination effect. *Physica A*, 424, 62-74.
- Yuan, H., 2009. A novel trajectory smoothing algorithm based on empirical mode decomposition. *Fifth international conference on image and graphics*, 223-226.
- Zhaohua Wu, Z., and Huang, N.E., 2009. Ensemble empirical mode decomposition: a noise-assisted data analysis method. *Advances in Adaptive Data Analysis*, 1 (1), 1–41.
- Zheng, Z., 2014. Recent developments and research needs in modeling lane Changing, *Transportation Research Part B*, 60, 16-34.
- Zheng, Z., Ahn, S., Chen, D., and Laval, J., 2011. Applications of wavelet transform for analysis of freeway traffic: Bottlenecks, transient traffic, and traffic oscillations. *Transportation Research Part B*, 45(2), 372-384.

Publications

- Mallikarjuna, C., Budde, T., and Pal, D., 2013. Analysis of the Lateral Gap Maintaining Behavior of Vehicles in Heterogeneous Traffic Stream. *Procedia - Social and Behavioral Sciences*, 104, 370-379.
- Pal, D., and Mallikarjuna, C., 2014. Correction of Vehicle's Trajectory Extracted from Video Image Processing. Poster presented at 19th international conference of Hong Kong Society for Transportation Studies (HKSTS), Hong Kong, 13-15 December.
- Pal, D., and Mallikarjuna, C., 2016. Impact of Variable Lateral Gap Maintaining Behavior of Vehicles on Macroscopic Traffic Relations. (Accepted for publication in proceeding of WCTRS 2016, full paper under review for special publication).
- Pal, D., and Mallikarjuna, C. Modeling of lateral Gap Maintaining Behavior of Vehicles in Heterogeneous Traffic Stream. (submitted for re-review after the first revision, *Journal of Transportation Engineering*, ASCE).
- Pal, D., and Mallikarjuna, C. Application of Wavelet Transforms and EMD in Extracting Microscopic Data under Heterogeneous Traffic Conditions. (Under review, *Journal of Transportation Engineering*, ASCE).
- Pal, D., and Mallikarjuna, C. Methodology for Correction of Vehicle Trajectory Extracted from Video Image Processing. (Under review, *Transportation Letters*).
- Pal, D., and Mallikarjuna, C. CA model for No-lane-disciplined Heterogeneous Traffic Flow. (Under preparation for *Journal of Advanced Transportation*).